Diboson and triboson production and polarization measurements

Saptaparna Bhattacharya

QCD@LHC

October 7-11th, 2024

Outline

- Triboson: recently observed processes
  - $WZ\gamma$ (CMS and ATLAS), $WW\gamma$ (CMS), $W\gamma\gamma$ (ATLAS)
- Dibosons (focus on polarization measurements):
  - WZ in CMS and ATLAS @ 13 TeV and 13.6 TeV
    - $ZZ \to 4\ell$

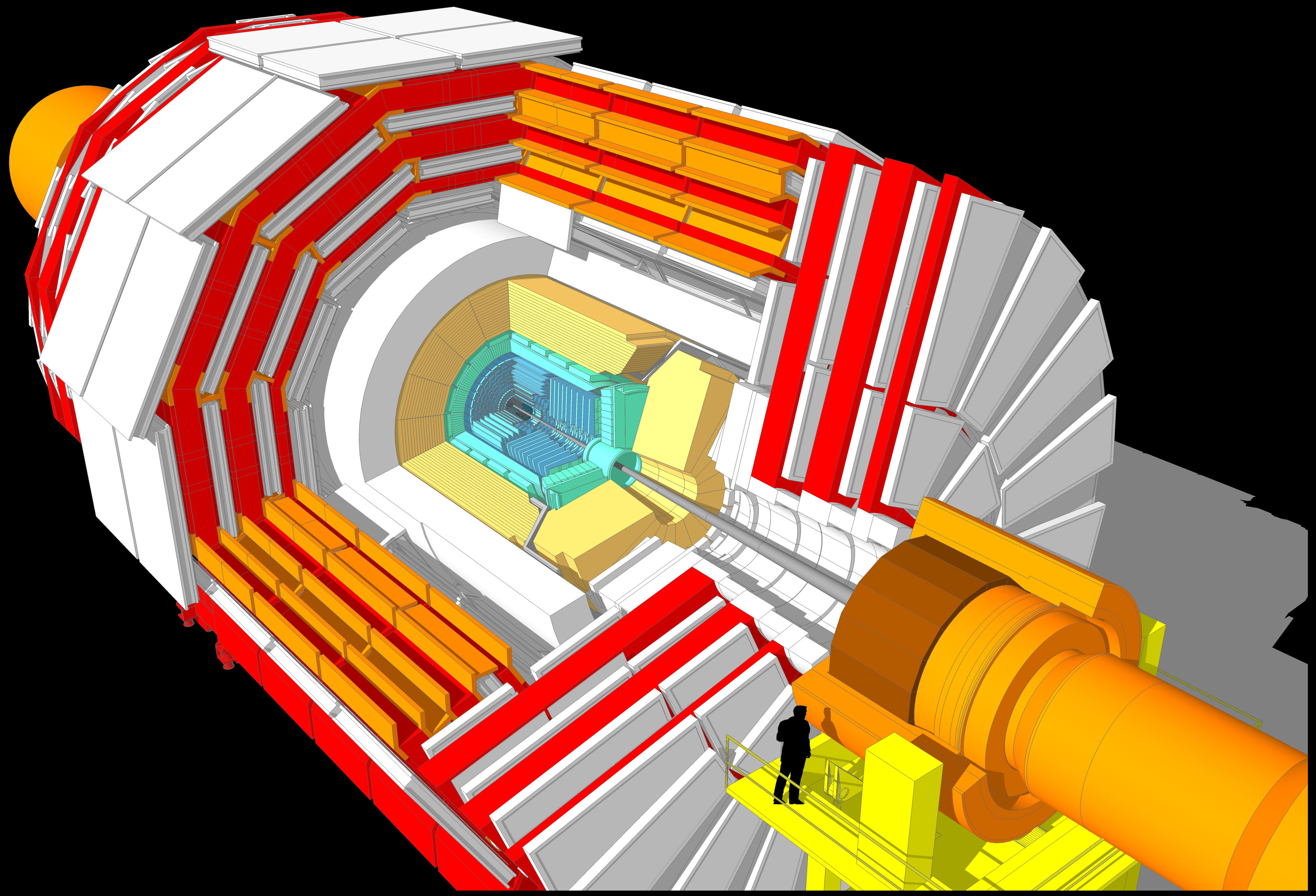

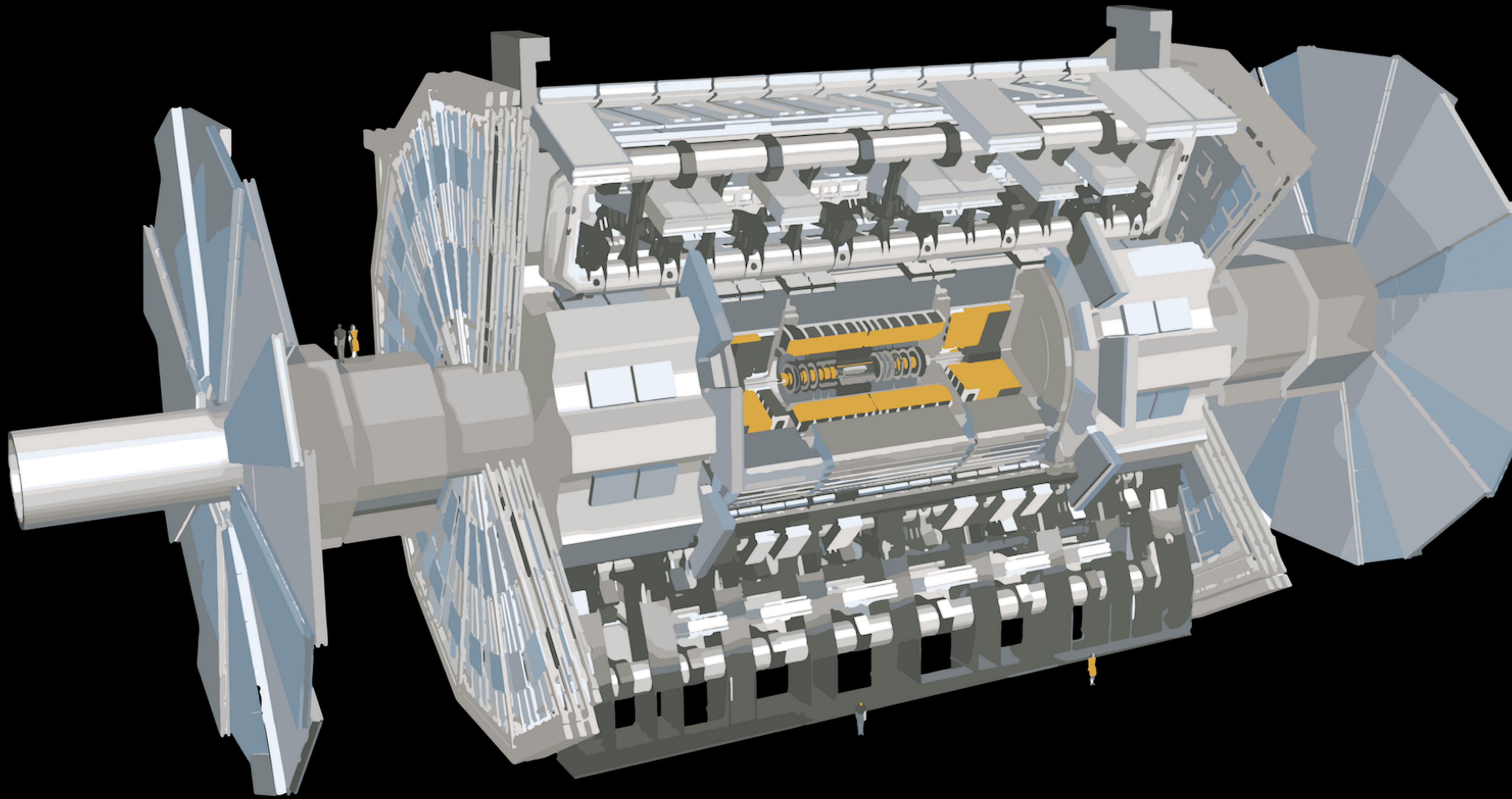

Overview of CMS cross section results

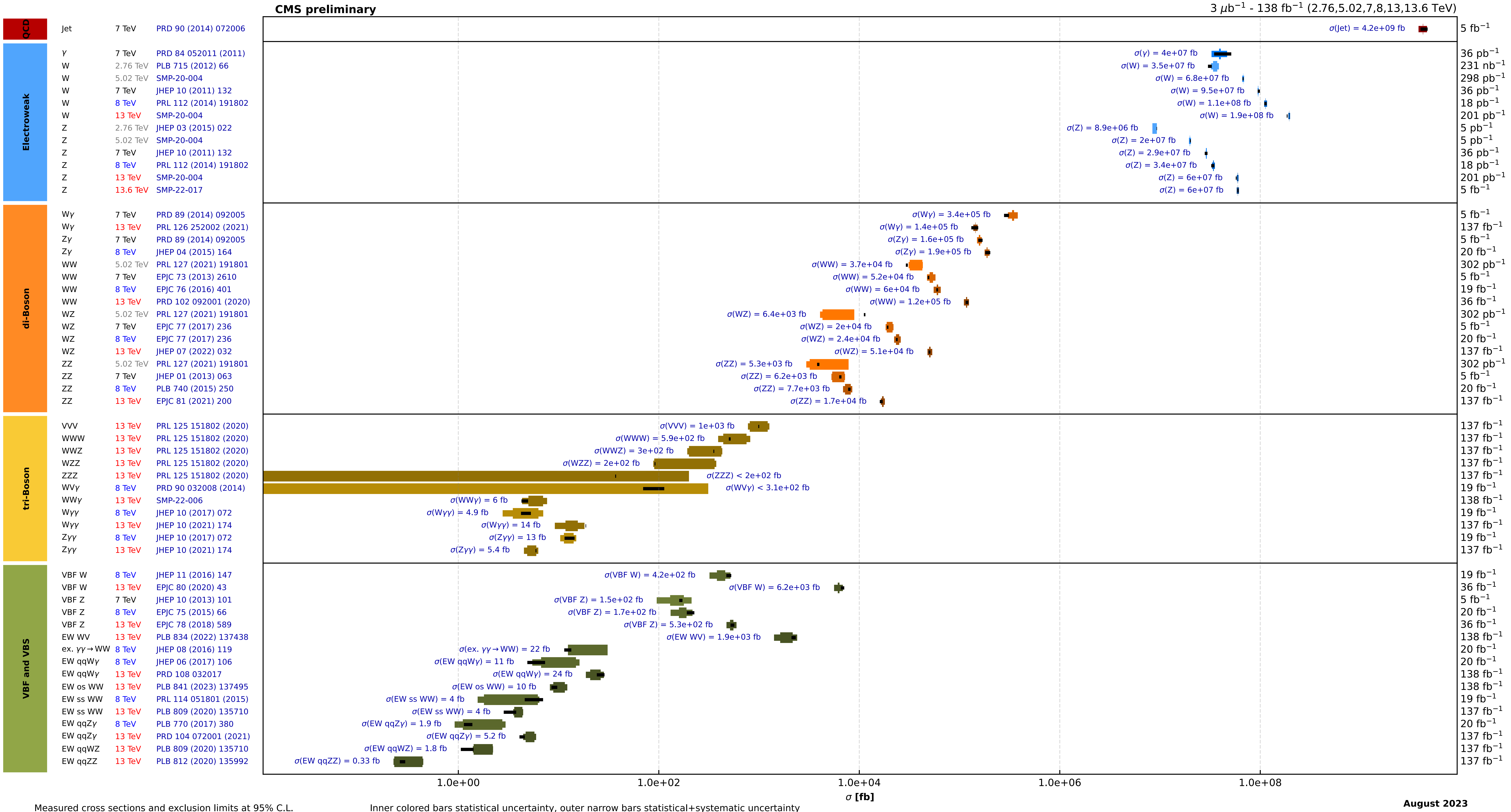

Measured cross sections and exclusion limits at 95% C.L.
See here for all cross section summary plots

Inner colored bars statistical uncertainty, outer narrow bars statistical+systematic uncertainty
Light to Dark colored bars: 2.76, 5.02, 7, 8, 13, 13.6 TeV, Black bars: theory prediction

Standard Model Total Production Cross Section Measurements

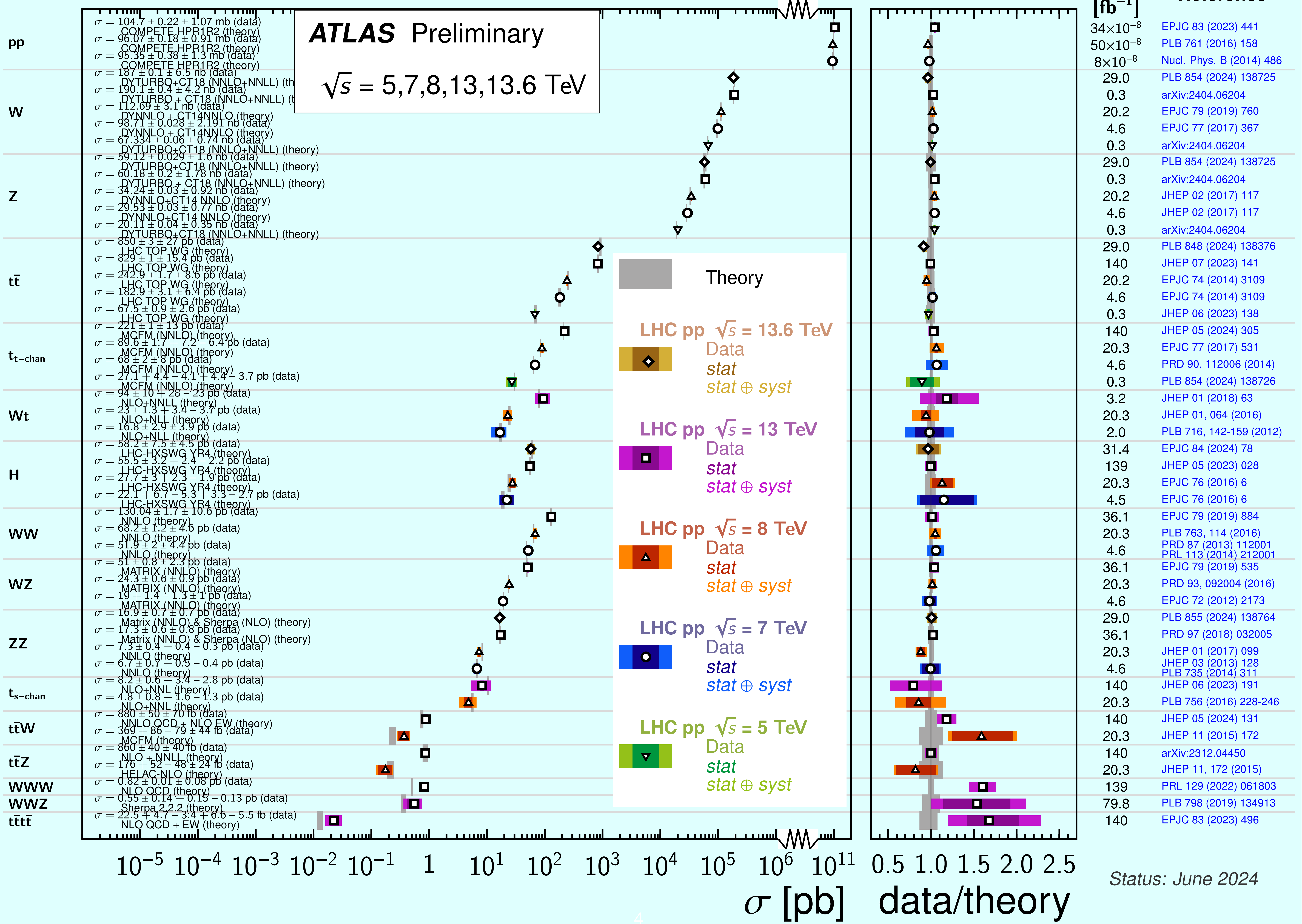

Tribosons

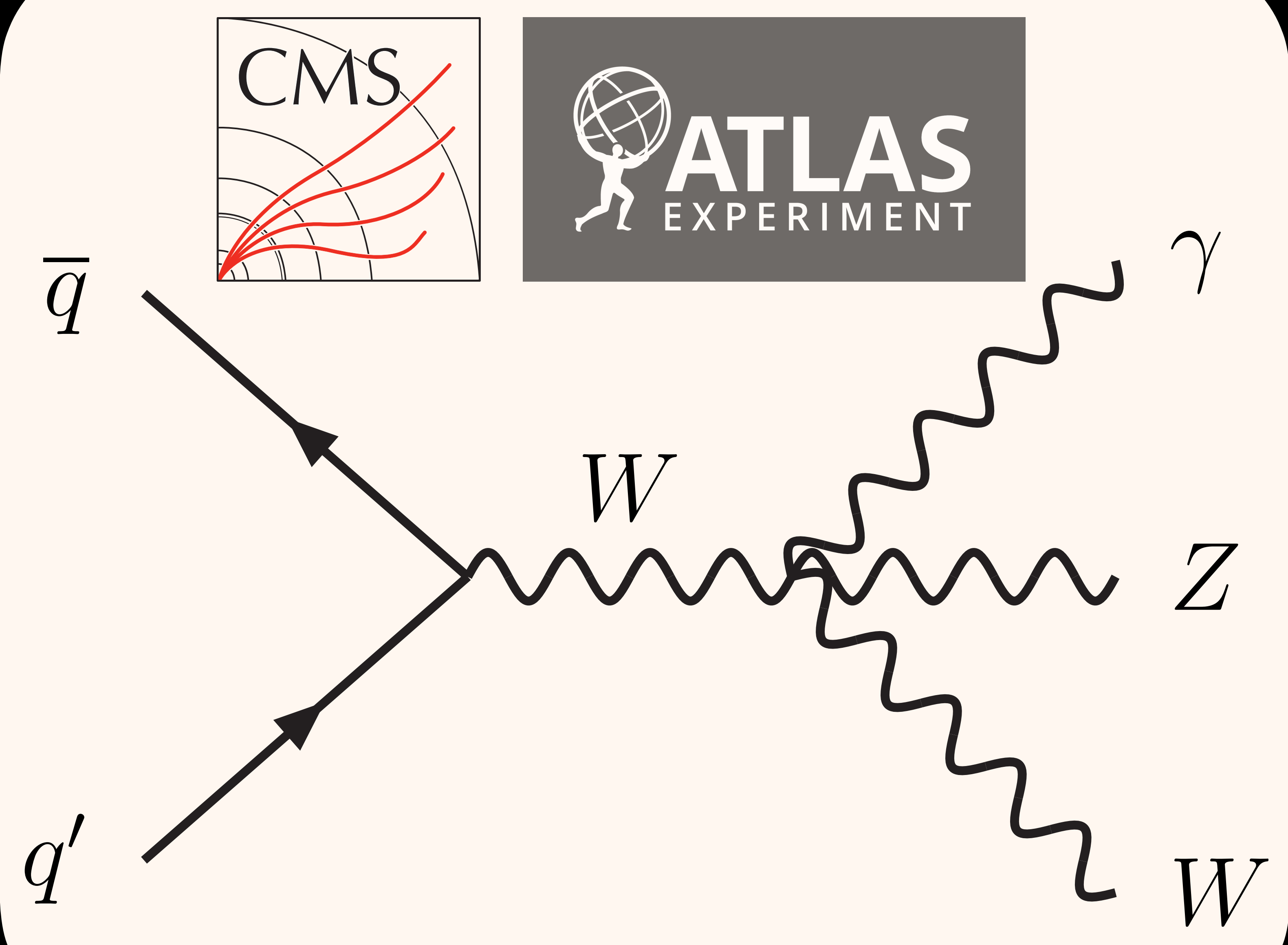

CMS
ATLAS
EXPERIMENT
$\overline{q}$
q'
W
γ
Z
W

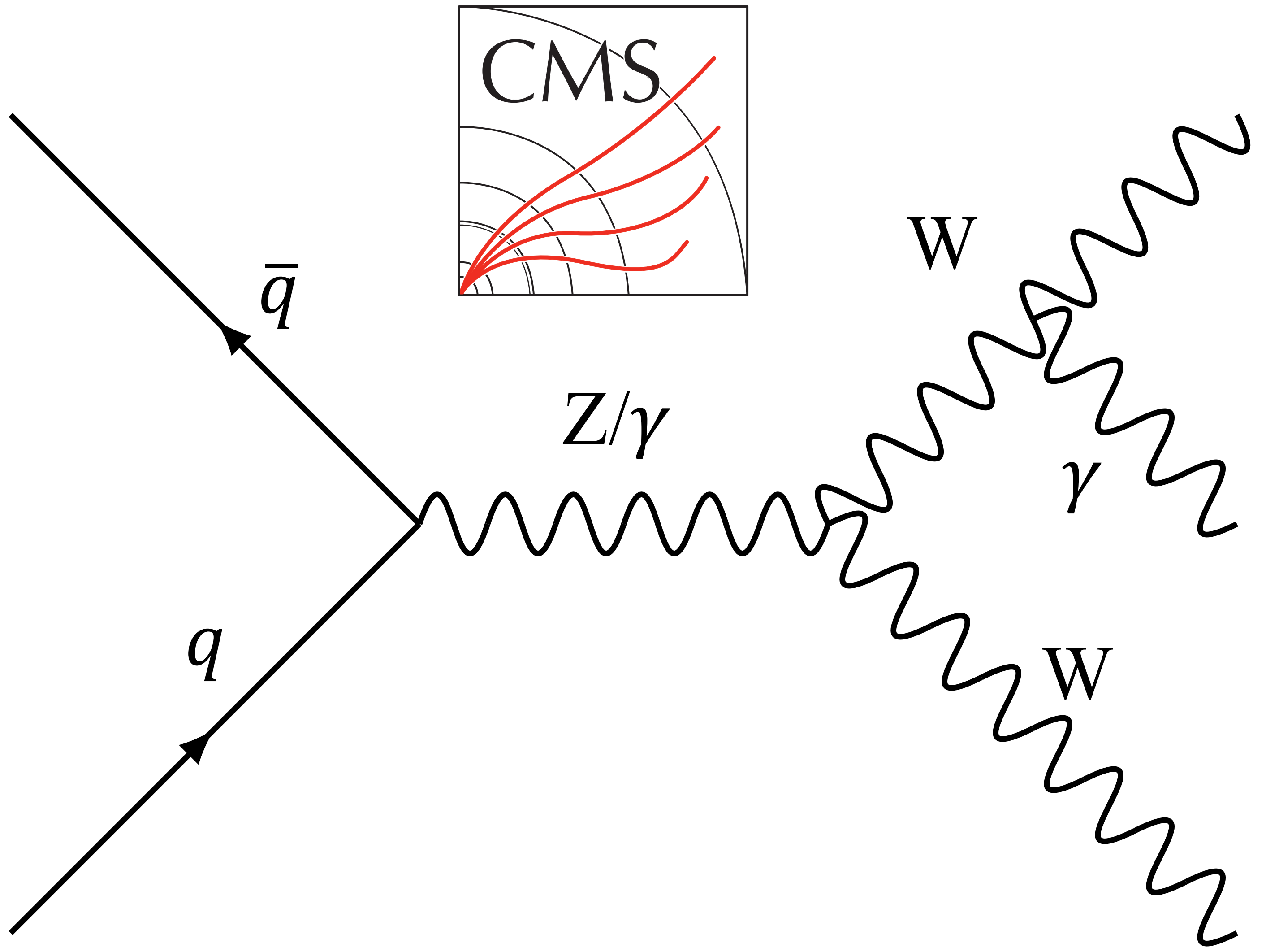

CMS
$\overline{q}$
q
Z/γ
W
γ
W

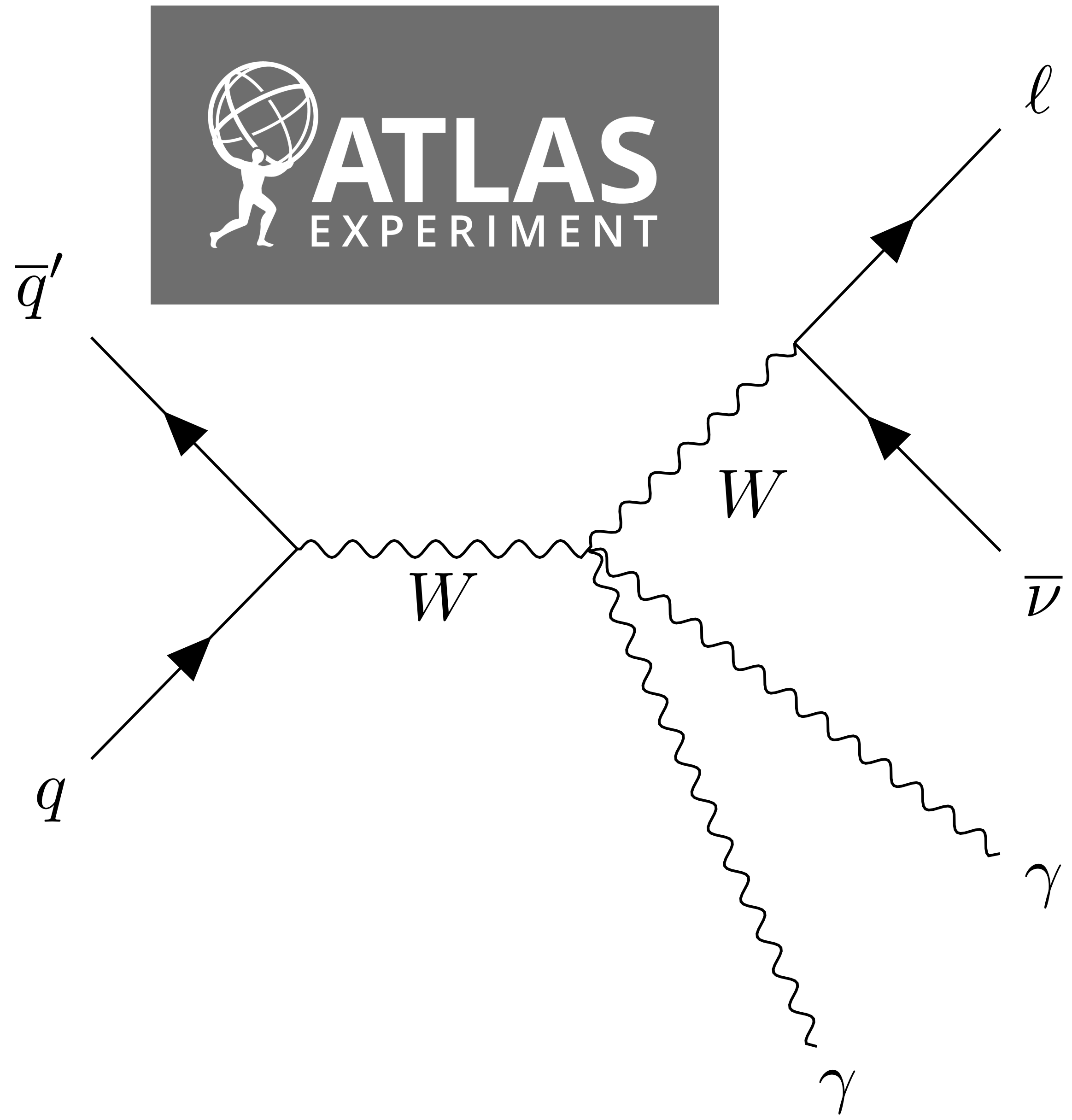

ATLAS
EXPERIMENT
$\overline{q}'$
q
W
W
ℓ
$\overline{\nu}$
γ
γ

https://cds.cern.ch/record/2905175

Observation of $WZ\gamma$ production at $\sqrt{s} = 13$ TeV

- $WZ\gamma$ process observed (expected) with a significance of 5.4 (3.8) σ
- Final state defined by requiring three charged leptons ($WZ \to \ell\nu\ell\ell$) and a photon
- Fiducial cross section measured as: 5.48 ± 1.11 fb
  - Three electrons or muons with one Z-candidate, $p_T > 15$ GeV, $\Delta R(\ell,\gamma) > 0.3$ and $|\eta^\gamma| < 2.5$

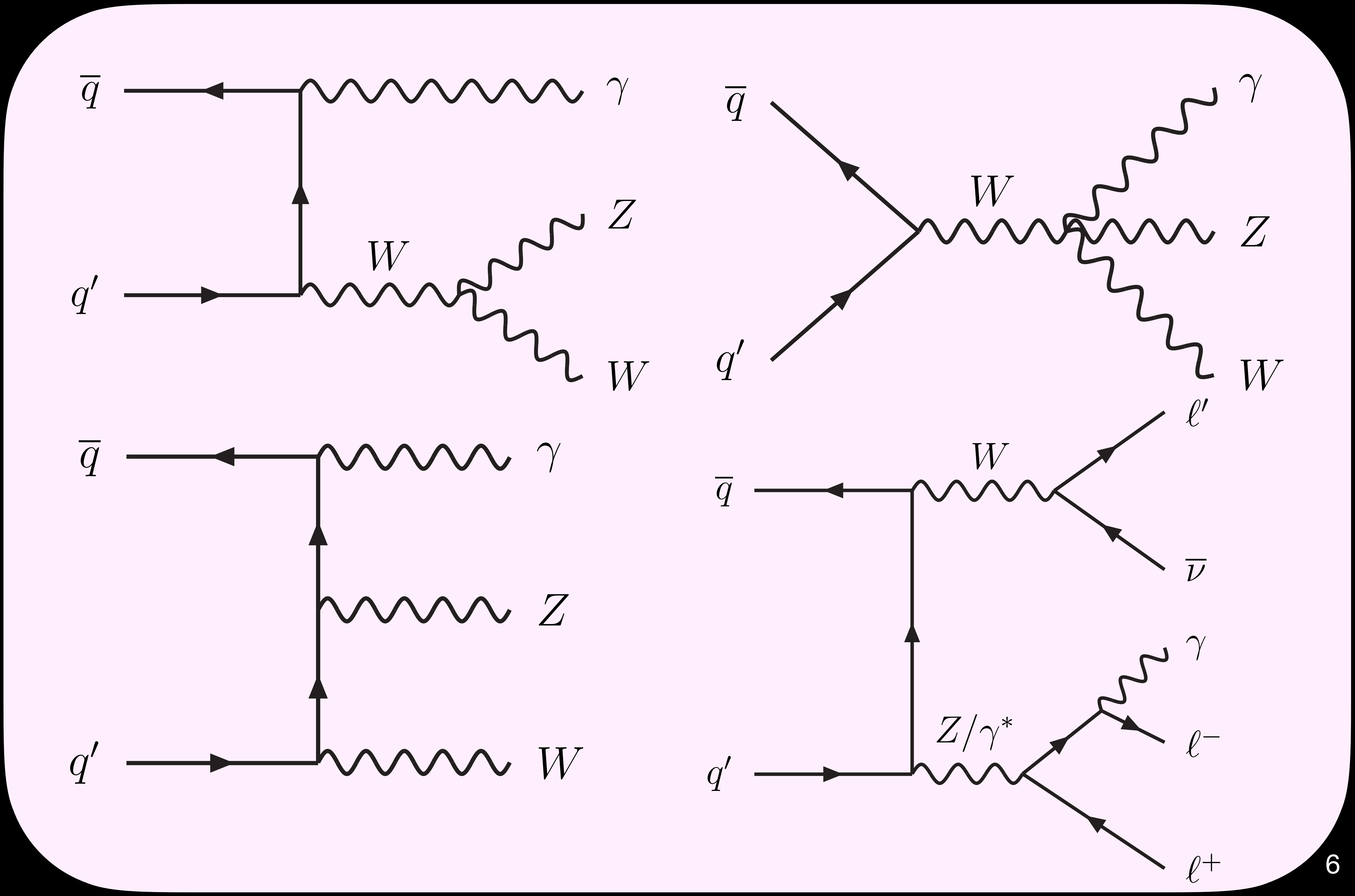

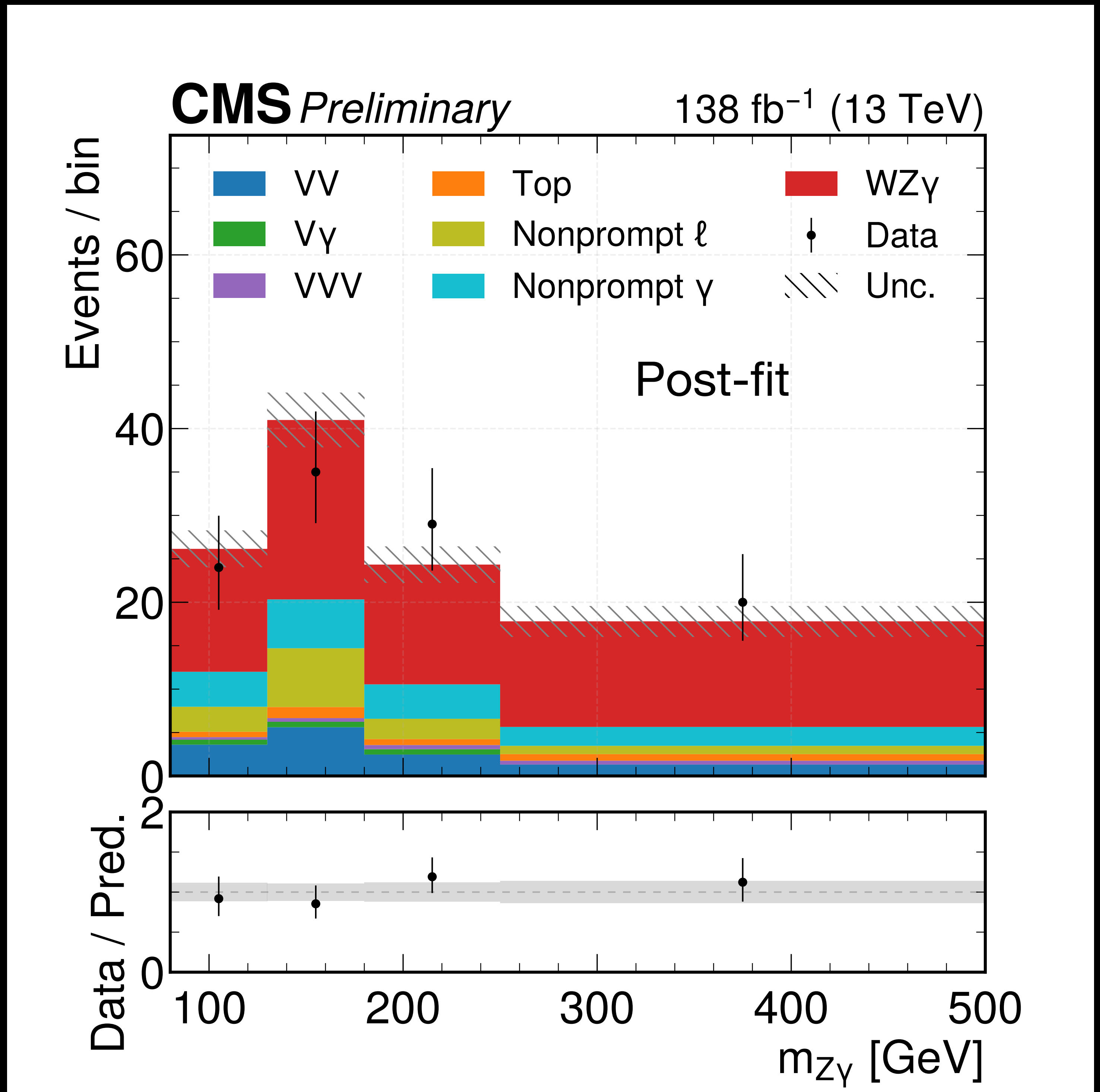

https://cds.cern.ch/record/2905175

Observation of $WZ\gamma$ production at $\sqrt{s} = 13$ TeV

- Simultaneous fit of signal and background regions
  - Major background sources
    - Non-prompt photon and leptons
    - Prompt ZZ with an ISR photon

Process	SR	Nonprompt ℓ CR	Nonprompt γ CR	ZZ CR
VV	13.0 ± 0.3	1.86 ± 0.12	0.16 ± 0.02	1016 ± 12
VVV	0.69 ± 0.05	0.36 ± 0.11	0.01 ± 0.01	0.10 ± 0.04
Vγ	1.38 ± 0.76	4.66 ± 2.05	438 ± 27	0.01 ± 0.01
Top	3.34 ± 0.55	227 ± 15	27.0 ± 5.9	0.30 ± 0.04
Nonprompt ℓ	12.9 ± 2.8	1792 ± 34	<0.1	<0.1
Nonprompt γ	15.8 ± 2.2	<0.1	195 ± 19	<0.1
WZG signal	60.8 ± 3.5	0.66 ± 0.01	0.20 ± 0.04	0.02 ± 0.01
Total background	48.5 ± 3.7	2027 ± 33	660 ± 21	1016 ± 12
Total prediction	109 ± 5	2027 ± 33	660 ± 21	1016 ± 12
Observed	108	2029	658	1017

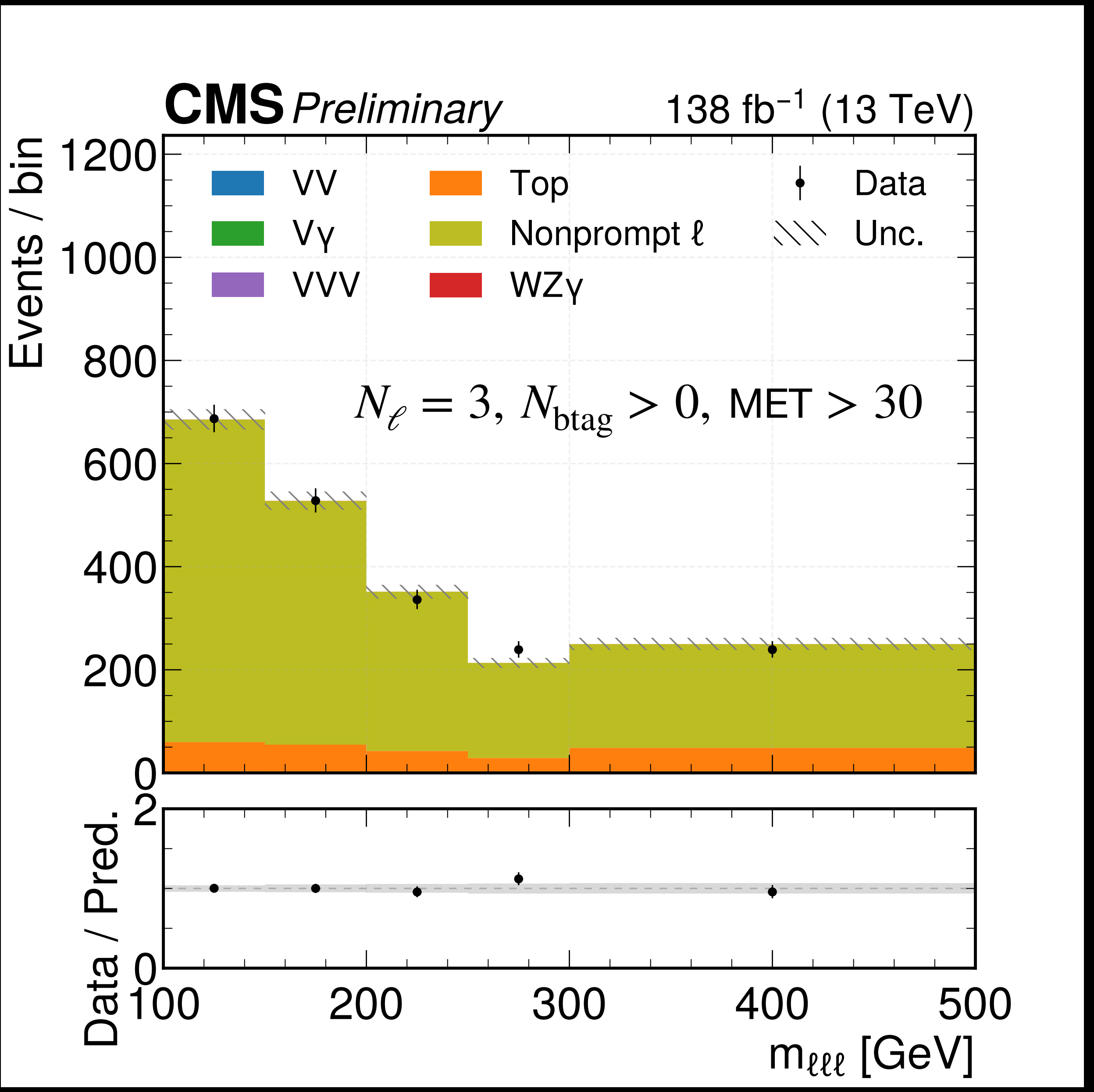

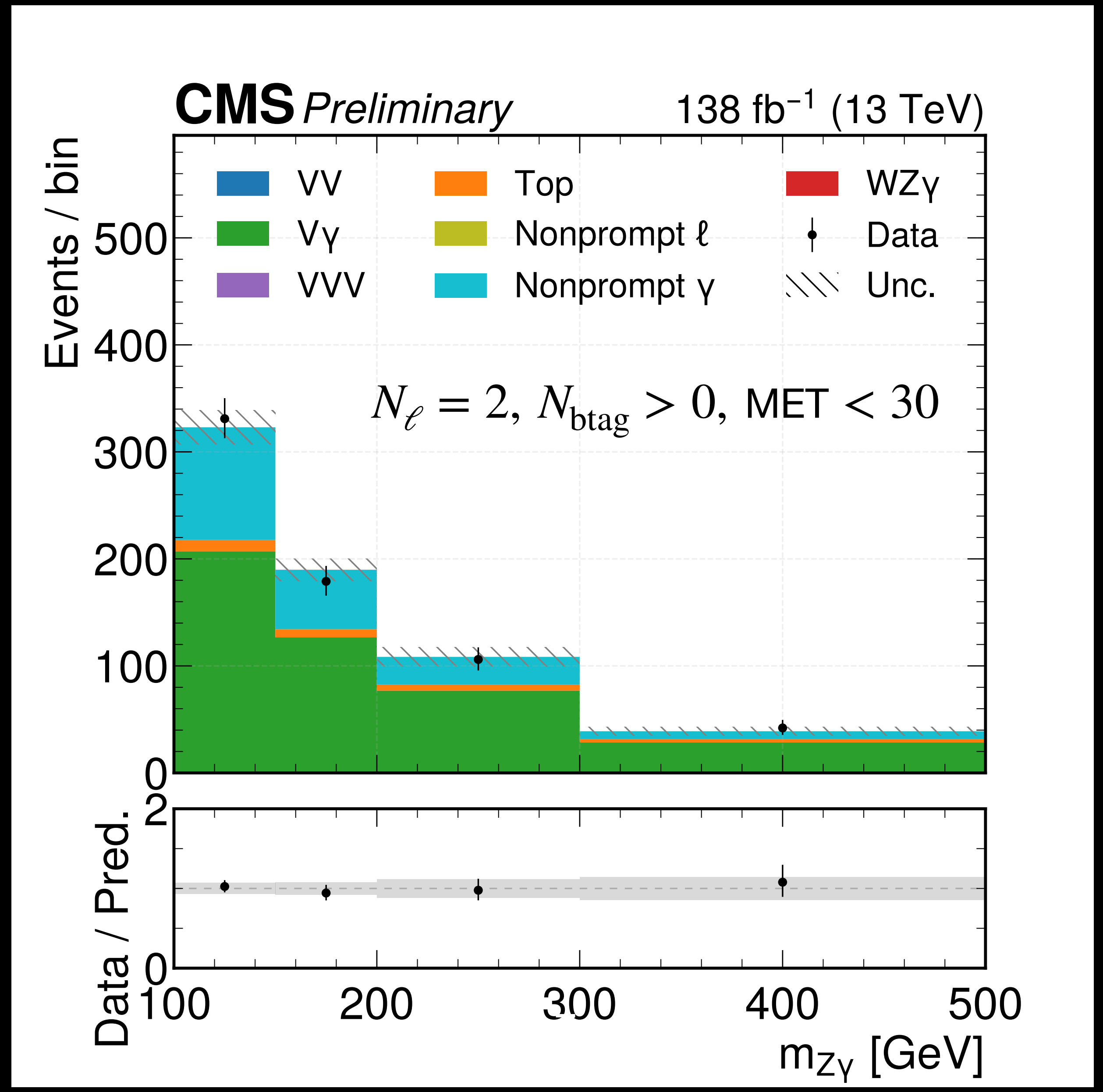

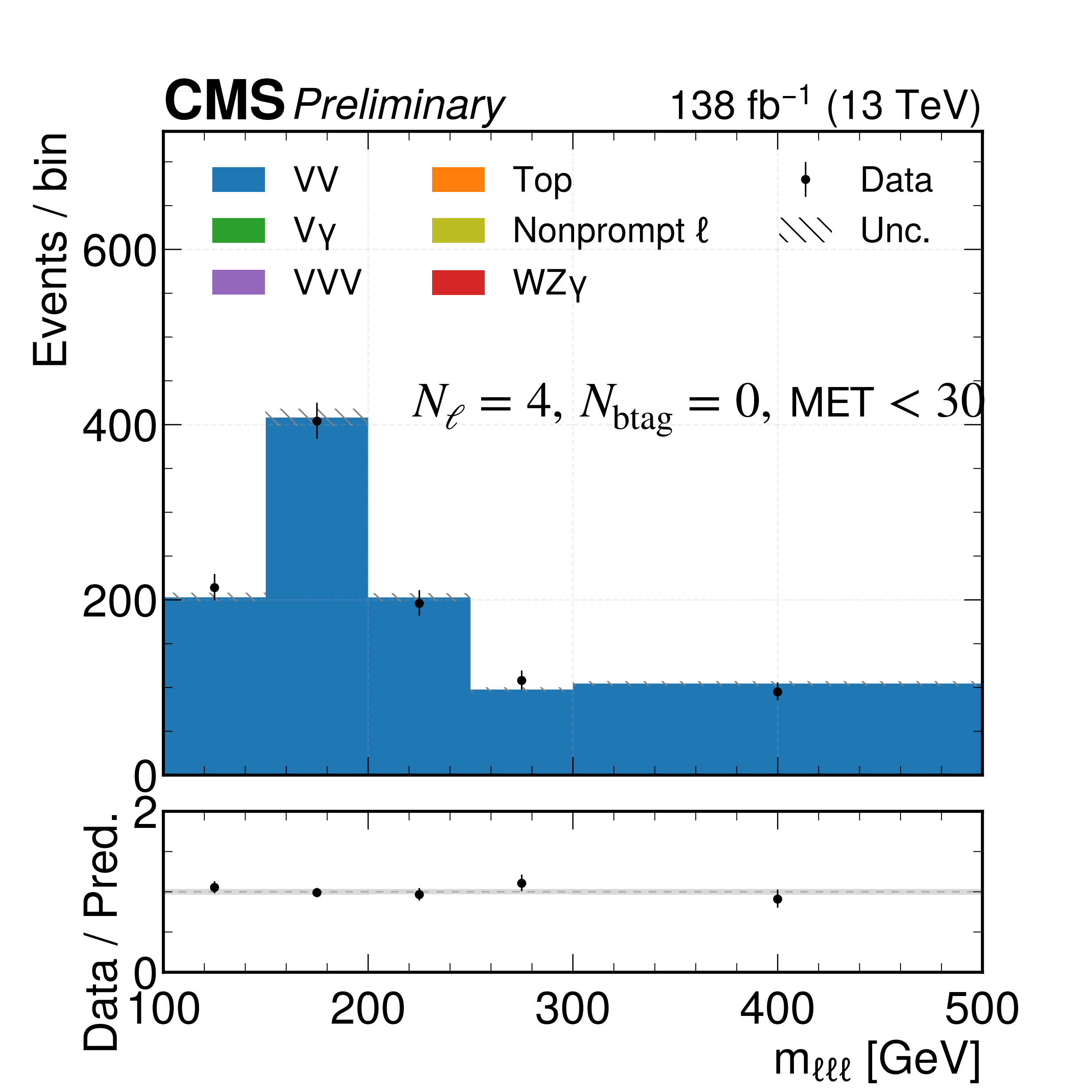

New physics at high energies manifesting at low energies

BSM implication of $WZ\gamma$

https://arxiv.org/pdf/2004.05174

EFT interpretation of dimension-8 operators featuring $SU(2)_L$ and $U(1)_Y$ field strength

Operators	Observed limits [TeV $^{-4}$]	Expected limits [TeV $^{-4}$]	Unitarity bound [TeV]
$F_{T,0}/\Lambda^4$	[-2.60, 2.60]	[-2.52, 2.52]	1.32
$F_{T,1}/\Lambda^4$	[-3.28, 3.24]	[-3.18, 3.14]	1.48
$F_{T,2}/\Lambda^4$	[-7.15, 7.05]	[-6.95, 6.85]	1.35
$F_{T,5}/\Lambda^4$	[-2.54, 2.56]	[-2.46, 2.50]	1.55
$F_{T,6}/\Lambda^4$	[-3.18, 3.22]	[-3.08, 3.14]	1.61
$F_{T,7}/\Lambda^4$	[-6.85, 7.05]	[-6.65, 6.85]	1.71

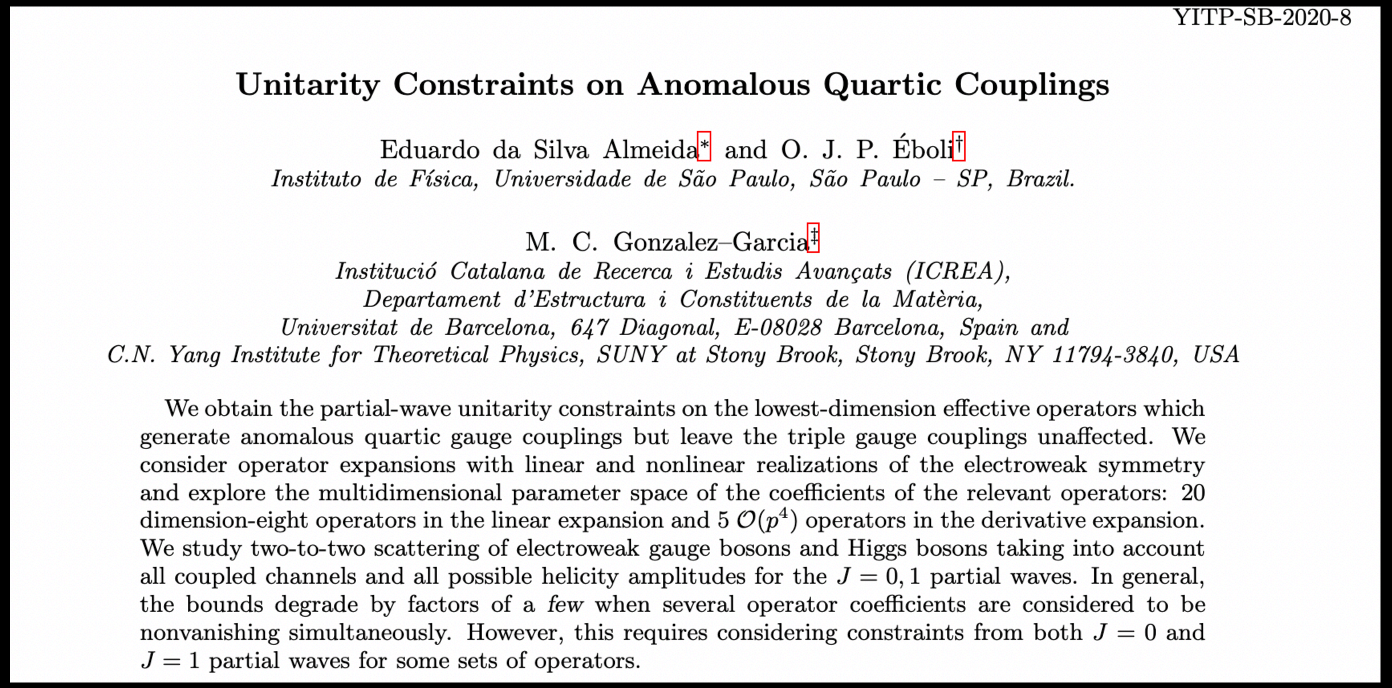
YITP-SB-2020-8

Unitarity Constraints on Anomalous Quartic Couplings

Eduardo da Silva Almeida* and O. J. P. Éboli†
Instituto de Física, Universidade de São Paulo, São Paulo – SP, Brazil.

M. C. Gonzalez–Garcia‡
Institució Catalana de Recerca i Estudis Avançats (ICREA), Departament d'Estructura i Constituents de la Matèria, Universitat de Barcelona, 647 Diagonal, E-08028 Barcelona, Spain and C.N. Yang Institute for Theoretical Physics, SUNY at Stony Brook, Stony Brook, NY 11794-3840, USA

We obtain the partial-wave unitarity constraints on the lowest-dimension effective operators which generate anomalous quartic gauge couplings but leave the triple gauge couplings unaffected. We consider operator expansions with linear and nonlinear realizations of the electroweak symmetry and explore the multidimensional parameter space of the coefficients of the relevant operators: 20 dimension-eight operators in the linear expansion and 5 $\mathcal{O}(p^4)$ operators in the derivative expansion. We study two-to-two scattering of electroweak gauge bosons and Higgs bosons taking into account all coupled channels and all possible helicity amplitudes for the $J = 0, 1$ partial waves. In general, the bounds degrade by factors of a *few* when several operator coefficients are considered to be nonvanishing simultaneously. However, this requires considering constraints from both $J = 0$ and $J = 1$ partial waves for some sets of operators.

$$\mathcal{L} = \mathcal{L}_{SM} + \sum_i \frac{c_i}{\Lambda^2}\mathcal{O}_i + \sum_j \frac{f_j}{\Lambda^4}\mathcal{O}_j$$

The $WZ\gamma$ process is also sensitive to mediation by axion-like particles

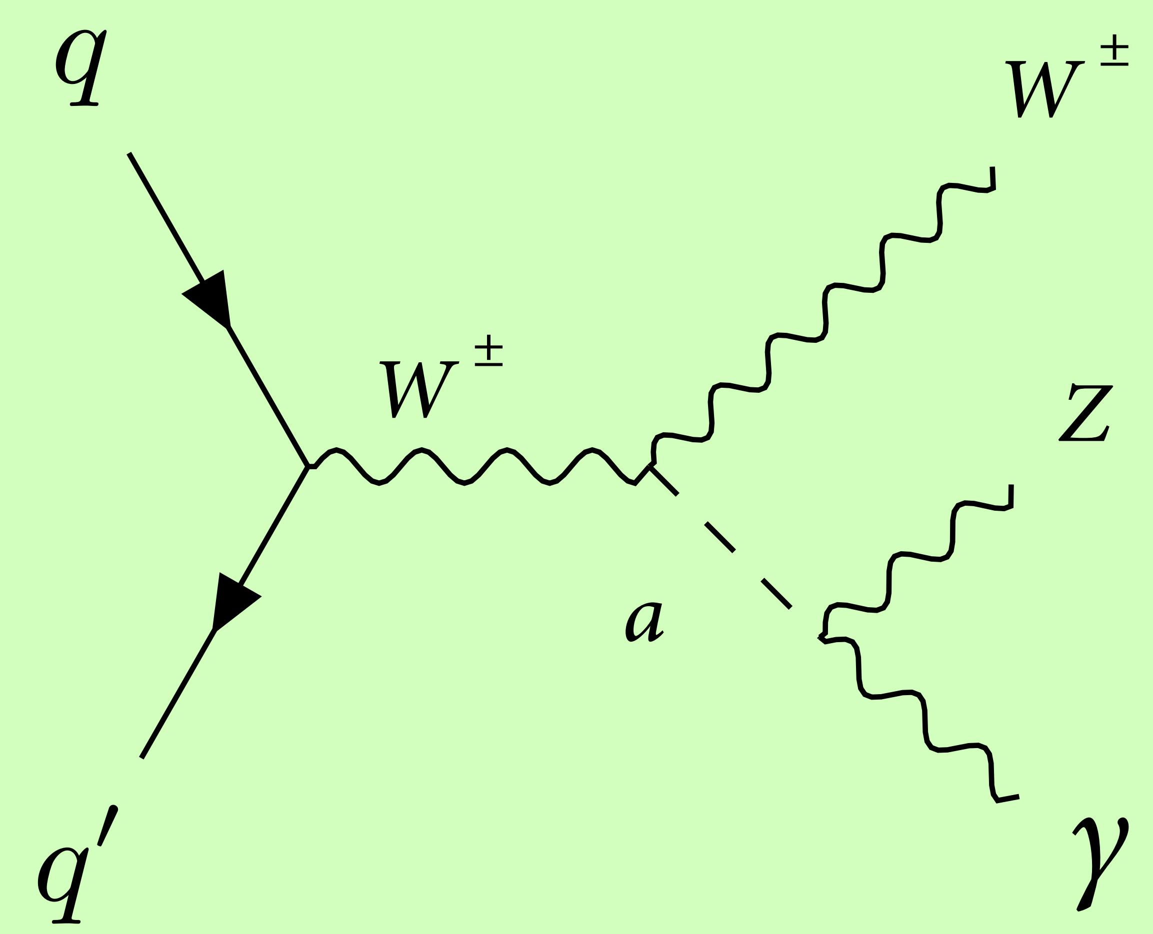

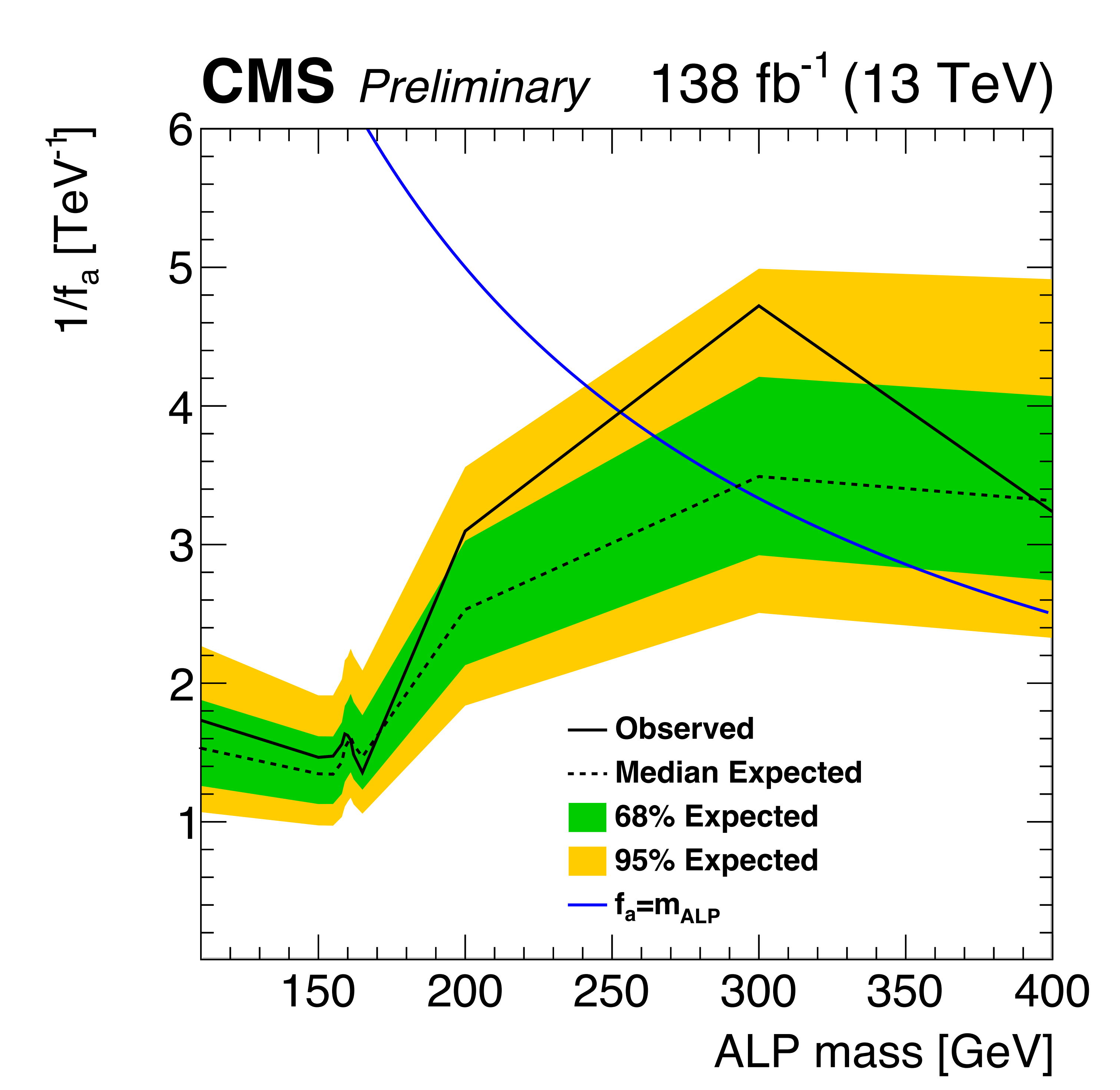

Observation of $WZ\gamma$ production at $\sqrt{s} = 13$ TeV

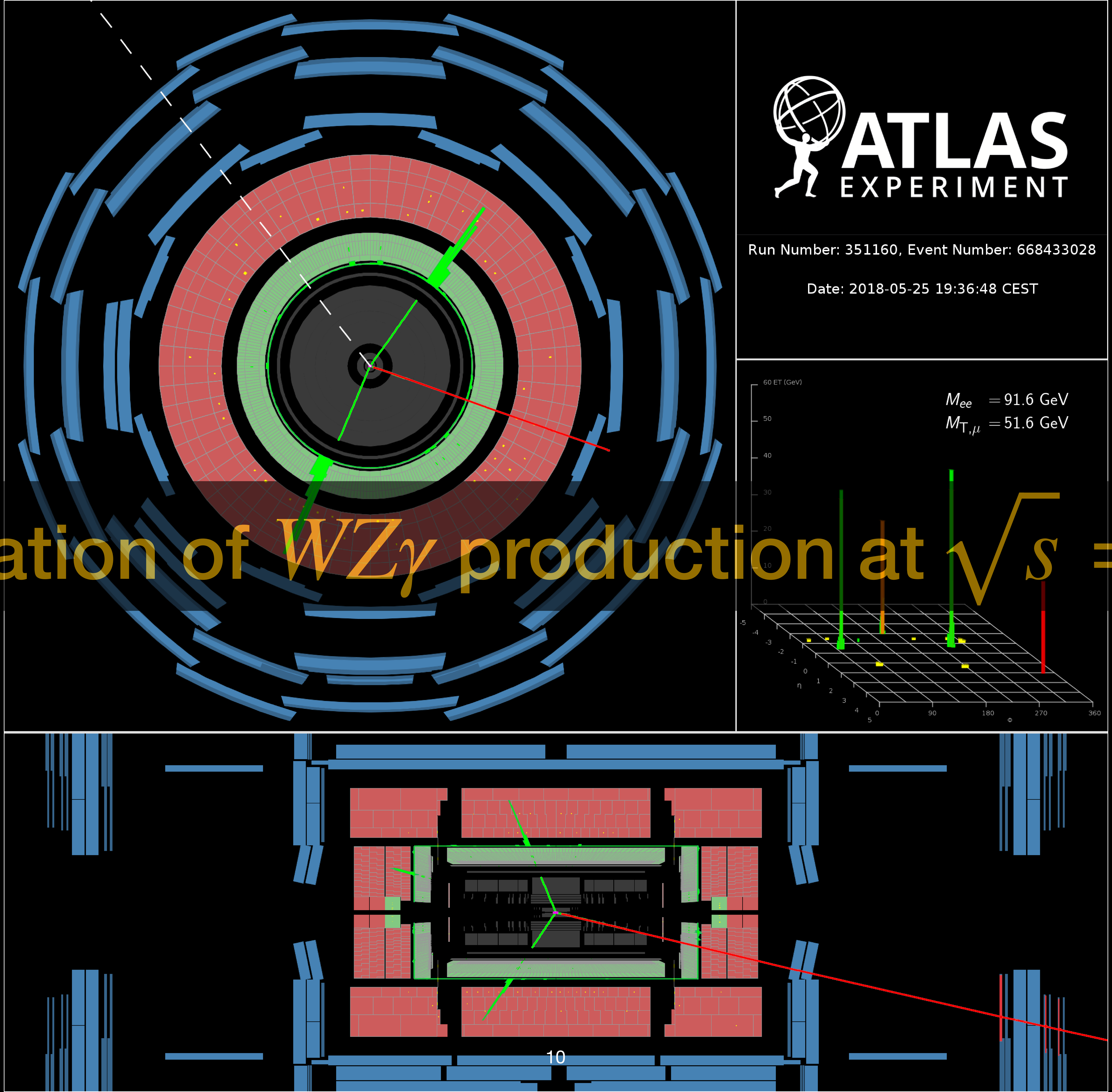

https://arxiv.org/abs/2305.16994

Observation of $WZ\gamma$ production at $\sqrt{s} = 13$ TeV

- Final state: $W \to \ell\nu,\ Z \to \ell^+\ell^-(\ell = e, \mu)$
- $WZ\gamma$ observed with a significance of 6.3 σ
- Cross section (fiducial):
  - 2.01 ± 0.30 (stat.) ± 0.16 (syst.) fb
- $K_{\mathrm{EW}} = \sigma_{\mathrm{fid.}}^{\mathrm{NLO\ EW}} / \sigma_{\mathrm{fid.}}^{\mathrm{LO}} = 1.05$

Fiducial requirements

	Photons	Leptons (e, μ)	Neutrino
$\lvert\eta\rvert$	$\lvert\eta^{\gamma}\rvert < 2.37$	$\lvert\eta^{\ell}\rvert < 2.5$	–
p_{T}	$p_{\mathrm{T}}^{\gamma} > 15\,GeV$	$p_{\mathrm{T}}^{\ell_1,\ell_2,\ell_3} > 30, 20, 20\,GeV$	$p_{\mathrm{T}}^{\nu} > 20\,GeV$
Isolation	$E_{\mathrm{T}}^{\mathrm{cone0.2}}/p_{\mathrm{T}}^{\gamma} < 0.07$	–	–
ℓ_Z assignment	for $eee/\mu\mu\mu$ channels, choose smallest $\lvert m_{\ell\ell} - m_Z\rvert$		
ΔR	$\Delta R(\ell, \gamma) > 0.4$		
Z invariant mass	$m_{\ell\ell} > 81\,GeV$		

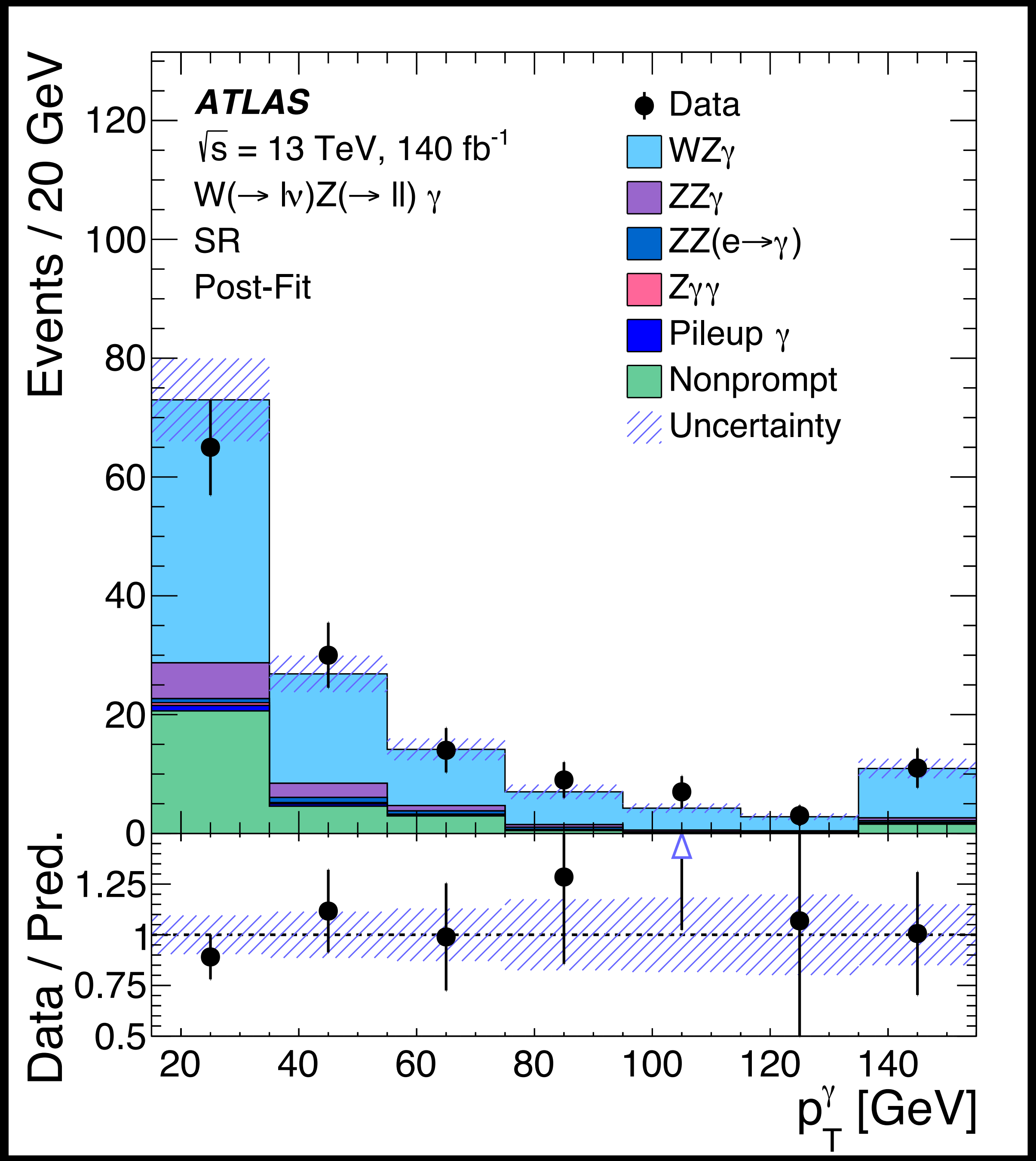

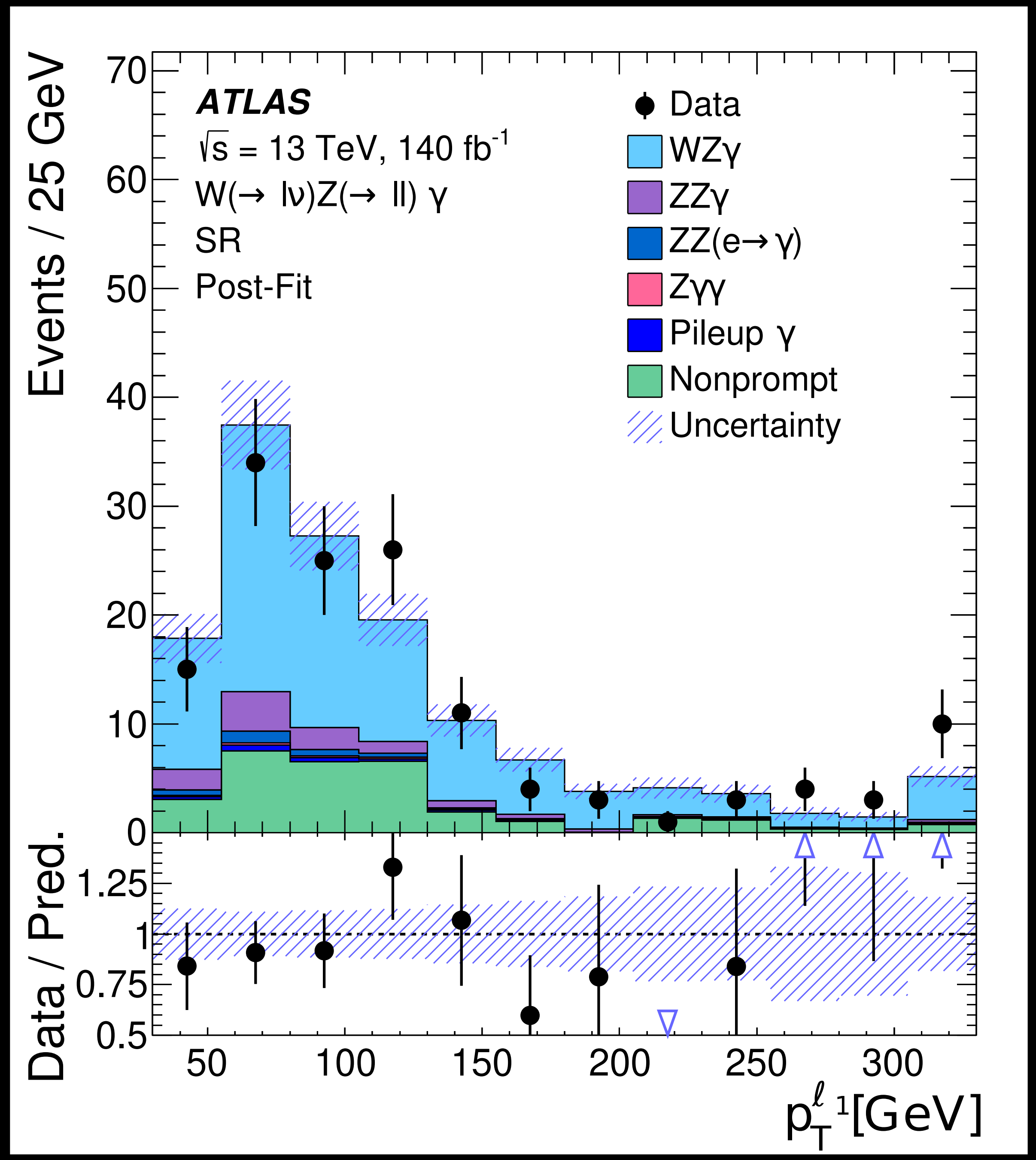

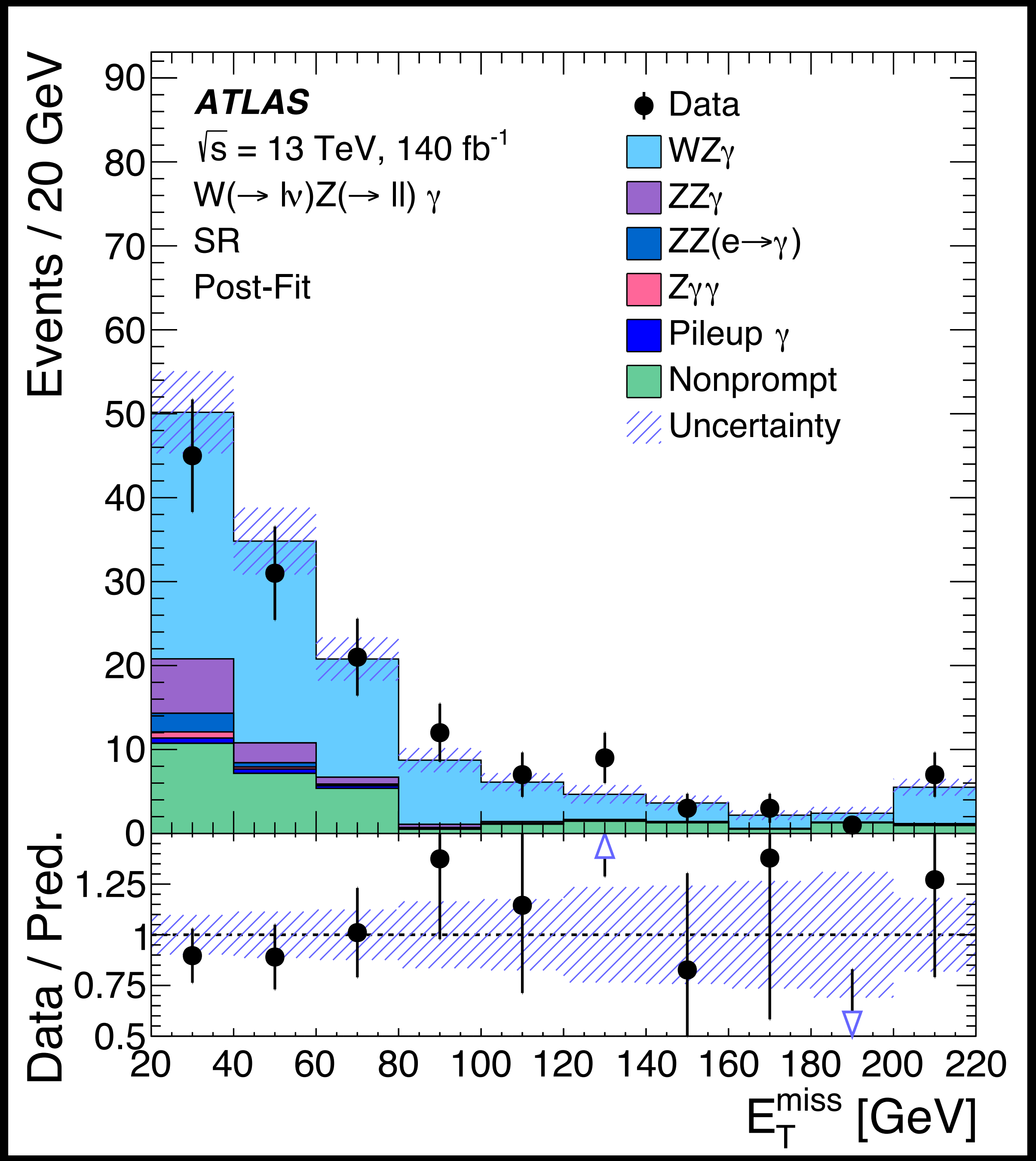

- Clean final state with large number of signal events with respect to the background contributions

Observation of $WW\gamma$ production at $\sqrt{s} = 13$ TeV

- $WW\gamma$ process observed (expected) with a significance of 5.6 (5.1) σ
- Fiducial cross section measured as: 5.9 ± 0.8 (stat.) ± 0.8 (syst.) ± 0.7 (modeling*) fb
- Associated search for H with a photon explored → generated by coupling of the Higgs boson to light quarks

Phys. Rev. Lett. 132 (2024) 121901

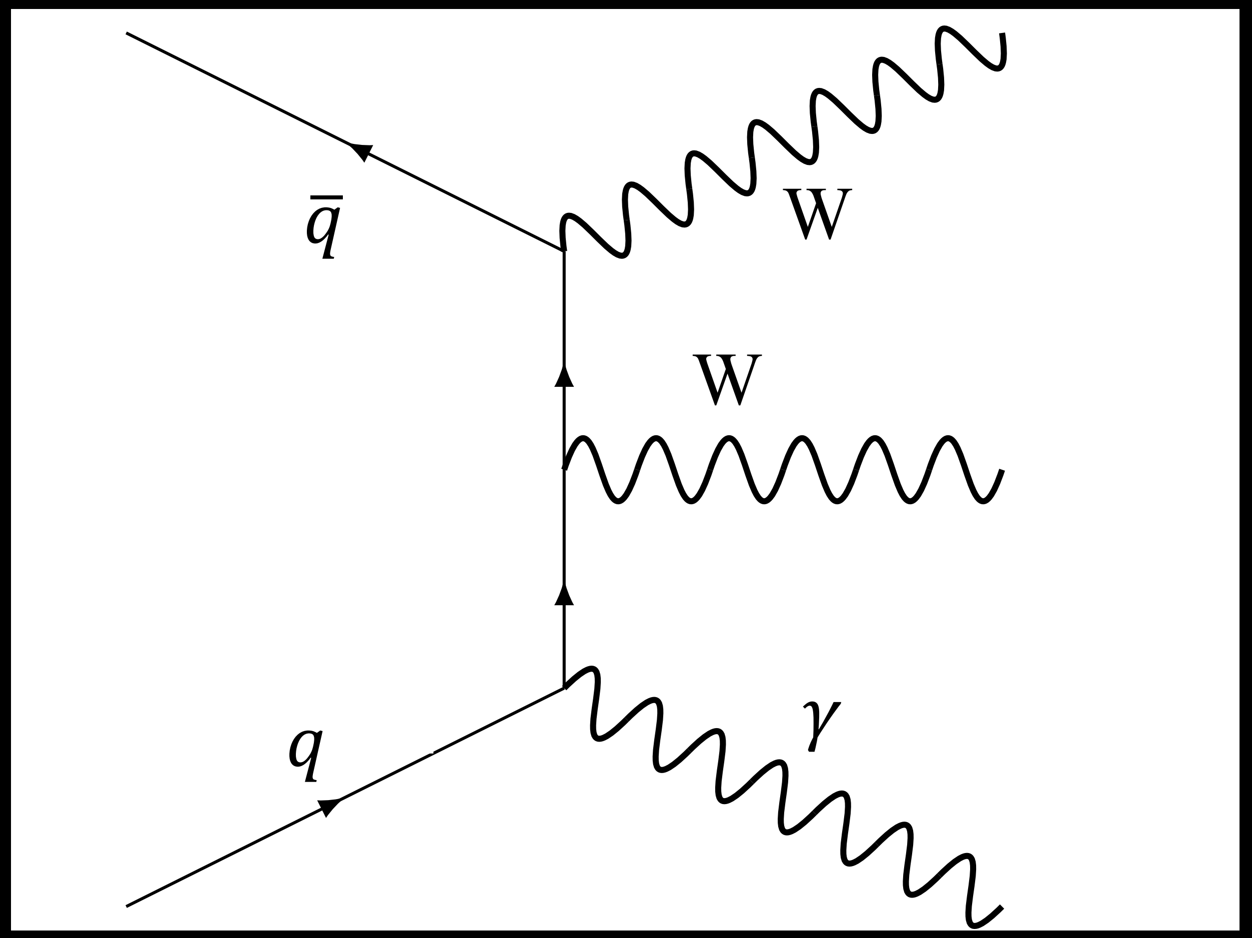

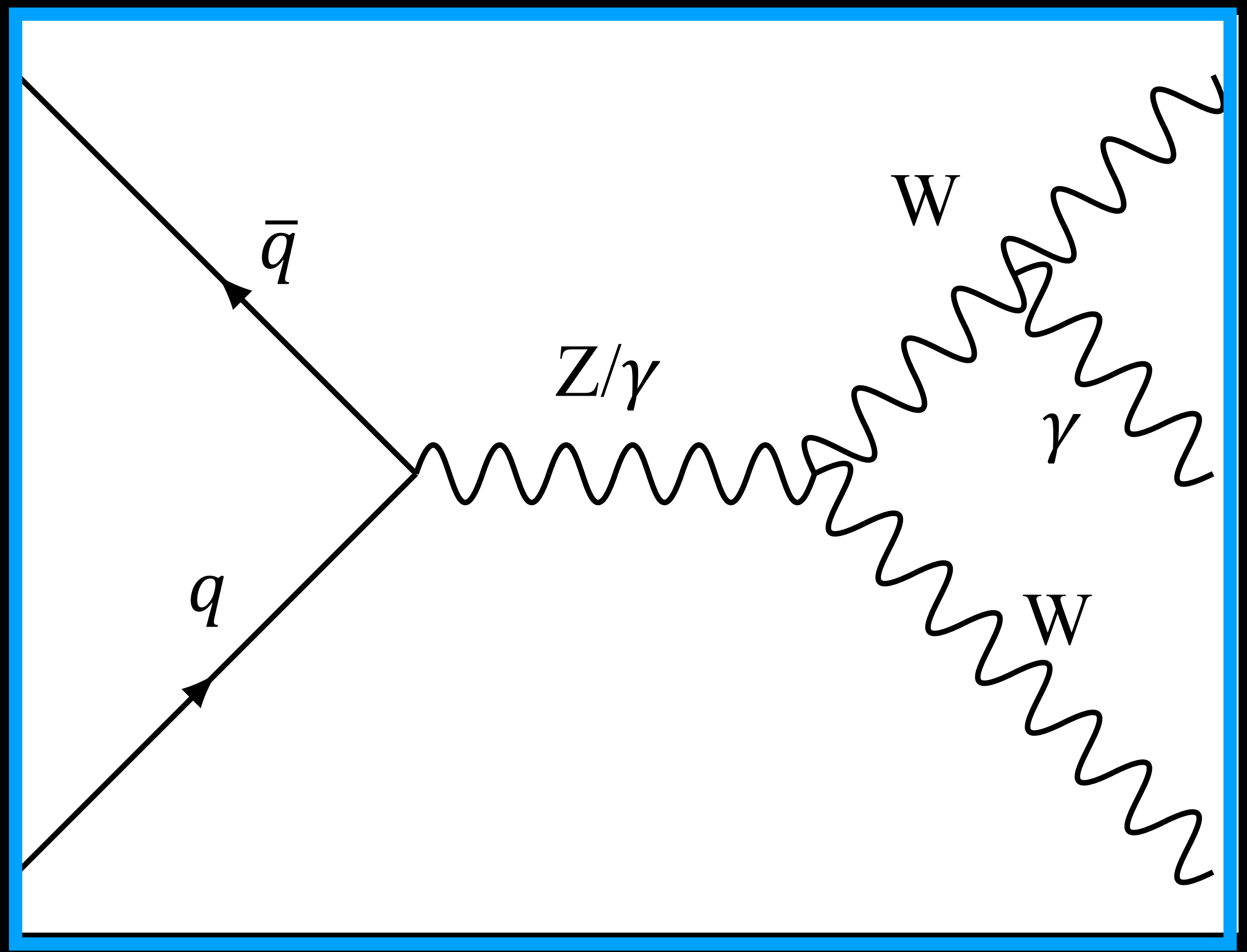

Trilinear coupling

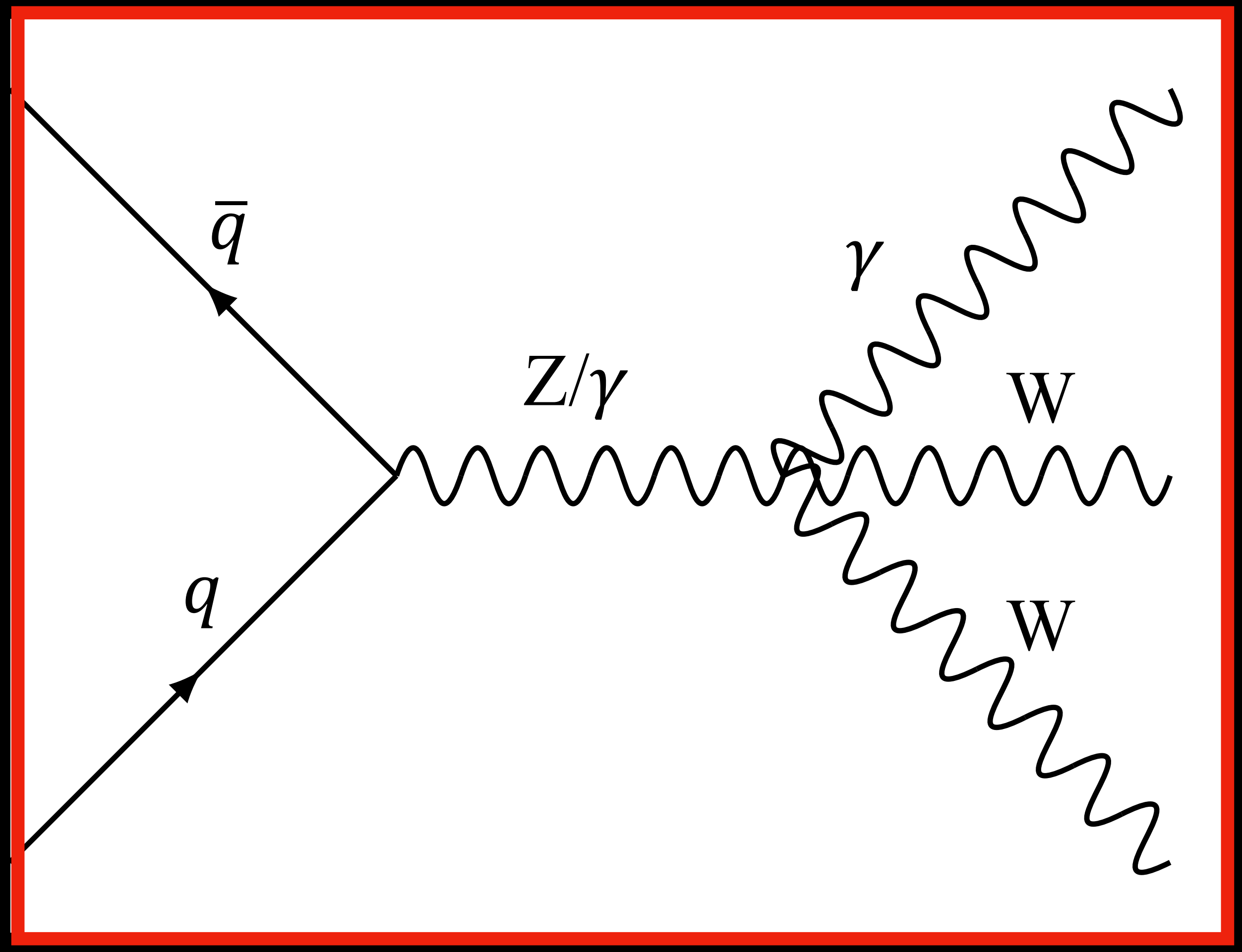

Quartic coupling

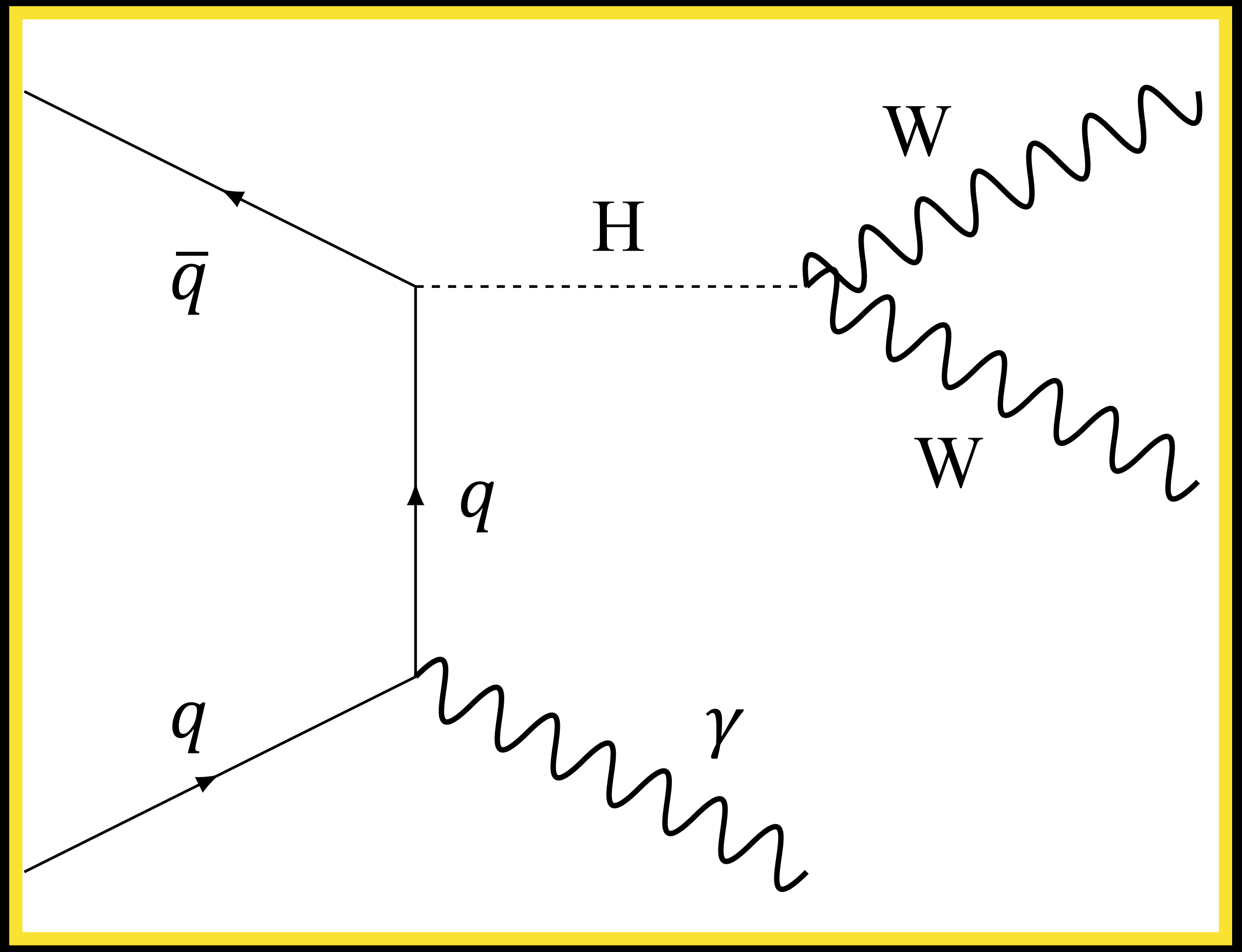

Associated production ($H\gamma$)

*The theoretical modeling uncertainties include the renormalization and factorization of QCD scales, PDFs, and parton shower modeling

Observation of $WW\gamma$ production at $\sqrt{s} = 13$ TeV

- $WW\gamma \rightarrow e^+\nu_e\mu^-\bar{\nu}_\mu\gamma$ or $\mu^+\nu_\mu e^-\bar{\nu}_e\gamma$ final state
- Events with b-jets vetoed
- Additional loose leptons vetoed
- Backgrounds suppressed by
  - $M_{\ell\ell} > 10$ GeV
  - $p_T^{\ell\ell} > 15$ GeV
  - $m_T^{WW} > 10$ GeV

$$m_T^{WW} = \sqrt{2p_T^{\ell\ell}\, p_T^{\text{miss}}[1 - \cos\Delta\phi(\overrightarrow{p_T}^{\ell\ell}, \overrightarrow{p_T}^{\text{miss}})]}$$

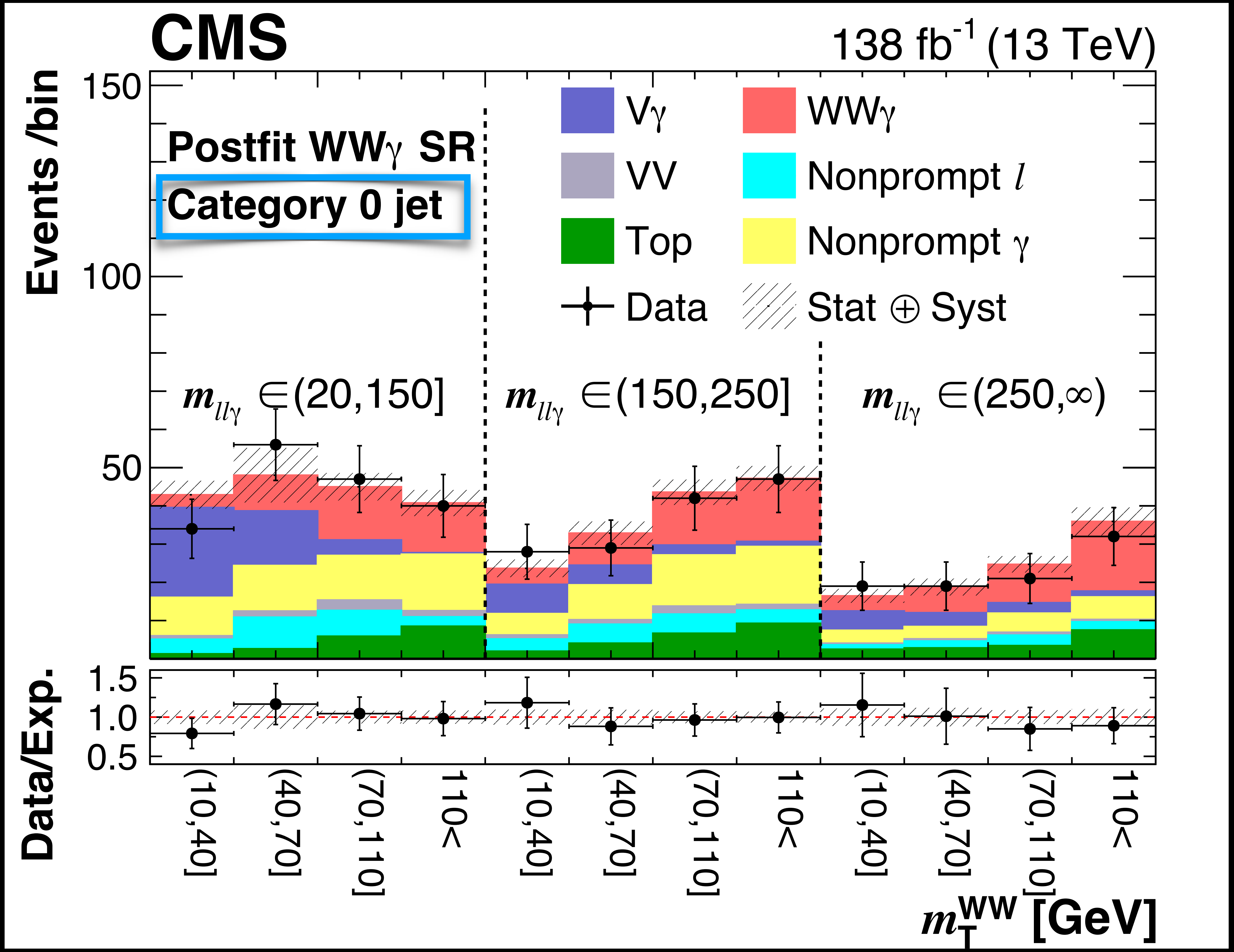

Signal extracted from a binned maximum likelihood fit using two dimensional distributions in m_T^{WW} and $m_{\ell\ell\gamma}$ (product of the Poisson probability mass functions for each bin forms the likelihood function)

Observation of $W\gamma\gamma$ production at $\sqrt{s} = 13$ TeV

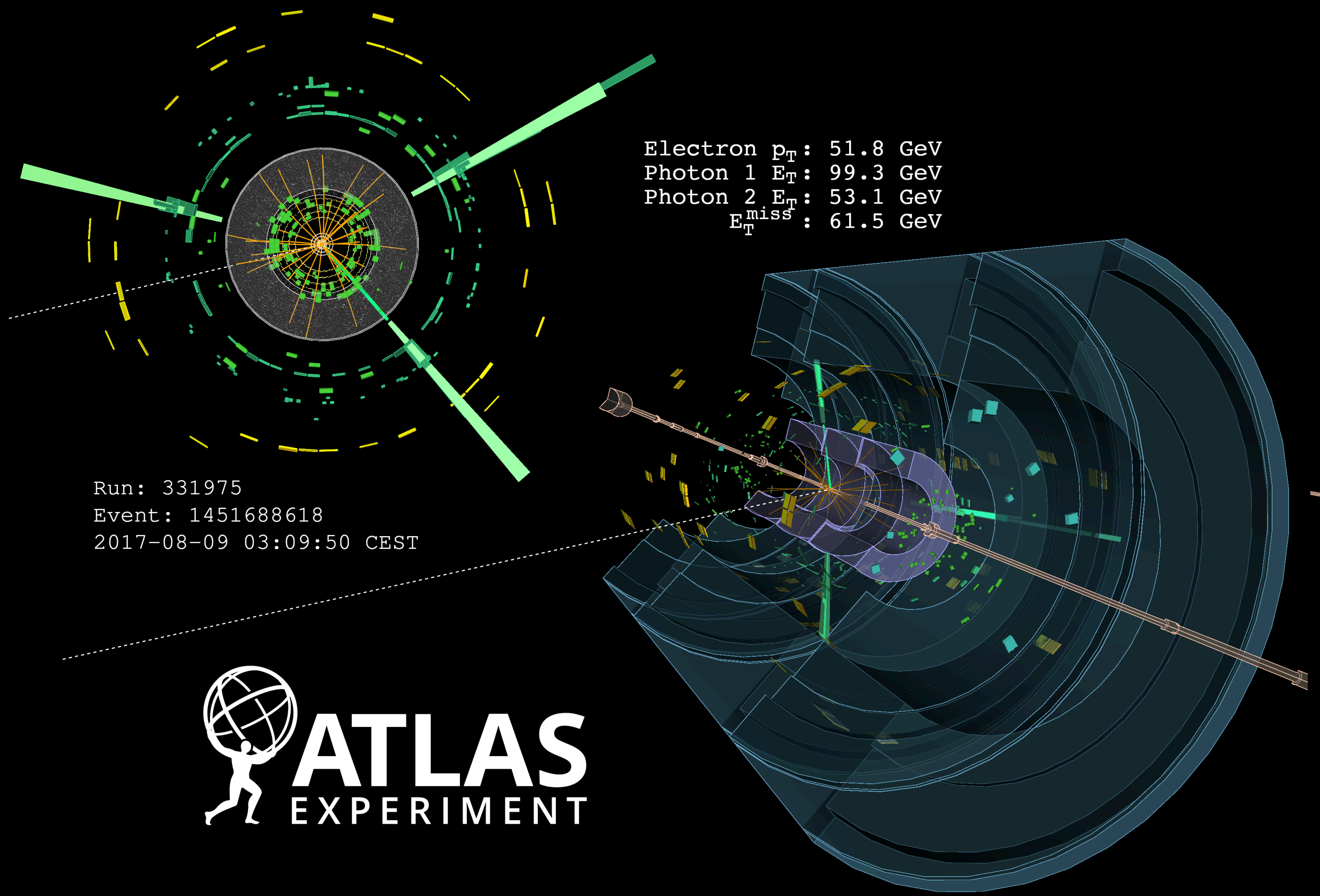

Final state with 2 photons and one electron

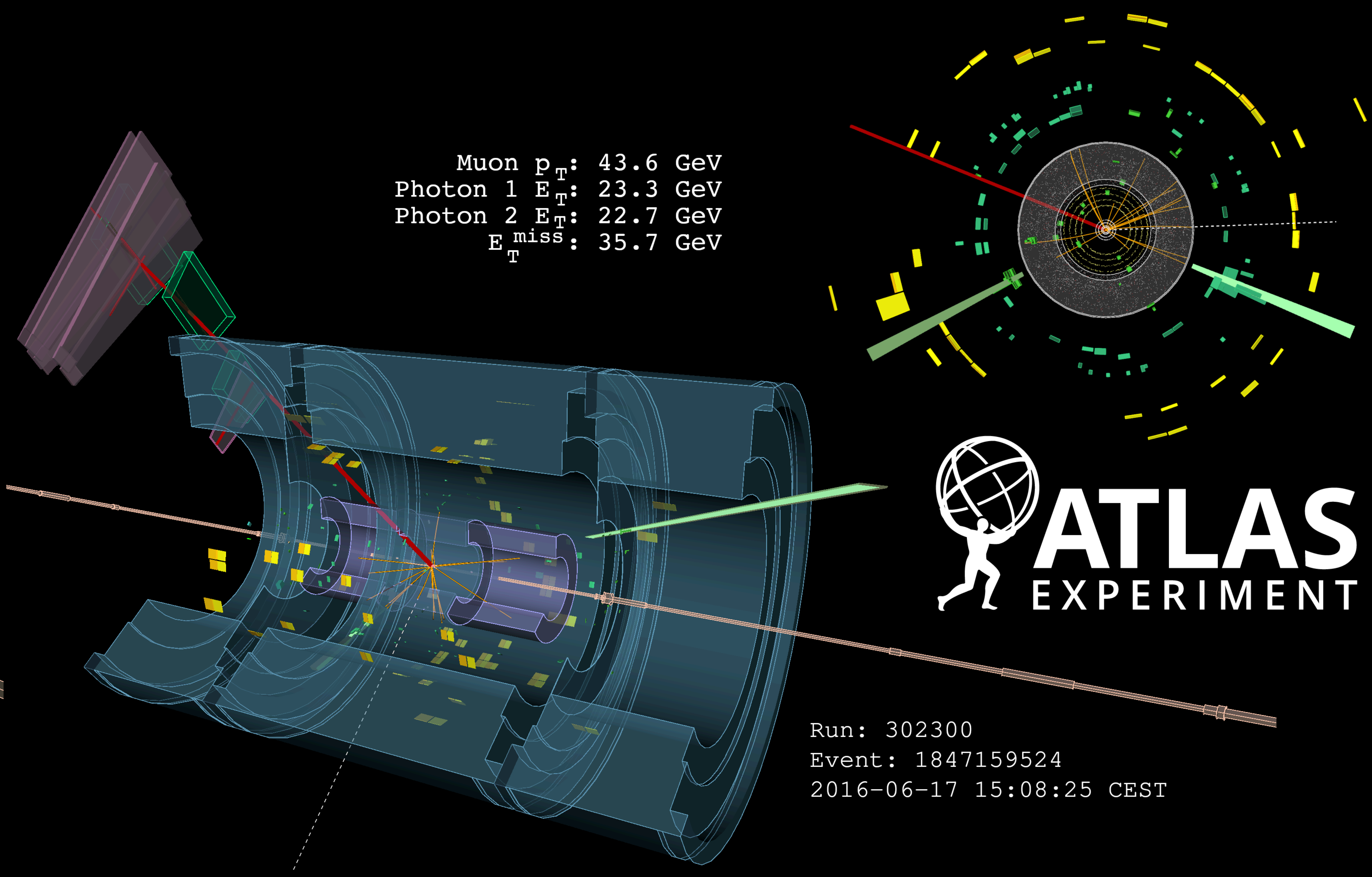

Final state with 2 photons and one muon

Observation of $W\gamma\gamma$ production at $\sqrt{s} = 13$ TeV

https://arxiv.org/abs/2308.03041

- $W\gamma\gamma$ observed with a significance of 5.6 σ
- Final state: $W \to \ell\nu$ ($\ell = e, \mu$)
- Fiducial cross section:
  - $\sigma_{\text{fid}} = 13.8 \pm 1.1\ (\text{stat.})^{+2.1}_{-2.0}\ (\text{syst.}) \pm 0.1\ (\text{lumi})$ fb
- Largest background from jets that fake a photon ($j \to \gamma$)

Source	SR	TopCR
$W\gamma\gamma$	410 ± 60	28 ± 5
Non-prompt $j \to \gamma$	420 ± 50	42 ± 20
Misidentified $e \to \gamma$	155 ± 11	120 ± 9
Multiboson ($WH(\gamma\gamma)$, $WW\gamma$, $Z\gamma\gamma$)	76 ± 13	5.2 ± 1.7
Non-prompt $j \to \ell$	35 ± 10	–
Top ($tt\gamma$, $tW\gamma$, $tq\gamma$)	30 ± 7	136 ± 32
Pileup	10 ± 5	–
Total	$1\,136 \pm 34$	332 ± 18
Data	$1\,136$	333

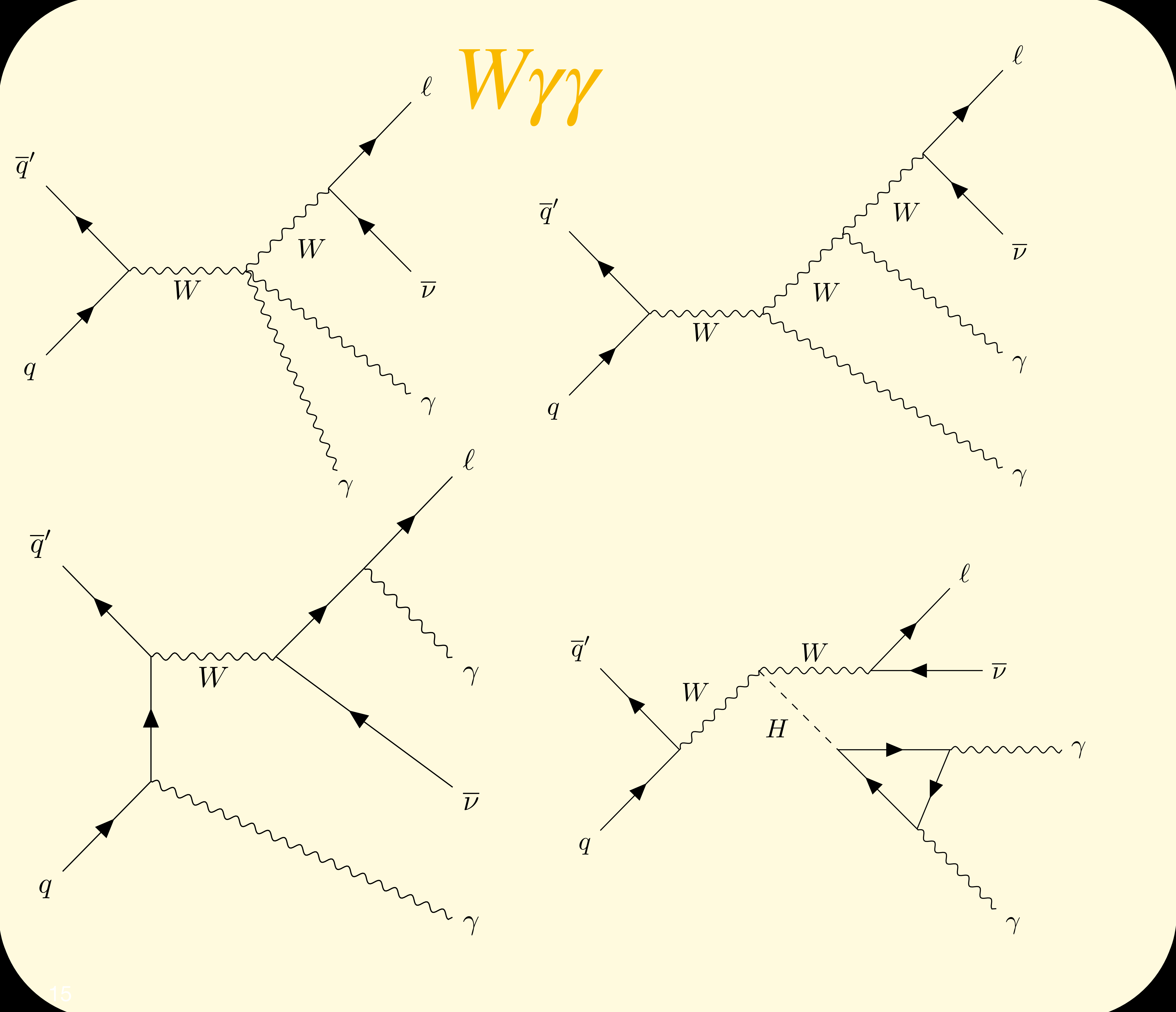

Observation of $W\gamma\gamma$ production at $\sqrt{s} = 13$ TeV

- Backgrounds estimated using data-driven methods
  - performing a two-dimensional template fit to the leading and sub-leading photon isolation distributions
- Largest uncertainty associated with $j \rightarrow \gamma$ background

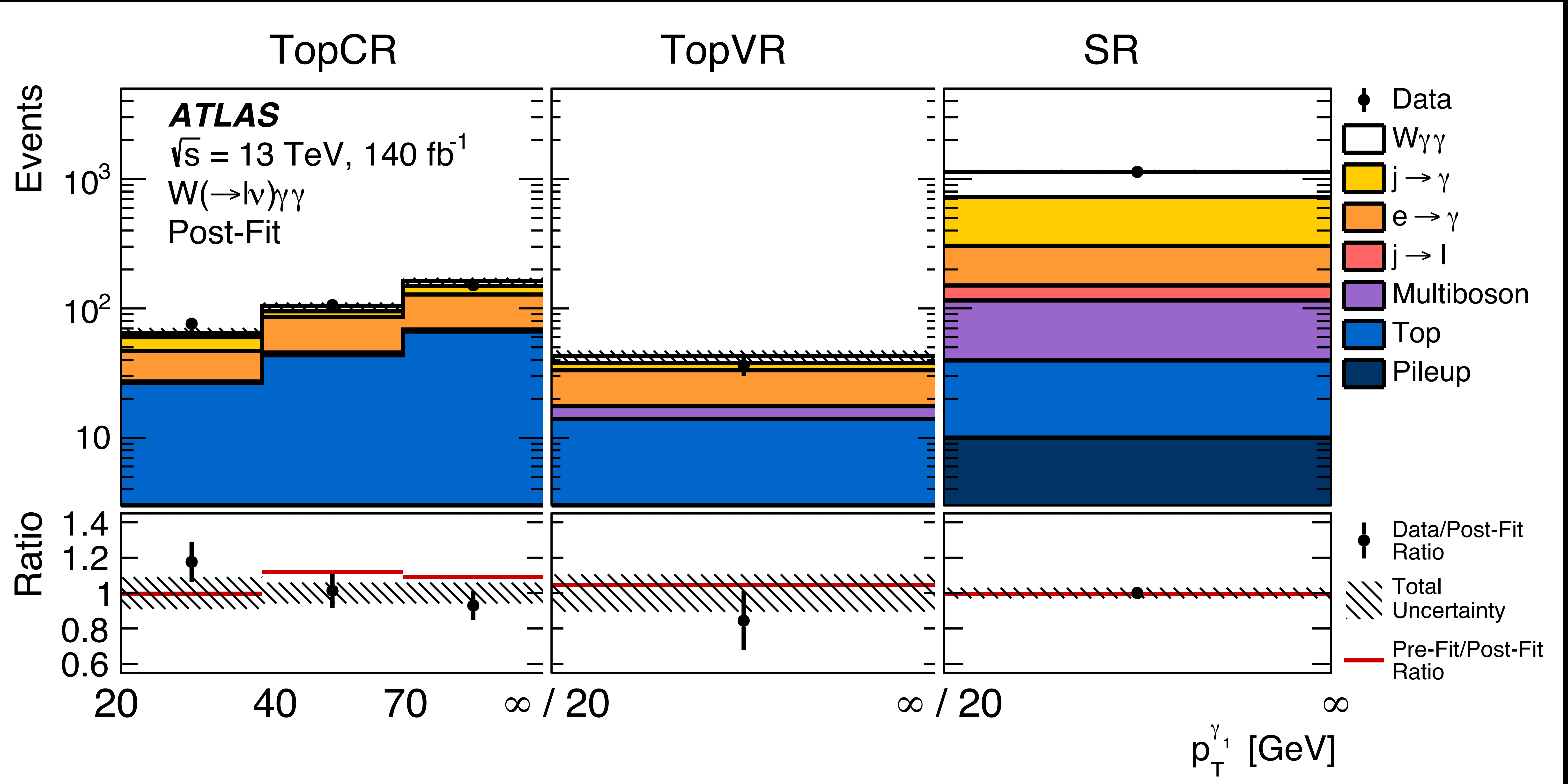

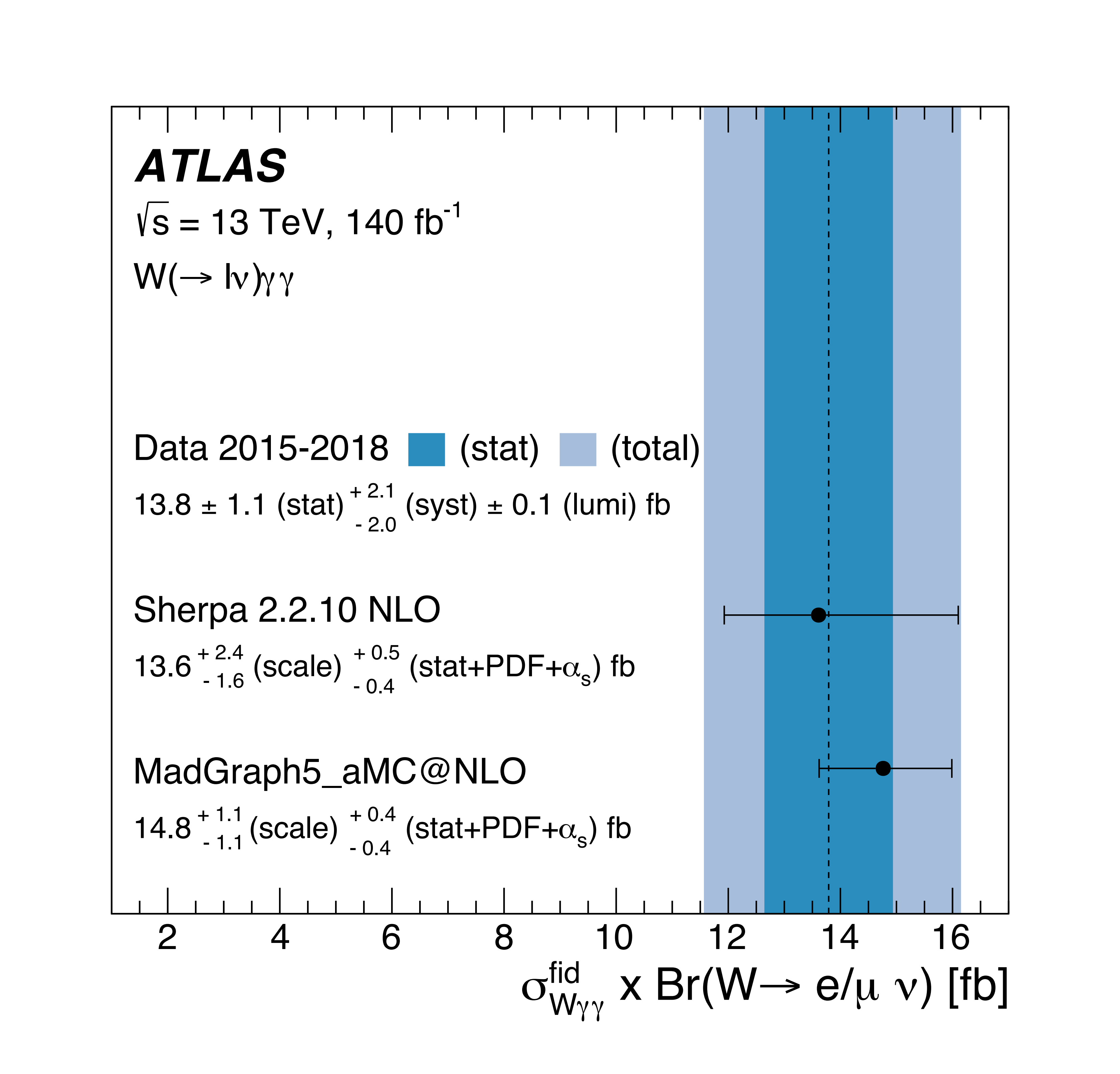

NLO electroweak corrections included

Dibosons

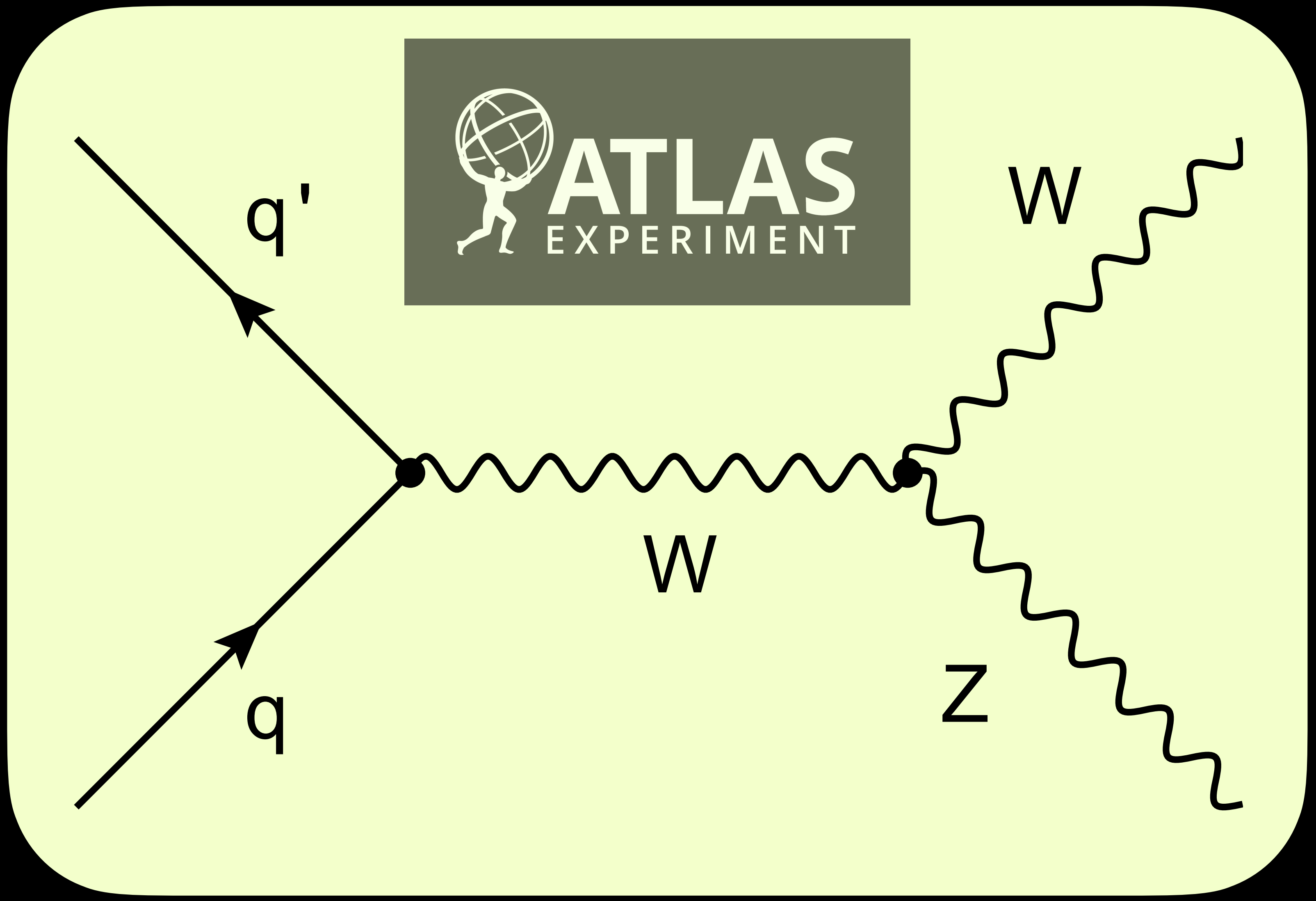
q'
ATLAS
EXPERIMENT
W
W
q
Z

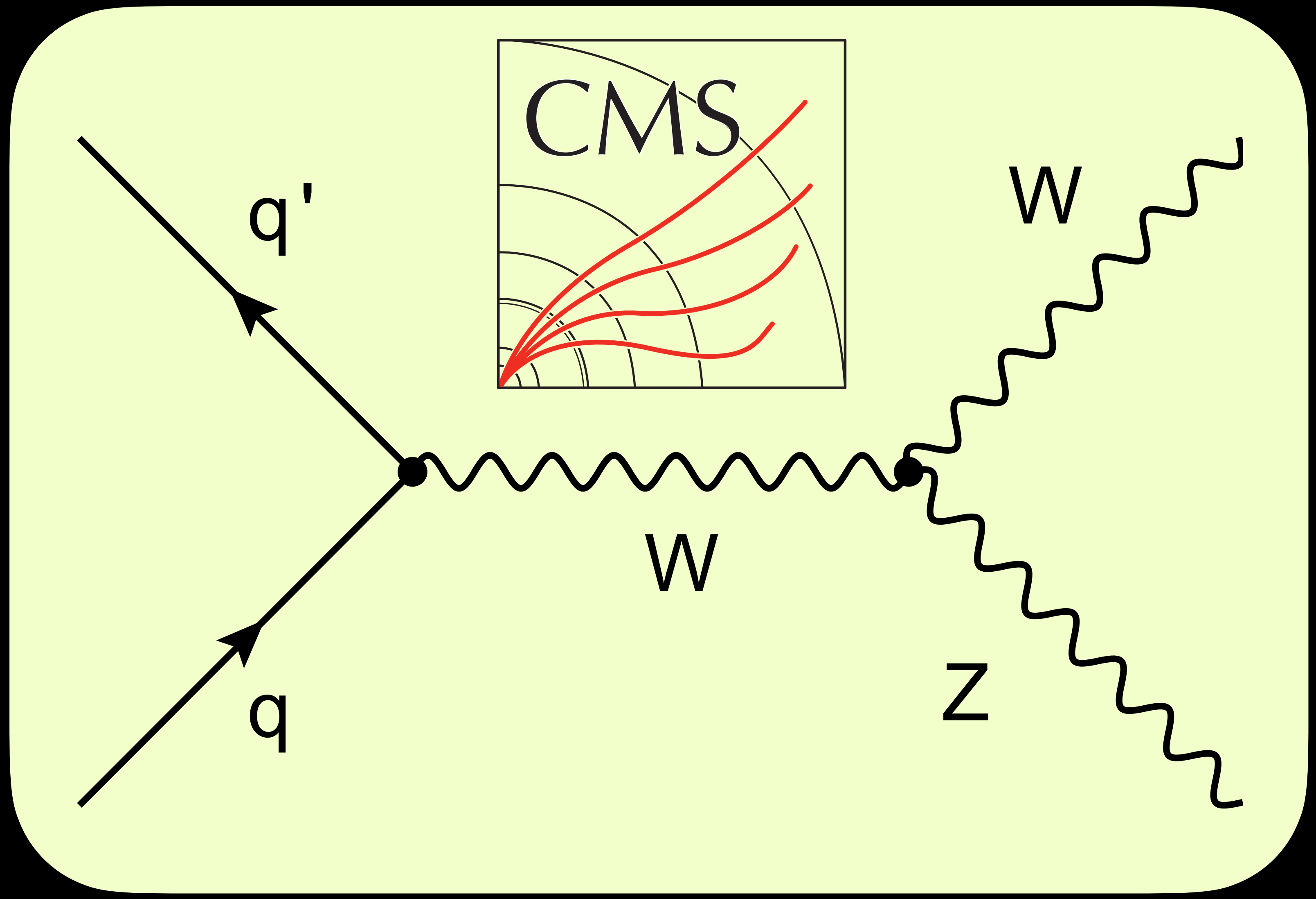
q'
CMS
W
W
q
Z

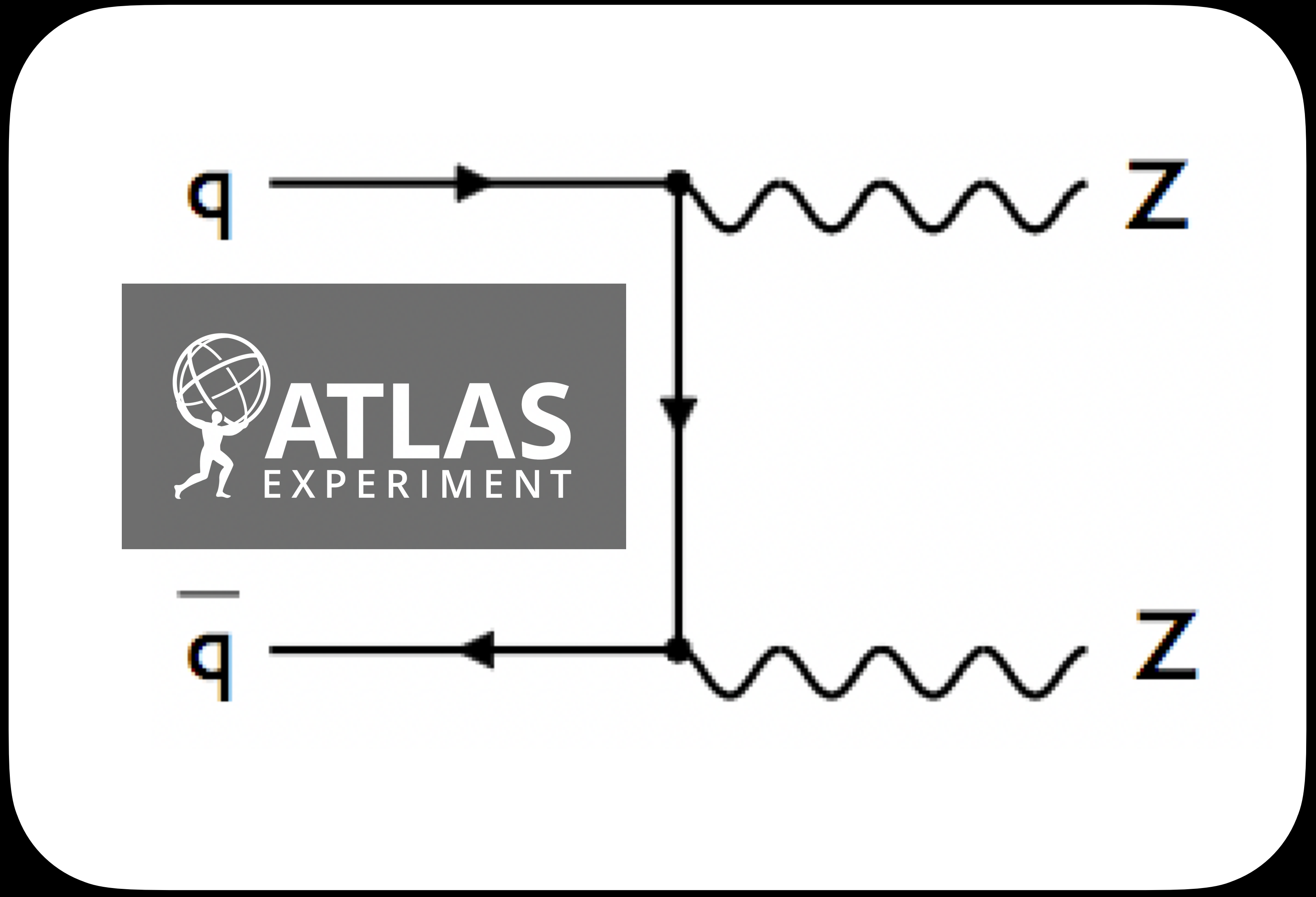
q
Z
ATLAS
EXPERIMENT
$\bar{q}$
Z

Why study polarization?

Studying the Higgs mechanism *Higgslessly*!

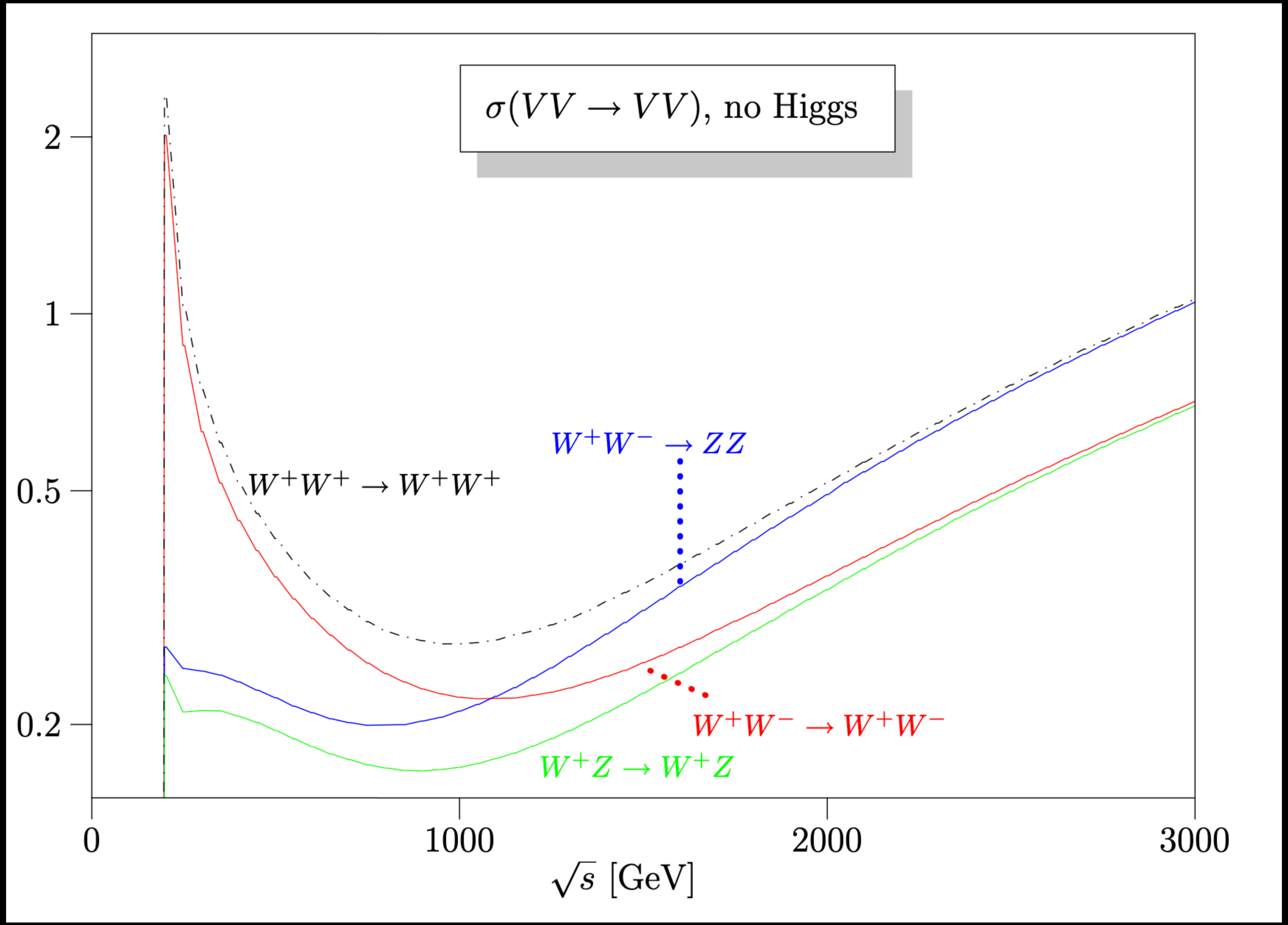

Study of different polarization states in diboson processes → sensitive probe of electroweak symmetry breaking

arXiv:0806.4145

ChatGPT

"However, it is important to note that the precise role of the Higgs boson in unitarizing WW scattering, in particular, is still an active area of research and there are ongoing studies to refine our understanding of this process."

Polarization is a frame-dependent measurement

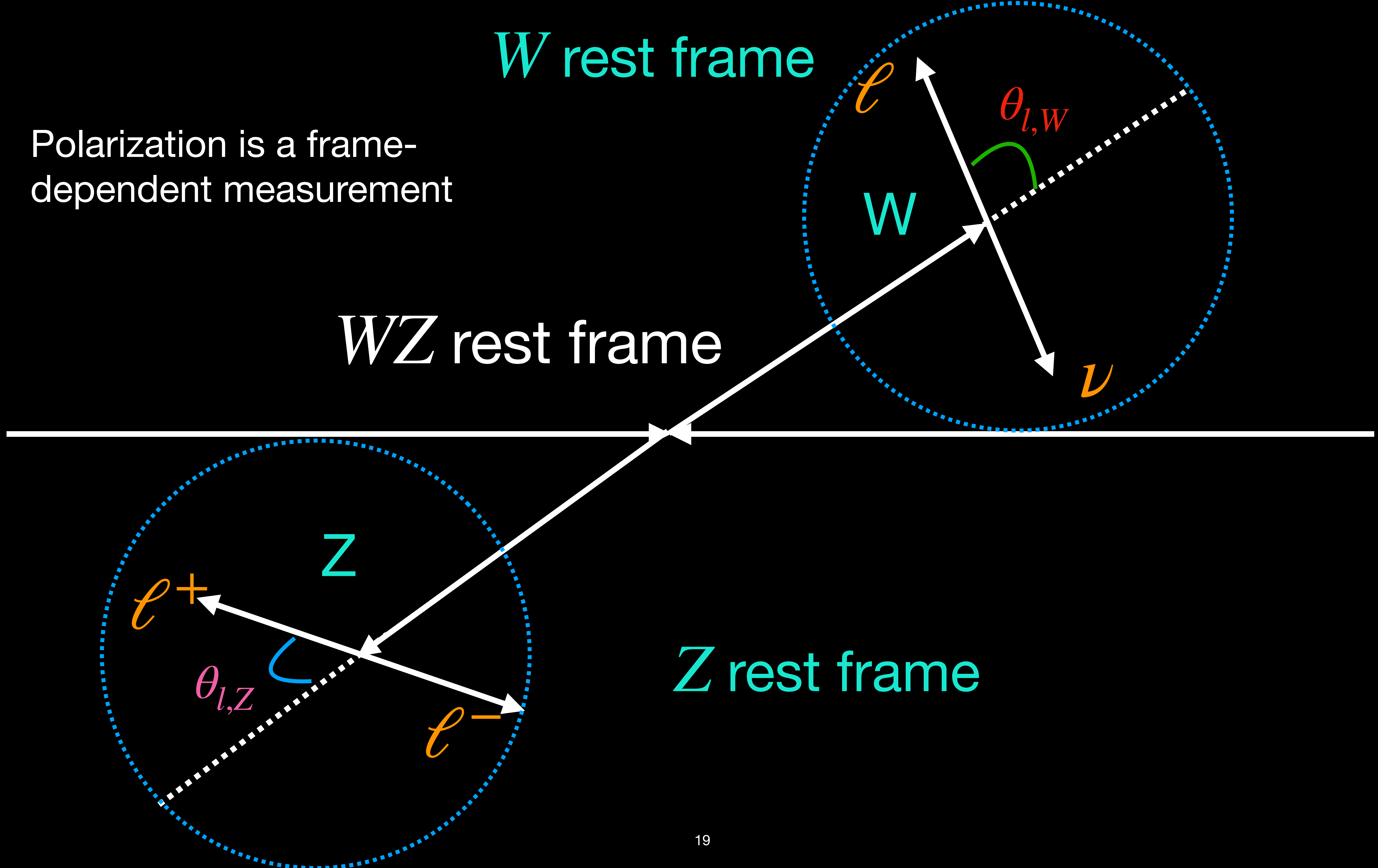

arXiv:2211.09435

Joint polarization measurement in WZ process

- Helicity fractions are frame dependent
- Joint polarization state:
  - f_{00} (f_{TT}) both bosons longitudinally (transversely) polarized
  - f_{0T} (f_{T0}): $W(Z)$ boson is longitudinally polarized, $Z(W)$ is transversely polarized
- Joint helicity fractions measured:
  - f_{00}: 7.1 σ, f_{0T}: 3.4 σ, f_{T0}: 7.1 σ, f_{TT}: 11 σ

	Data	Powheg+Pythia	NLO QCD
		$W^{\pm}Z$	
f_{00}	0.067 ± 0.010	0.0590 ± 0.0009	0.058 ± 0.002
f_{0T}	0.110 ± 0.029	0.1515 ± 0.0017	0.159 ± 0.003
f_{T0}	0.179 ± 0.023	0.1465 ± 0.0017	0.149 ± 0.003
f_{TT}	0.644 ± 0.032	0.6431 ± 0.0021	0.628 ± 0.004
		$W^{+}Z$	
f_{00}	0.072 ± 0.016	0.0583 ± 0.0012	0.057 ± 0.002
f_{0T}	0.119 ± 0.034	0.1484 ± 0.0022	0.155 ± 0.003
f_{T0}	0.152 ± 0.033	0.1461 ± 0.0022	0.147 ± 0.003
f_{TT}	0.66 ± 0.04	0.6472 ± 0.0026	0.635 ± 0.004
		$W^{-}Z$	
f_{00}	0.063 ± 0.016	0.0600 ± 0.0014	0.059 ± 0.002
f_{0T}	0.11 ± 0.04	0.1560 ± 0.0027	0.166 ± 0.003
f_{T0}	0.21 ± 0.04	0.1470 ± 0.0027	0.152 ± 0.003
f_{TT}	0.62 ± 0.05	0.6370 ± 0.0033	0.618 ± 0.004

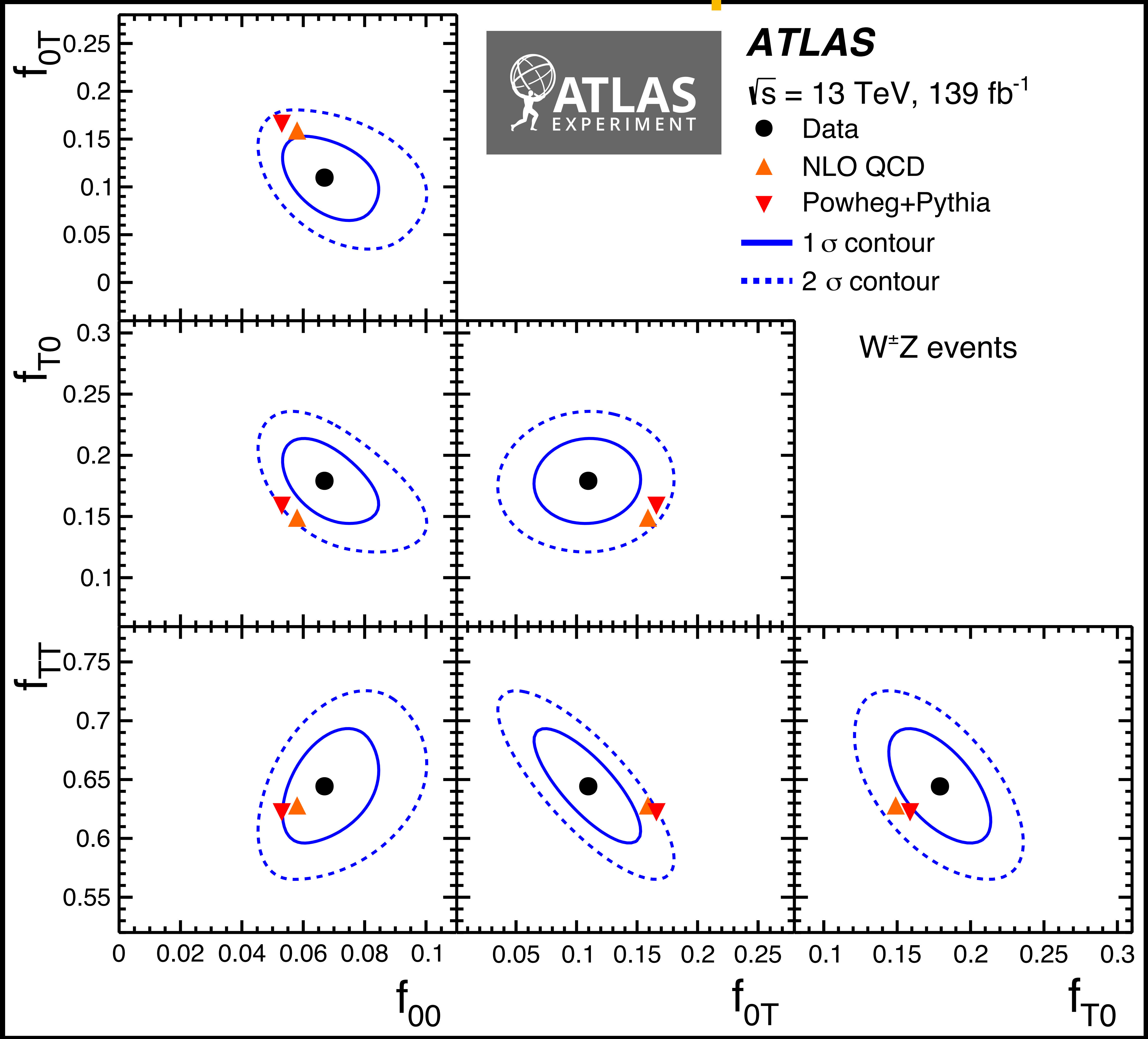

$$\rho_{\lambda_W \lambda_W' \lambda_Z \lambda_Z'} \equiv \frac{1}{C_{norm}} \times \sum_{\mu_q \mu_{\bar{q}}} F^{(\mu_q \mu_{\bar{q}})}_{\lambda_W \lambda_Z} F^{(\mu_q \mu_{\bar{q}})\,*}_{\lambda_W' \lambda_Z'}$$

Complete 9X9 matrix hard to determine, focus on 4 linear combinations arXiv:2211.09435

Joint polarization measurement in WZ process

- Frame defined as:
  - Decay angles in the $W^{\pm}/Z$ rest frame relative to the $W^{\pm}/Z$ direction in the $W^{\pm}/Z$ center-of-mass frame
- Deep Neural Network (DNN) trained with several kinematic variables: transverse momenta of the three leptons and the neutrino and angular variables ($\Delta\phi(\ell^{W},\nu), \Delta\phi(\ell_1^{Z},\ell_2^{Z}), p_T^{WZ}$)
- DNN classifier trained: components of the vector output, one for each joint-polarization state, combined in single output node at last layer
- Four categories defined to disentangle mixed helicity states (0T and T0)
  - $|\cos\theta^*_{\ell W}| < 0.5, |\cos\theta^*_{\ell Z}| < 0.5$
  - $|\cos\theta^*_{\ell W}| > 0.5, |\cos\theta^*_{\ell Z}| < 0.5$
  - $|\cos\theta^*_{\ell W}| < 0.5, |\cos\theta^*_{\ell Z}| > 0.5$
  - $|\cos\theta^*_{\ell W}| > 0.5, |\cos\theta^*_{\ell Z}| > 0.5$

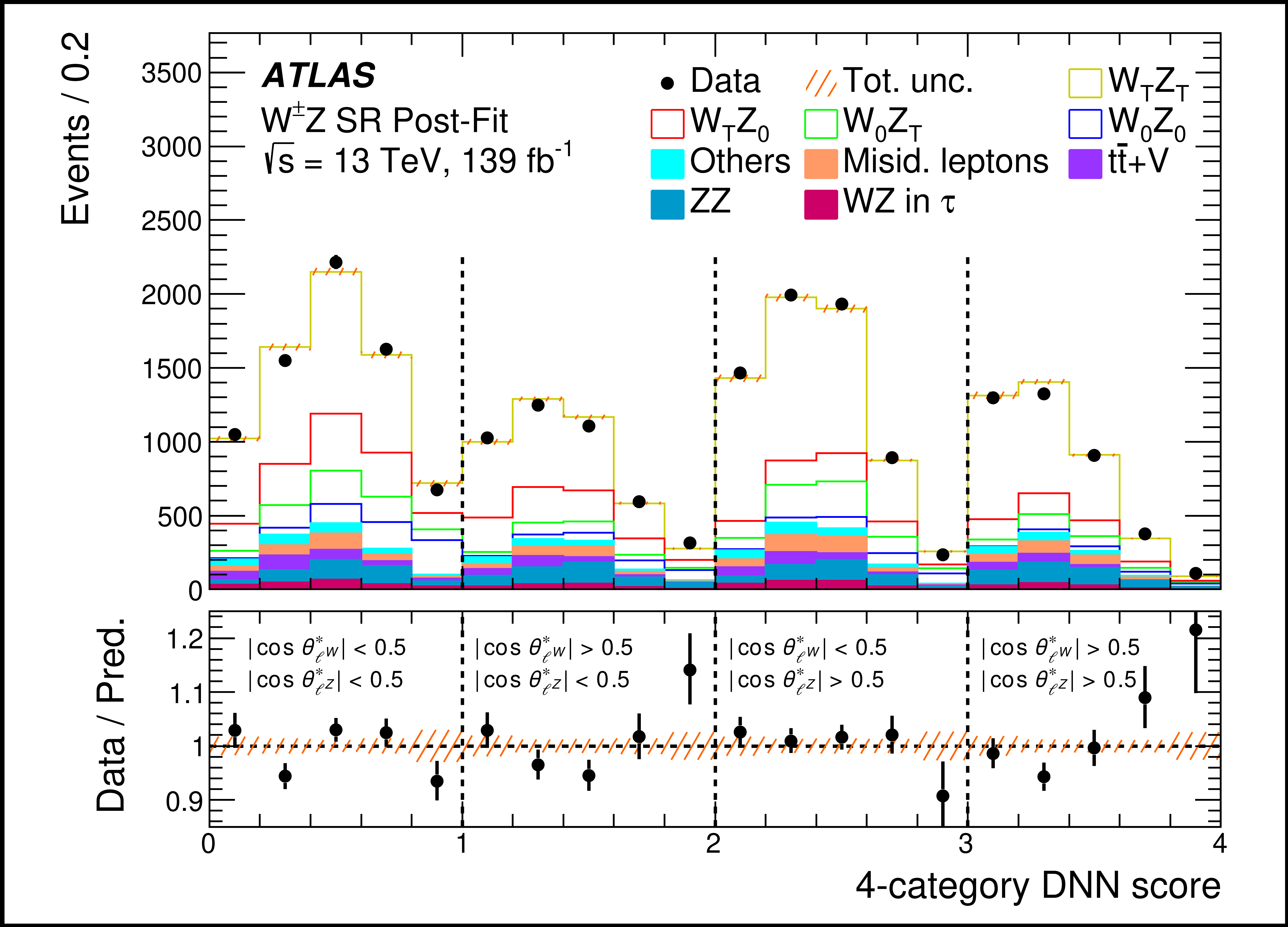

https://arxiv.org/abs/2402.16365

Polarization measurement in WZ (high p_T^Z)

- Boosted decision tree trained to measure polarization fractions (7 variables):
  - New: measurement of fractions in high p_T^Z regime and low p_T^{WZ}
    - Leads to an improvement of 20-30% in f_{00}

ATLAS EXPERIMENT

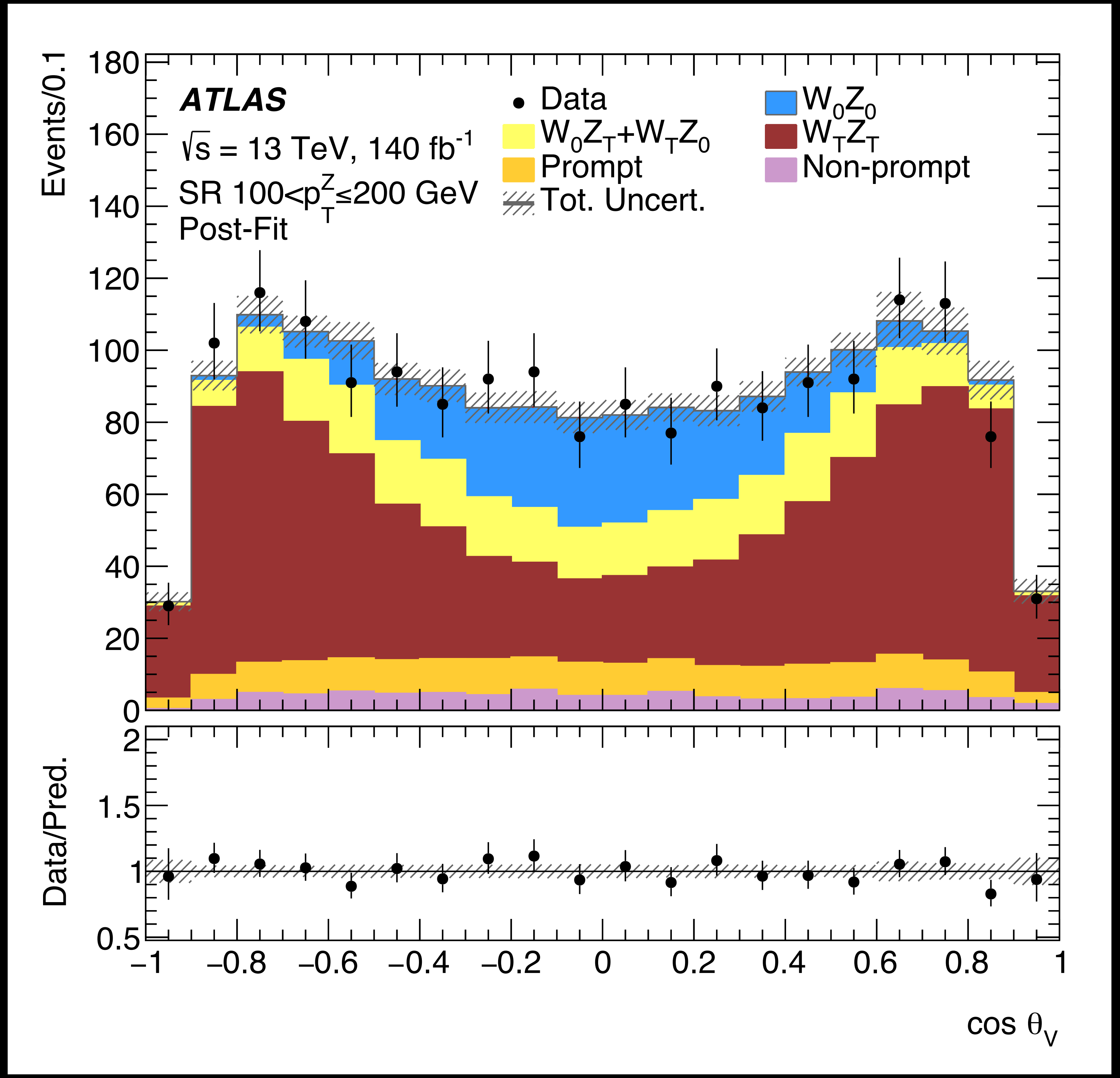

θ_V : scattering angle of the W boson in the WZ rest frame with respect to the z-axis

	Measurement		Prediction		
	$100 < p_T^Z \leq 200$ GeV	$p_T^Z > 200$ GeV		$100 < p_T^Z \leq 200$ GeV	$p_T^Z > 200$ GeV
f_{00}	$0.19\ ^{+0.03}_{-0.03}$ (stat) $^{+0.02}_{-0.02}$ (syst)	$0.13\ ^{+0.09}_{-0.08}$ (stat) $^{+0.02}_{-0.02}$ (syst)	f_{00}	0.152 ± 0.006	0.234 ± 0.007
f_{0T+T0}	$0.18\ ^{+0.07}_{-0.08}$ (stat) $^{+0.05}_{-0.06}$ (syst)	$0.23\ ^{+0.17}_{-0.18}$ (stat) $^{+0.06}_{-0.10}$ (syst)	f_{0T}	0.120 ± 0.002	0.062 ± 0.002
f_{TT}	$0.63\ ^{+0.05}_{-0.05}$ (stat) $^{+0.04}_{-0.04}$ (syst)	$0.64\ ^{+0.12}_{-0.12}$ (stat) $^{+0.06}_{-0.06}$ (syst)	f_{T0}	0.109 ± 0.001	0.058 ± 0.001
f_{00} obs (exp) sig.	5.2 (4.3) σ	1.6 (2.5) σ	f_{TT}	0.619 ± 0.007	0.646 ± 0.008

Fraction of events where both bosons are longitudinally polarized measured with an observed significance of 5.2 σ (1.6 σ) in the phase space: $100 < p_T^Z < 200$ GeV ($p_T^Z > 200$ GeV)

https://arxiv.org/abs/2402.16365

Radiation Amplitude Zero effect in WZ at 13 TeV

ATLAS EXPERIMENT

- Dominant helicity amplitude with two transversely-polarized bosons exactly zero
  - when scattering angle of the W boson in the WZ rest frame (w.r.t the incoming antiquark direction) approaches 90^0 → Radiation Amplitude Zero (RAZ)
  - arises from the gauge structure in the SM
- RAZ ⇒ drop at 0 in the $\Delta Y(WZ)$ (rapidity difference between W and Z bosons) and $\Delta Y(l_W Z)$ (rapidity difference between lepton from W decay and Z boson) distributions
- First observation of RAZ effect in WZ production, seen in $W\gamma$ previously (SMP-20-005), longitudinally polarized $W's$ make observation challenging
- Next-to-leading order (NLO) QCD correction dilute the effect, hadronic activity reduced by placing stringent requirement on p_T^{WZ}

https://arxiv.org/abs/2402.16365

Radiation Amplitude Zero effect in WZ at 13 TeV

Unfolded distributions

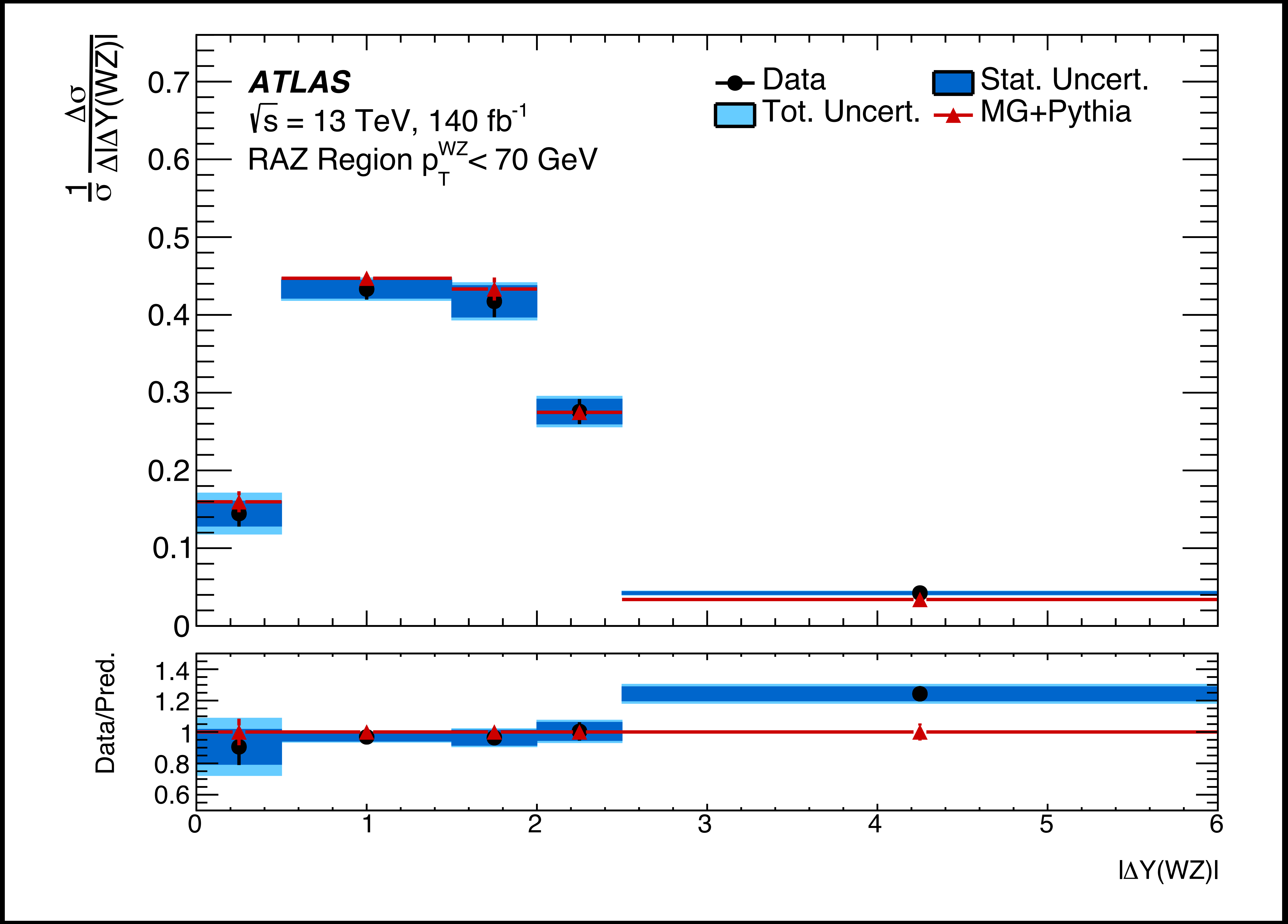

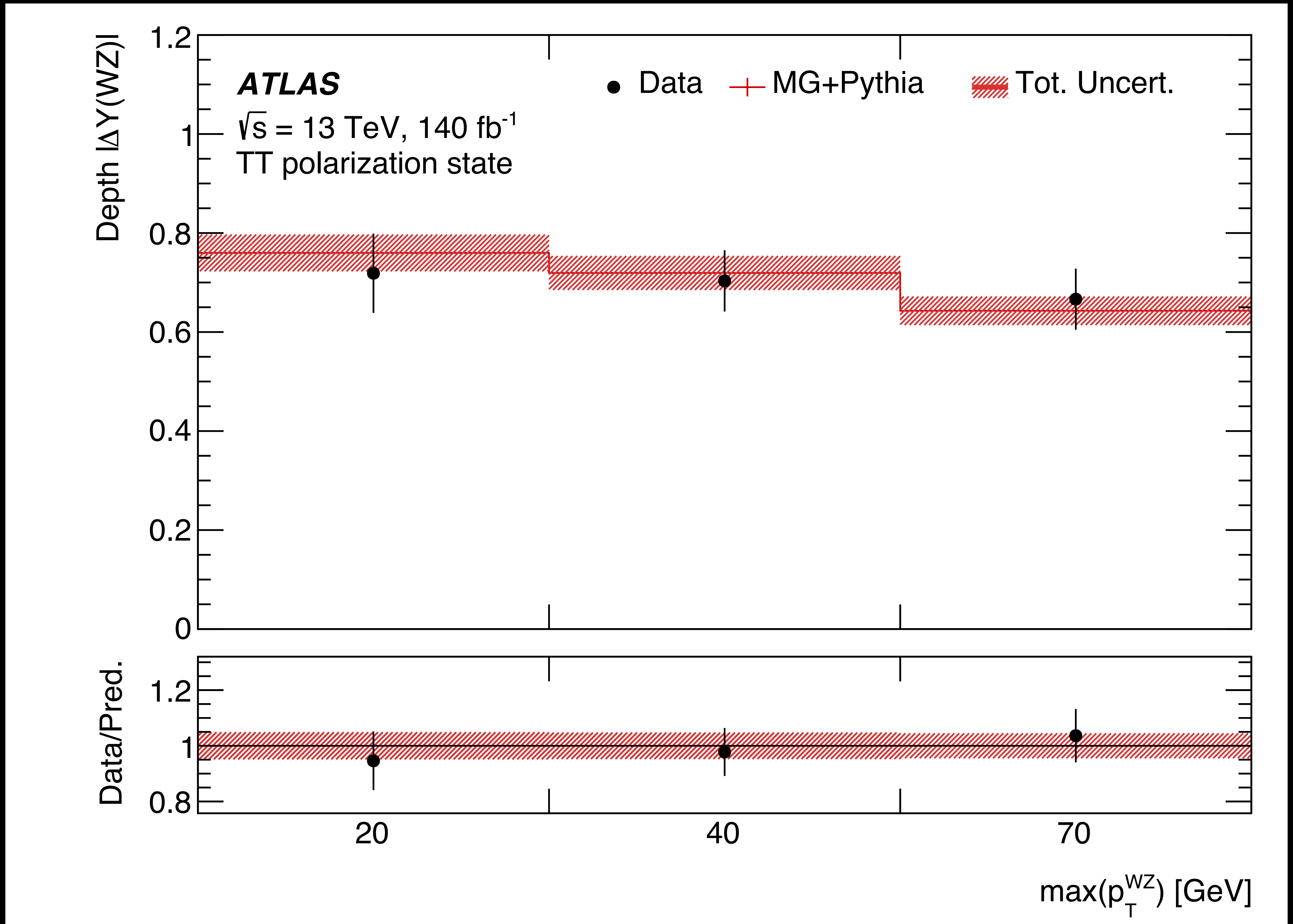

Effect expected for only transversely polarized bosons, all other polarization components are subtracted

Depth of the RAZ dip defined as

$$\mathscr{D} = 1 - 2 \times \left(\frac{N(|\Delta Y(WZ)| < 0.5)}{N(0.5 < |\Delta Y(\ell_W Z)| < 1.5)} \right), +\mathscr{D} \Rightarrow \text{dip}$$

JHEP 07 (2022) 032, https://cds.cern.ch/record/2905015

Measurement of the WZ process

- Electroweak process: sensitive to the PDFs of u and d quarks; relatively unaffected by the gluon
- High WZ cross section makes it the dominant process that can be studied in the trilepton final state
- Ratio of $\frac{W^{+}Z}{W^{-}Z}$ cross section is one of the most precisely measurable quantities
- Measured at several center-of-mass energies

13 TeV

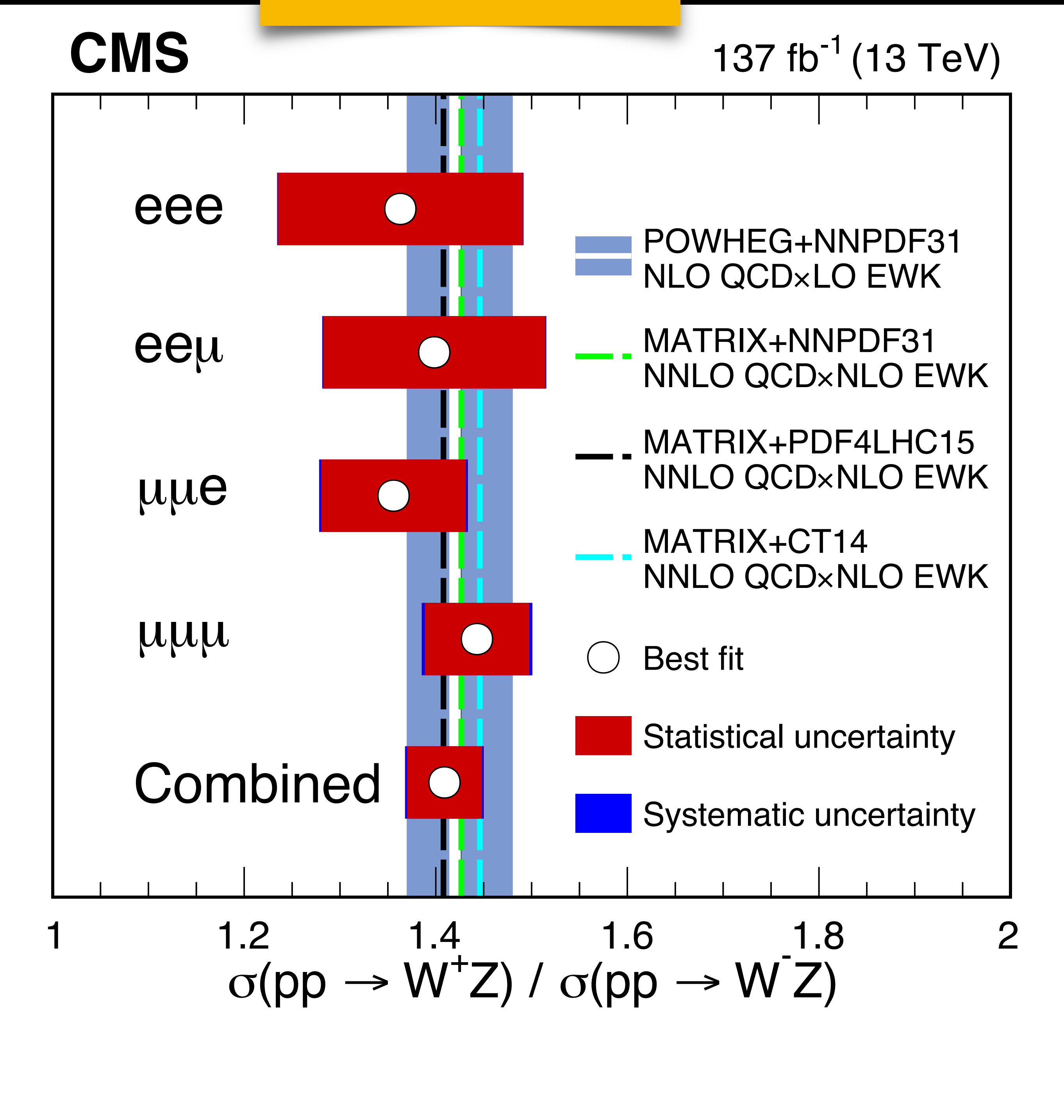

13.6 TeV

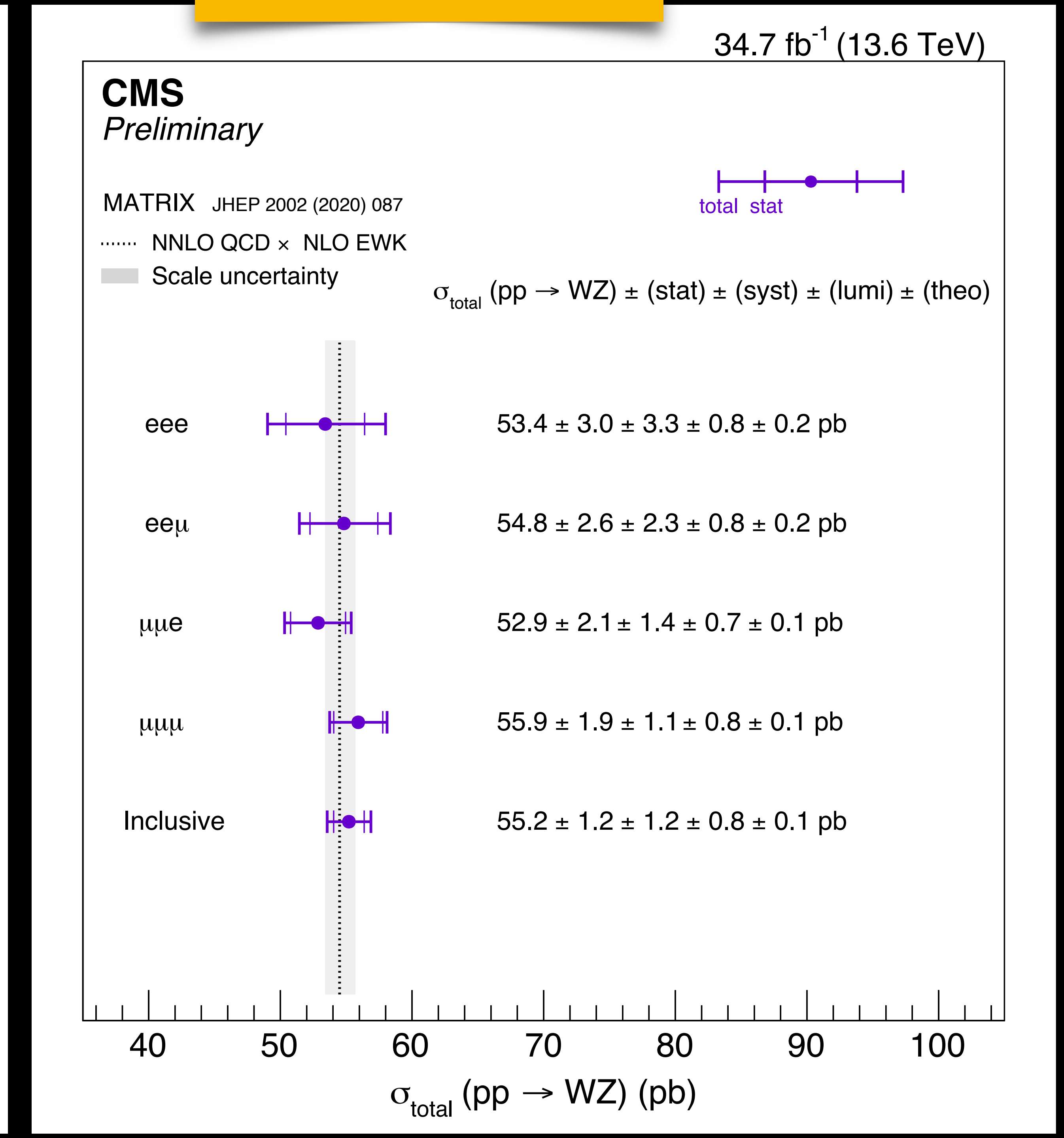

13 TeV

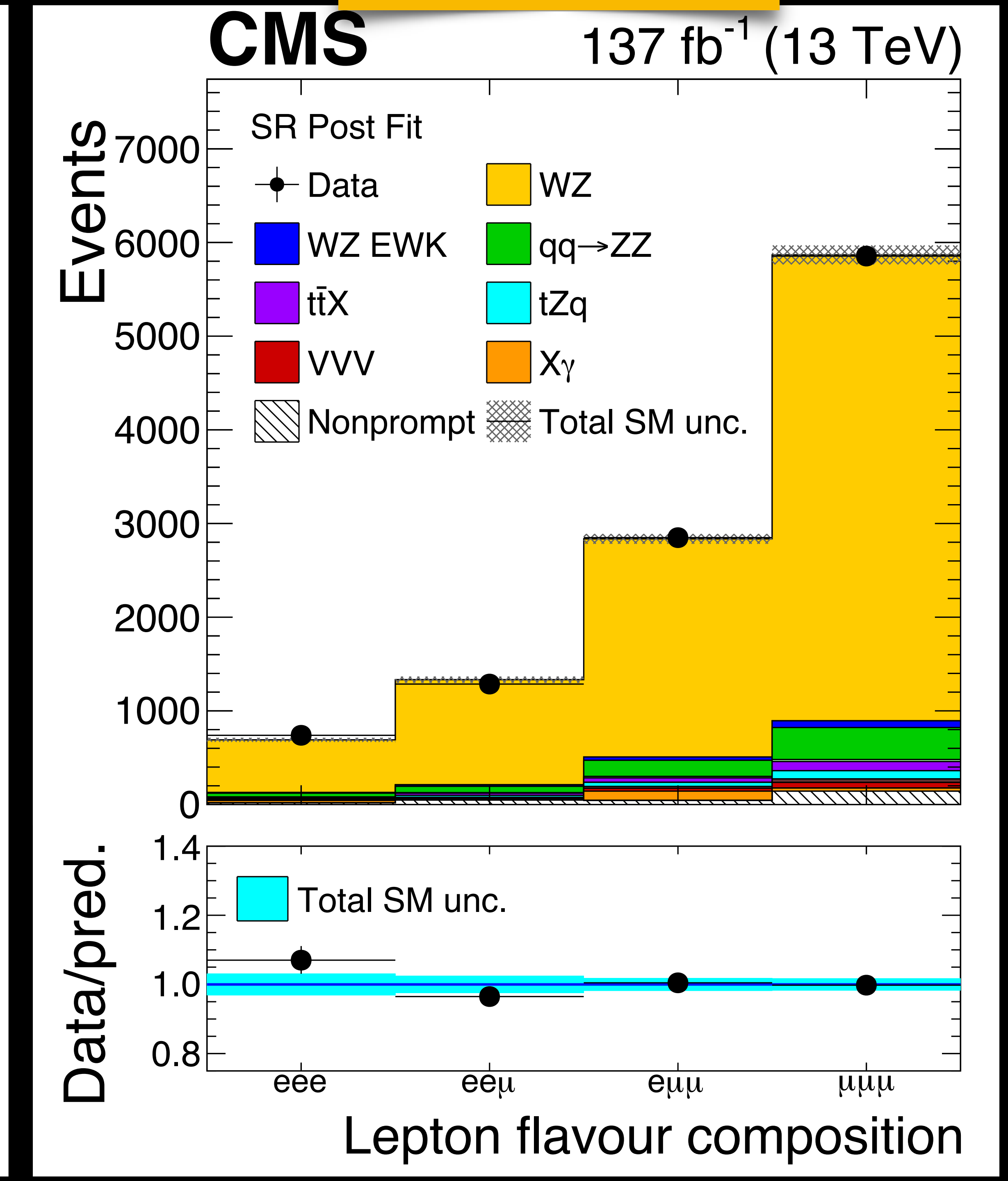

13 TeV

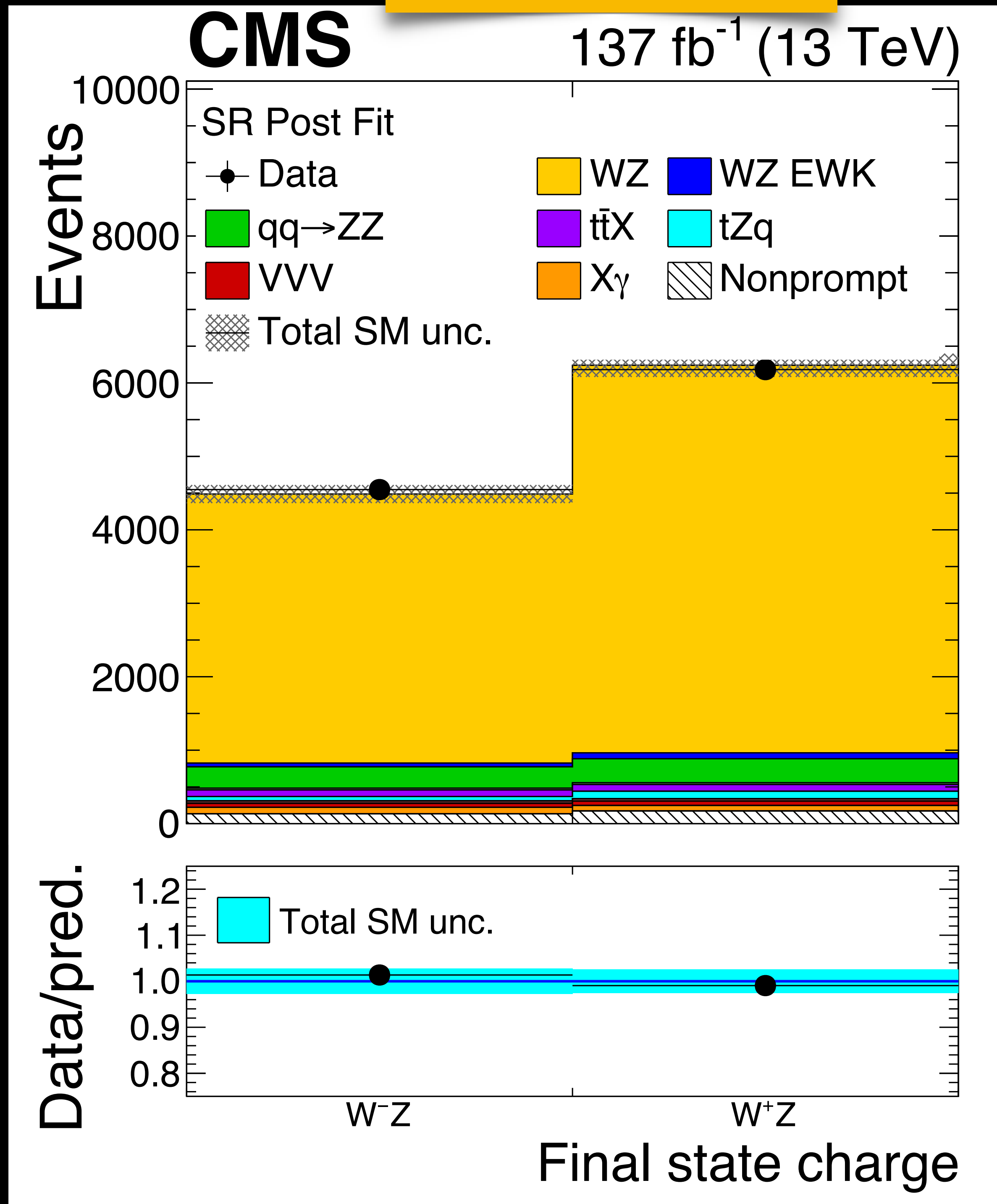

Measuring the W polarization in WZ processes

- Single boson spin density matrix derived from joint spin density matrix
  - Individual helicity fractions: f_0 (longitudinal), f_L and f_R (left and right handed transverse helicity states)
- θ^W: angular distance between the momenta of the W boson and the charged lepton from its primary decay

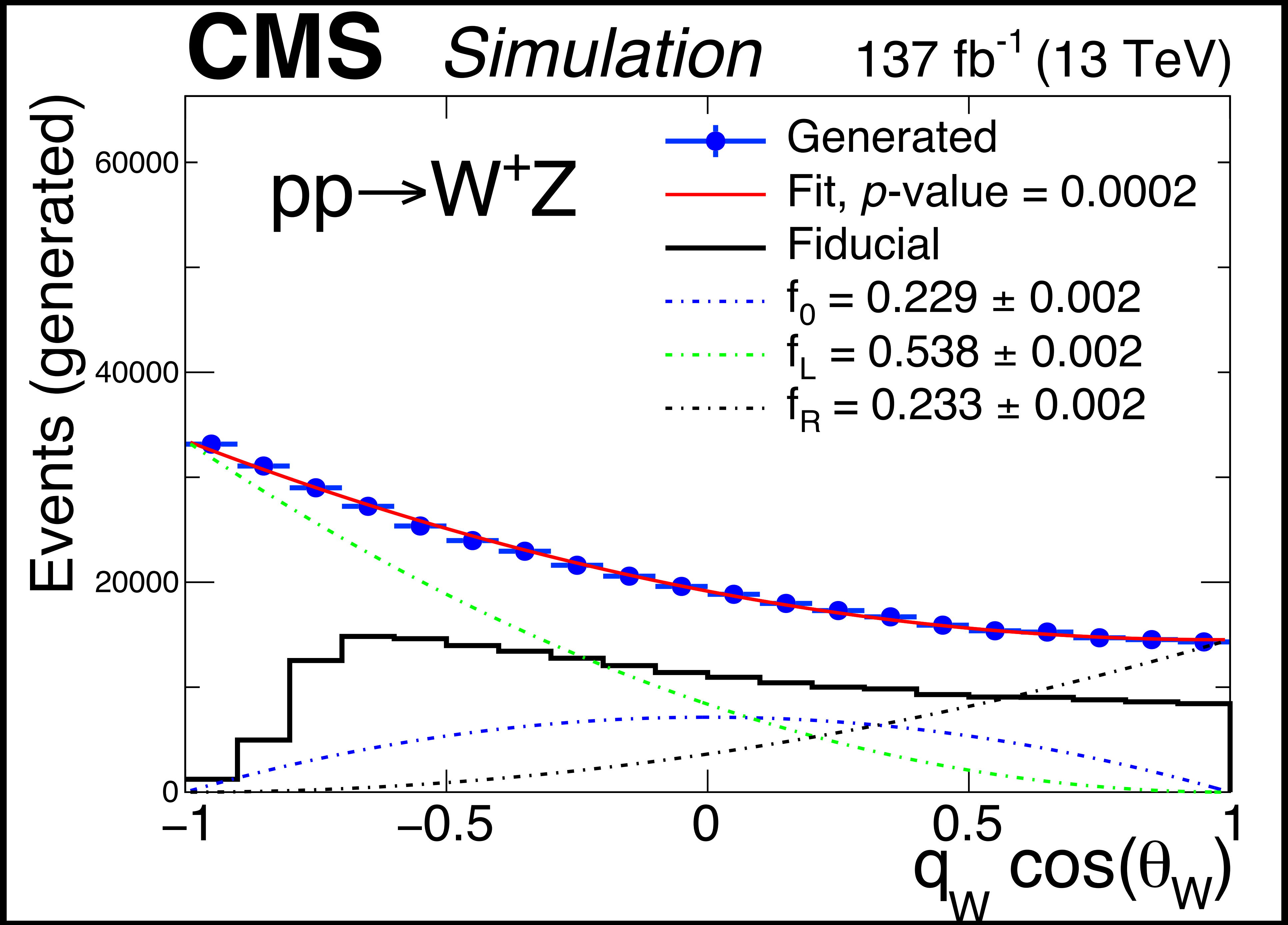

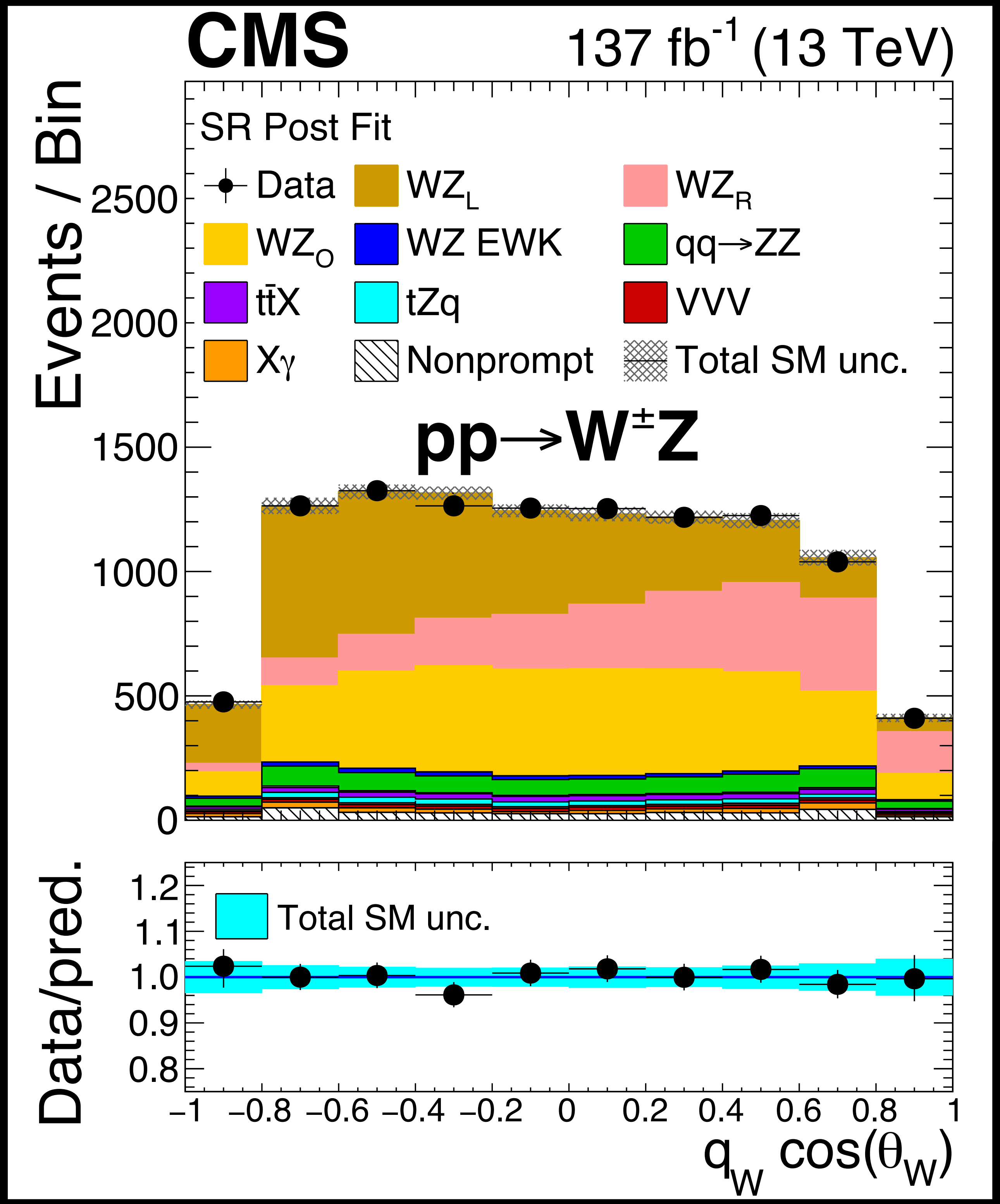

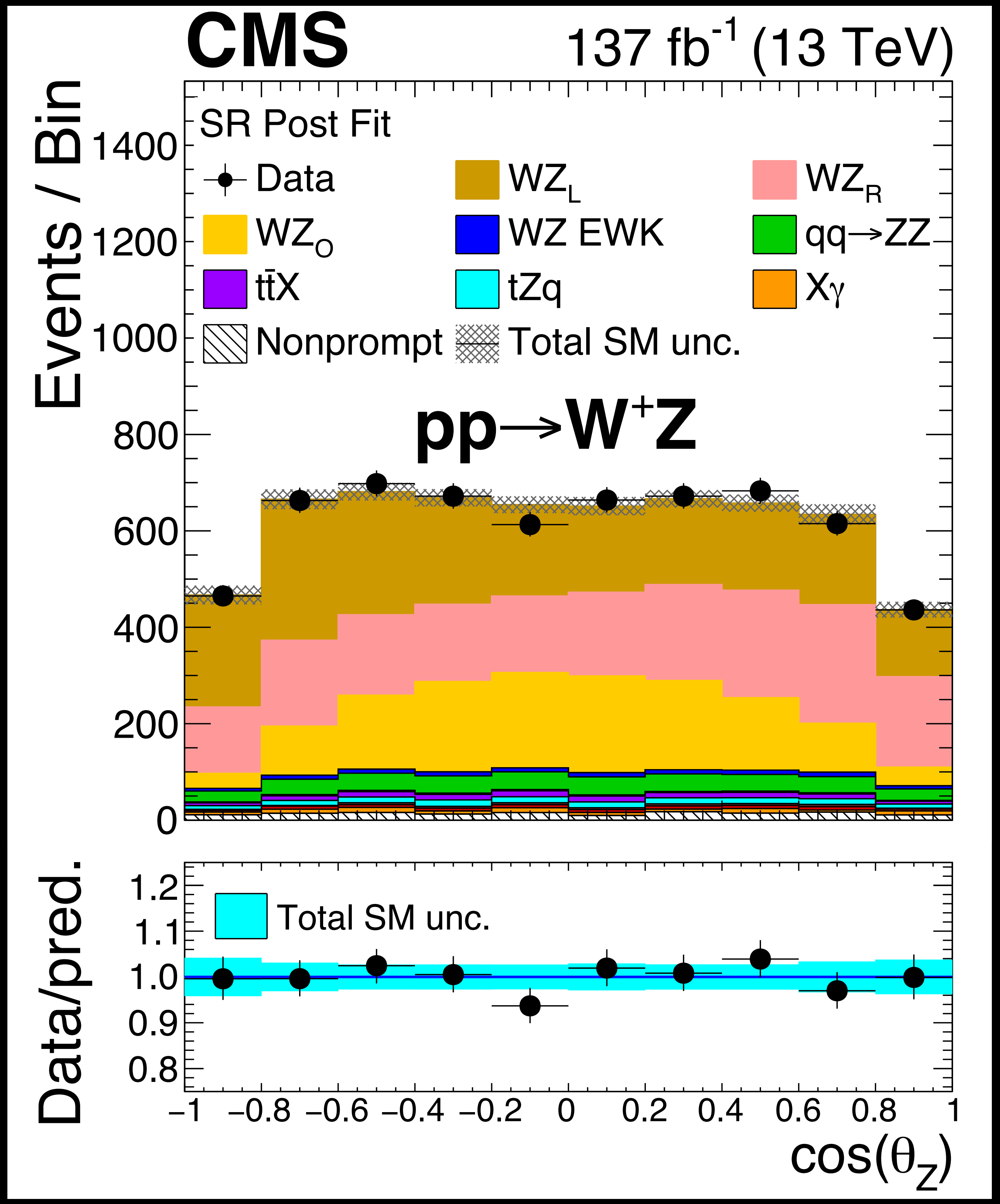

Measuring the Z_L polarization in $ZZ \rightarrow 4\ell$ process

https://arxiv.org/pdf/2310.04350

- Study of polarization in $ZZ \rightarrow 4\ell$
  - Require 2 Z-candidates
- Maximize sensitivity to Z_L by constructing BDT
- Reweighting for:
  - each polarization state (separately for $gg \rightarrow ZZ, q\bar{q} \rightarrow ZZ$)
  - interference effect between polarization states
  - higher order calculations

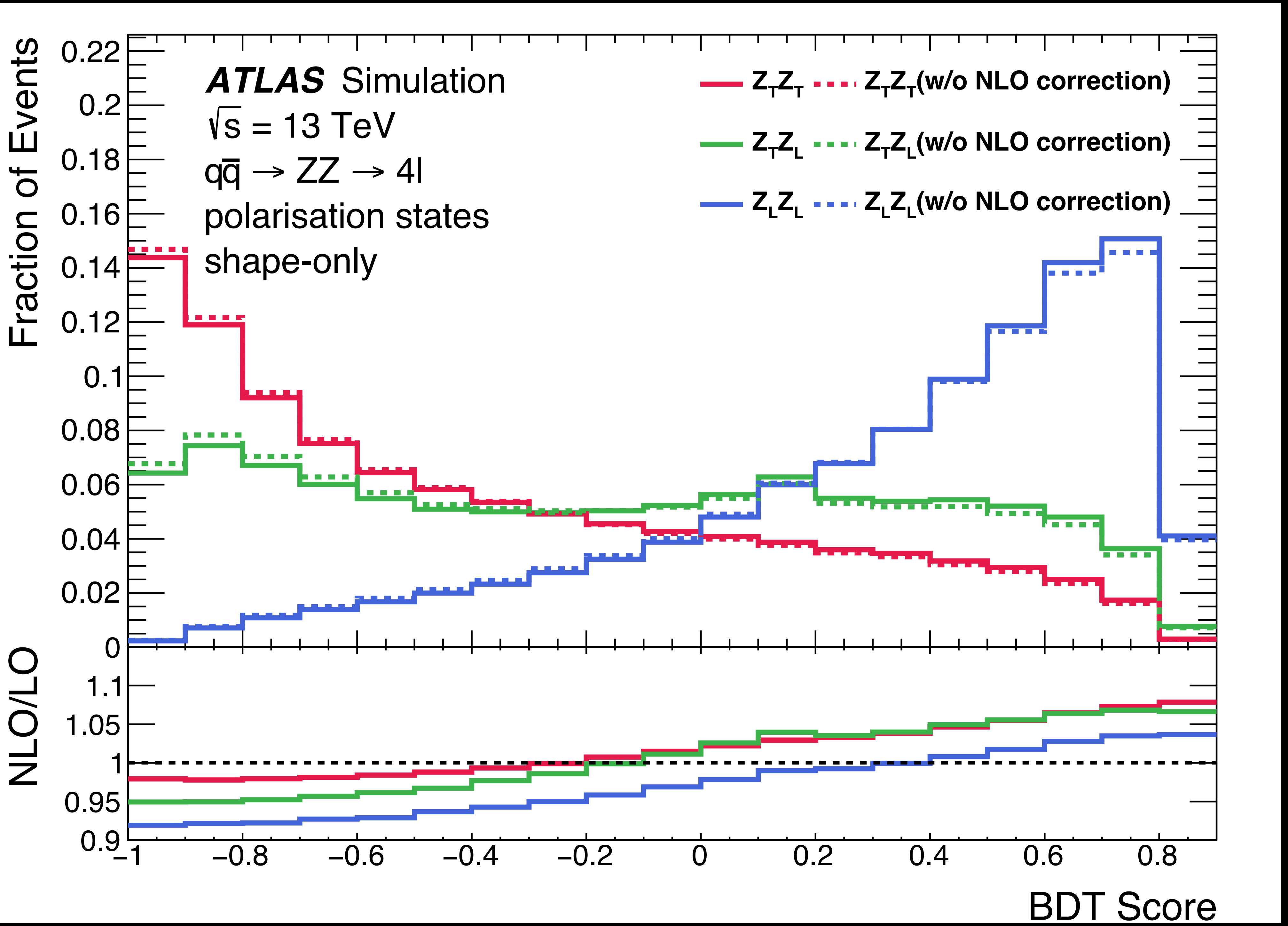

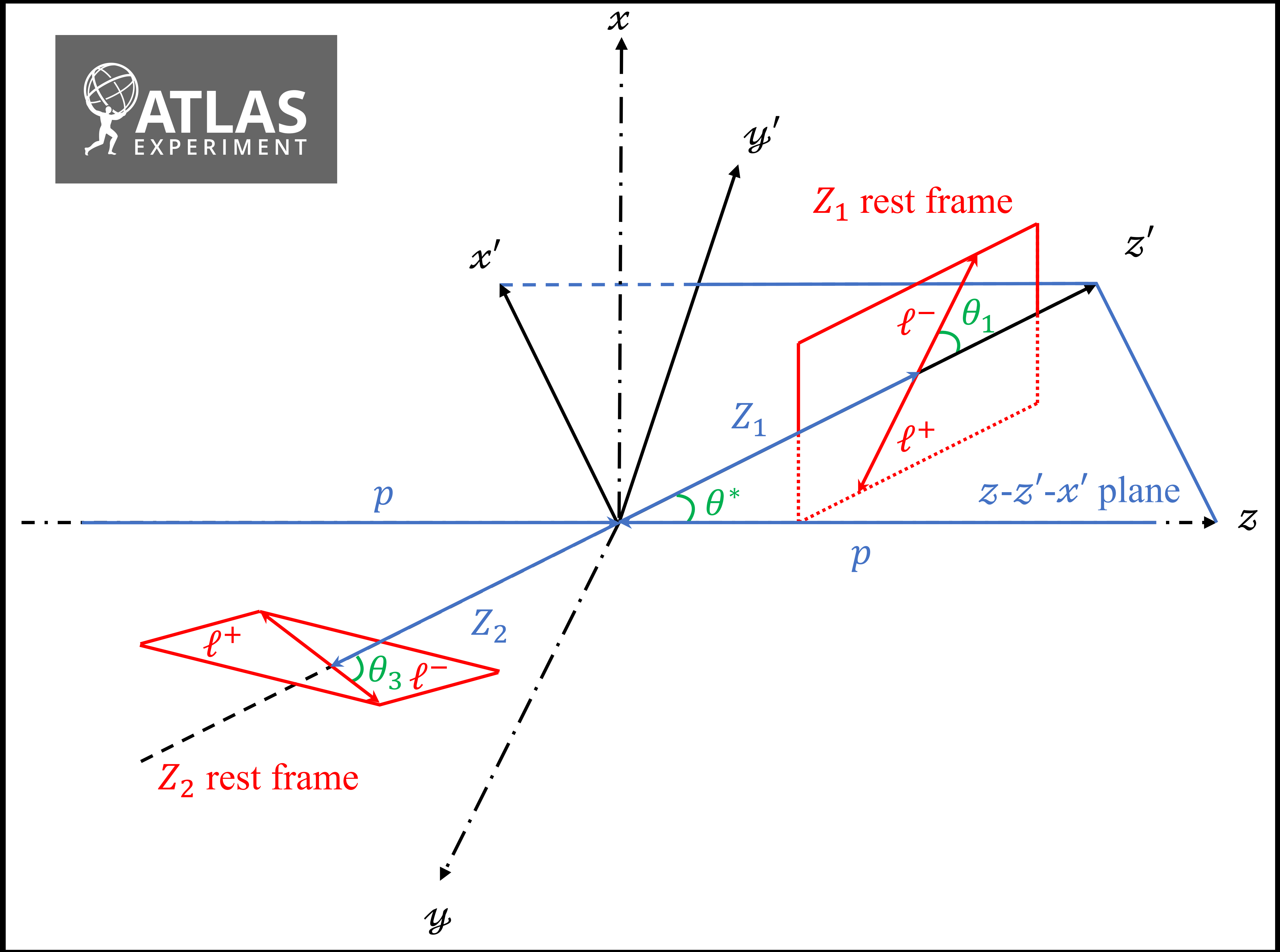

- Variables sensitive to polarization
- CP sensitive variables defined as the direction of motion of the Z_1 boson in the in the four-lepton rest frame

Measuring the Z_L polarization in $ZZ \to 4\ell$ processes

- $Z_L Z_L$ measured with 4.3 σ
- Analysis statistically limited, highest source of systematic uncertainty from $q\bar{q} \to ZZ$ interference modeling
- Clean final state with background contributions from Z+jets and $t\bar{t}$ events (non-prompt sources), background uncertainties have high statistical component

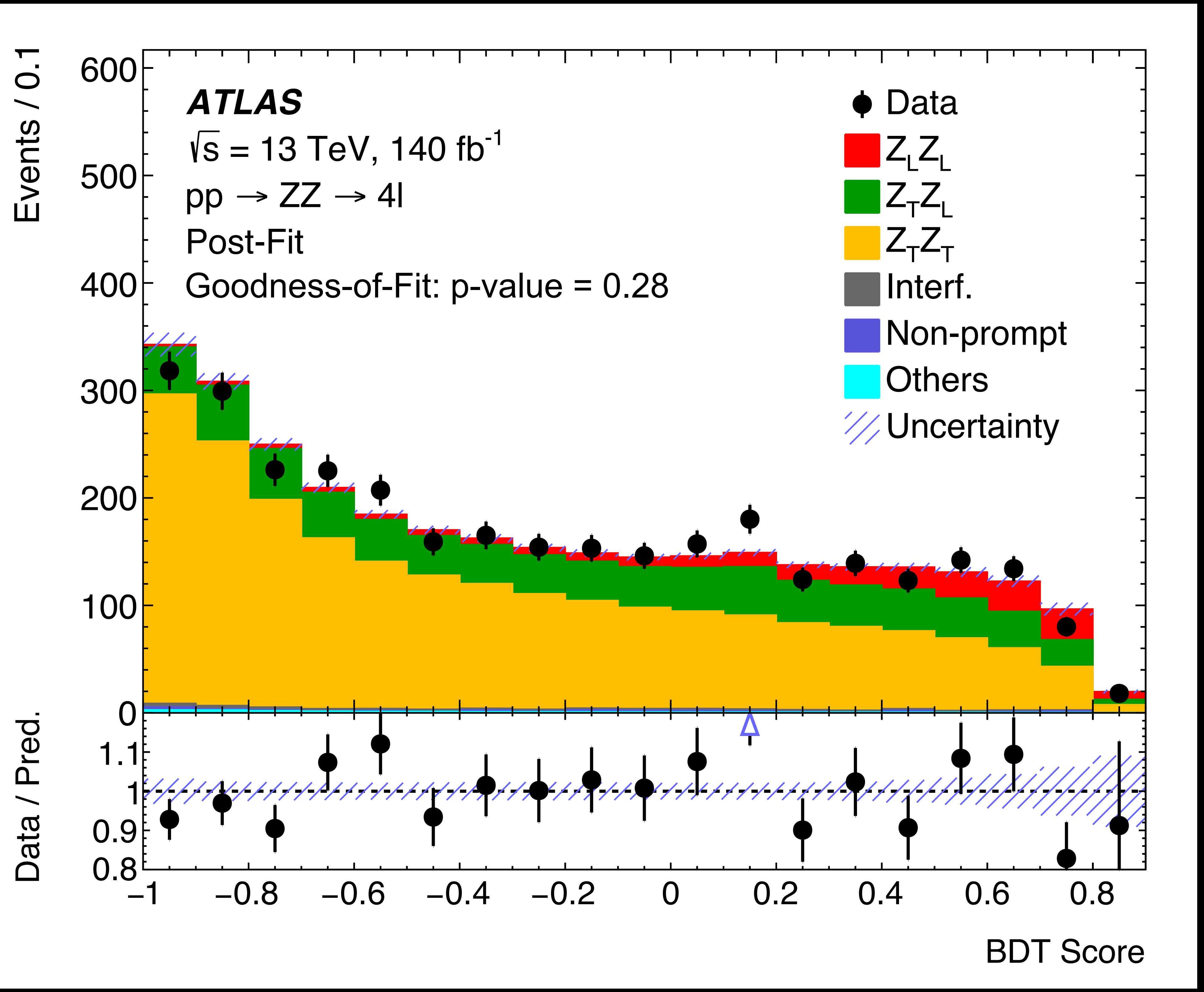

		Pre-fit	Post-fit
ZZ	$Z_L Z_L$	189.3 ± 8.7	220 ± 54
	$Z_T Z_L$	710 ± 29	711 ± 29
	$Z_T Z_T$	2170 ± 120	2147 ± 60
	Interference	33.7 ± 2.8	33.4 ± 2.7
Non-prompt		18.7 ± 7.1	18.5 ± 7.0
Others		20.0 ± 3.7	19.9 ± 3.7
Total		3140 ± 150	3149 ± 57
Data		3149	3149

Stress testing the SM over various energies with dibosons

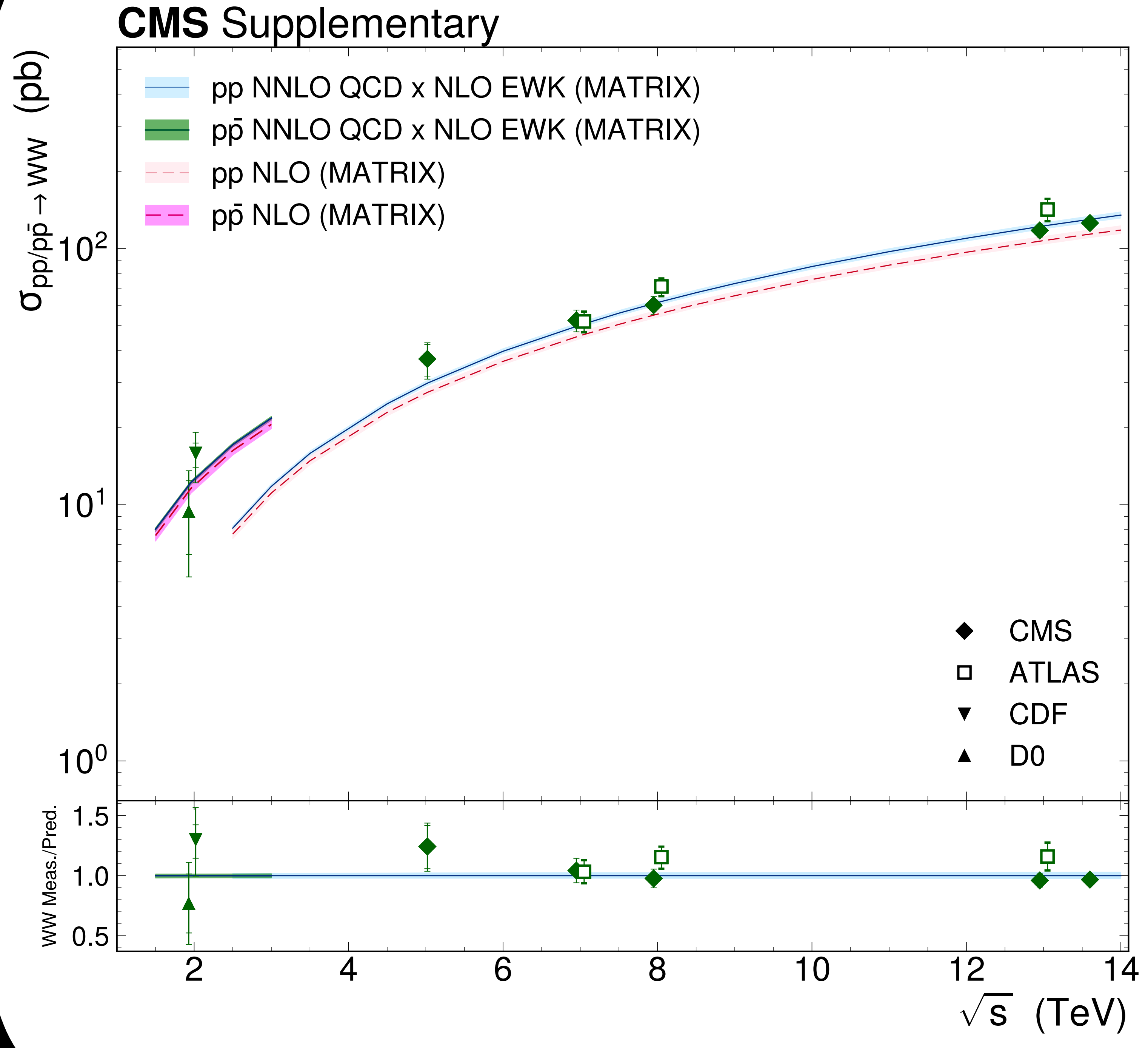

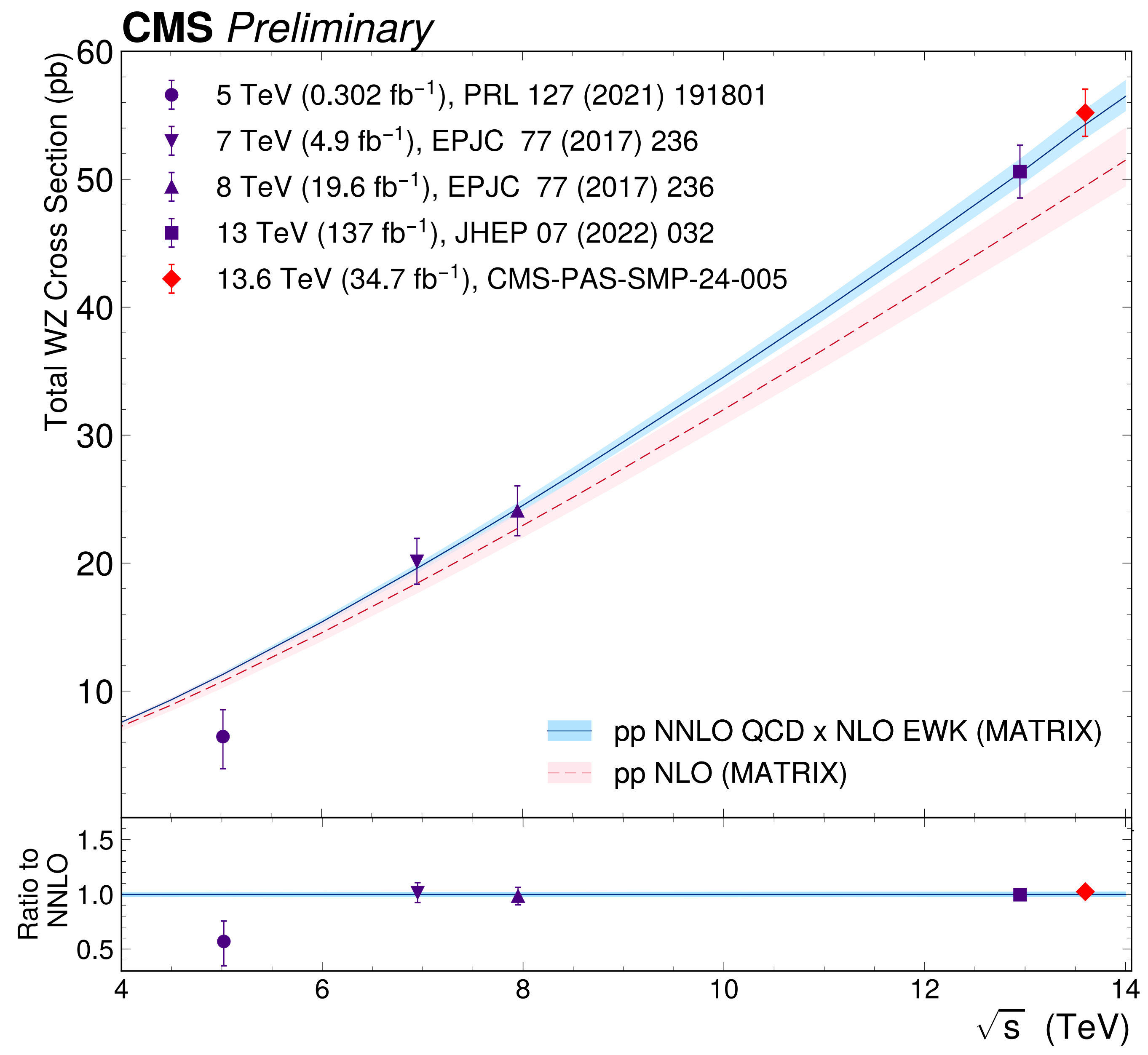

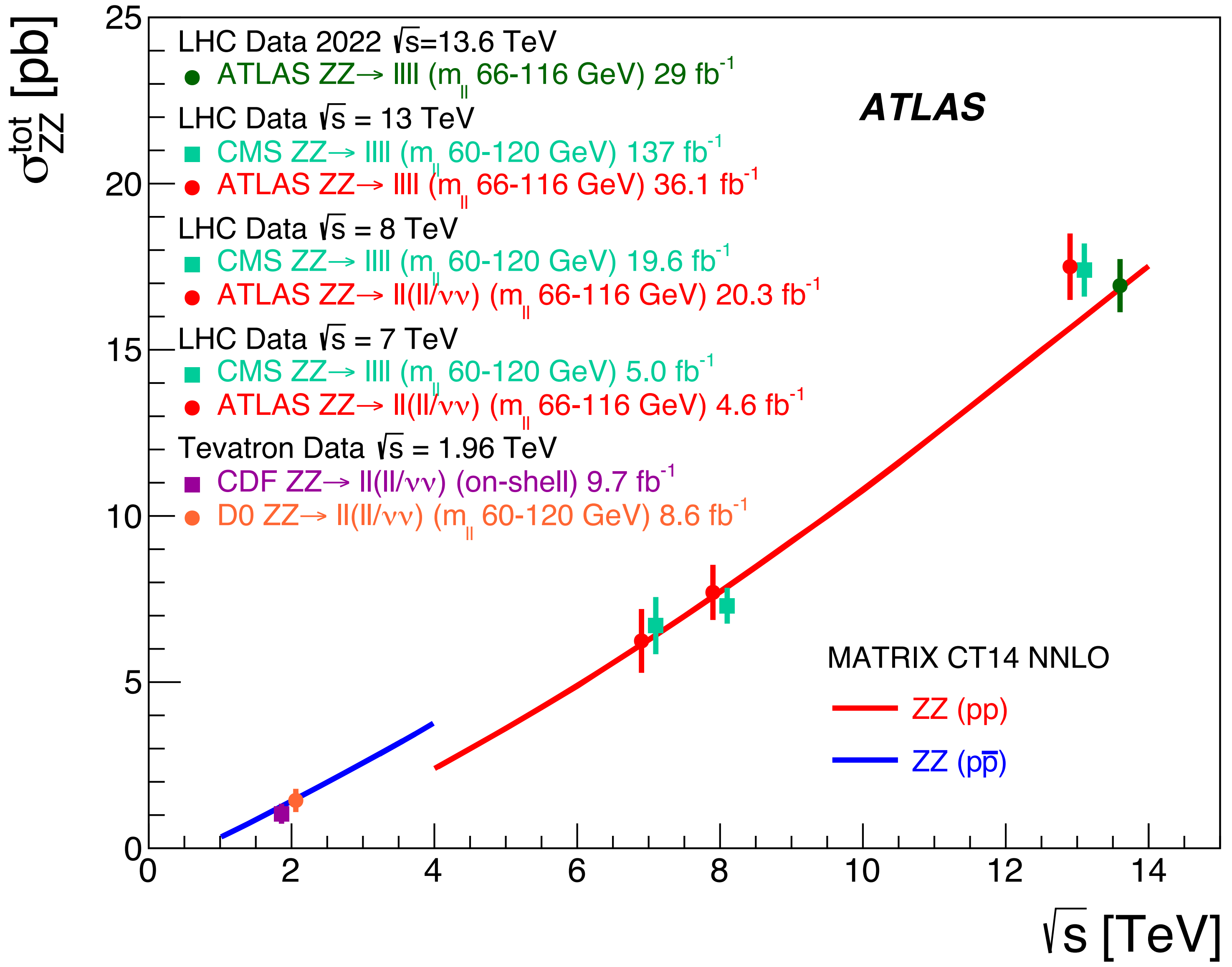

Conclusion

- The full Run 2 dataset allowed us to observe rare processes predicted by the SM
- Precision tests of diboson processes now possible
- Studying the Higgs mechanism *Higgslessly* with polarization measurements
- Run 3 luminosity already exceeds Run 2!

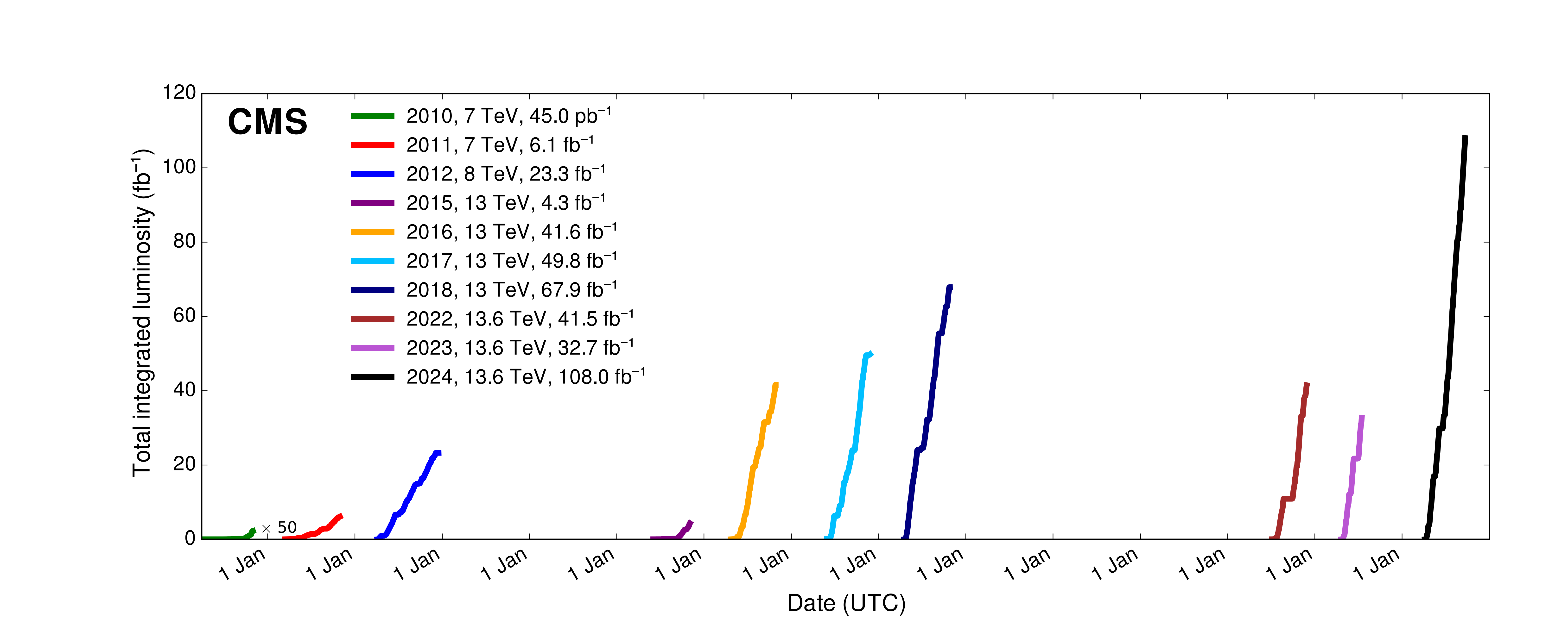

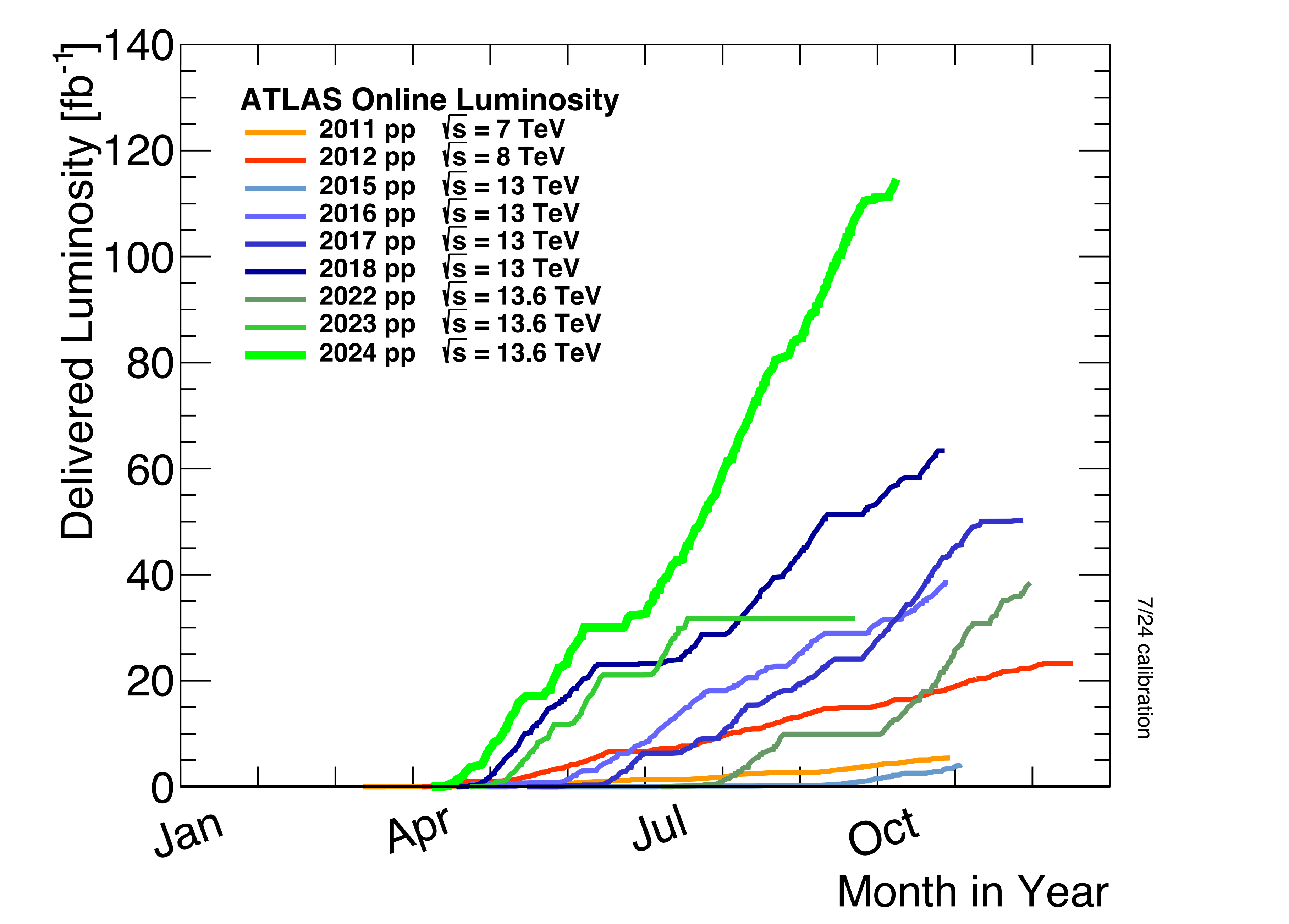

Additional Material

τ polarization in Z-boson decays

- Polarization of τ leptons is measured in $Z \to \tau\tau$ events
- Differential cross section of the $q\bar{q} \to Z \to \tau^+\tau^-$ in lowest order is expressed as:

$$\frac{d\sigma}{d\cos\theta_\tau} = F_0(\hat{s})(1+\cos^2\theta_\tau) + 2F_1(\hat{s})\cos\theta_\tau - h_\tau[F_2(\hat{s})(1+\cos^2\theta_\tau) + 2F_3(\hat{s})\cos\theta_\tau]$$

- Forward-backward asymmetry defined in terms of F_1 and F_2
- Polarization defined in terms of F_2 and F_0
  - Simplified when $\sqrt{\hat{s}} = M_Z$

Helicity states of incoming quarks and outgoing τ leptons: thin arrows show direction of movement, thick arrows show helicity

θ_τ: scattering angle of the τ^- with respect to the quark momentum in the rest frame of the Z boson

h_τ: helicity

τ polarization in Z-boson decays

- Tau spin observables constructed from several decay angles
- Optimal observable to measure τ helicity → polarimetric vector
  - Final-state dependent variable
  - Largest source of uncertainty from QCD normalization
- Measured value of τ polarization: $P_\tau(Z)$ = -0.144 ± 0.006 (stat) ± 0.014 (syst)
  - In agreement with LEP, SLD, ATLAS
- More precise than the previous ATLAS measurement, almost matches precision of single LEP experiments
- Weak mixing angle $\sin^2\theta_W^{\text{eff}}$ = 0.2319 ± 0.0019 (0.8% precision)

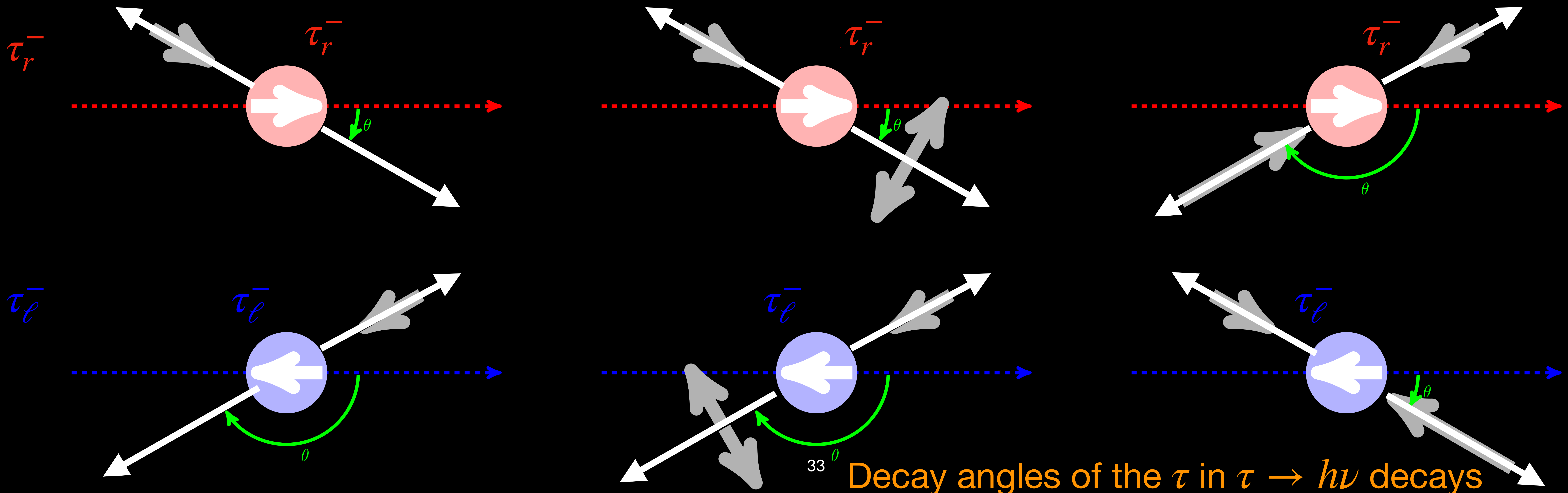

Decay angles of the τ in $\tau \to h\nu$ decays

Definition of signal, control and validation regions at a glance

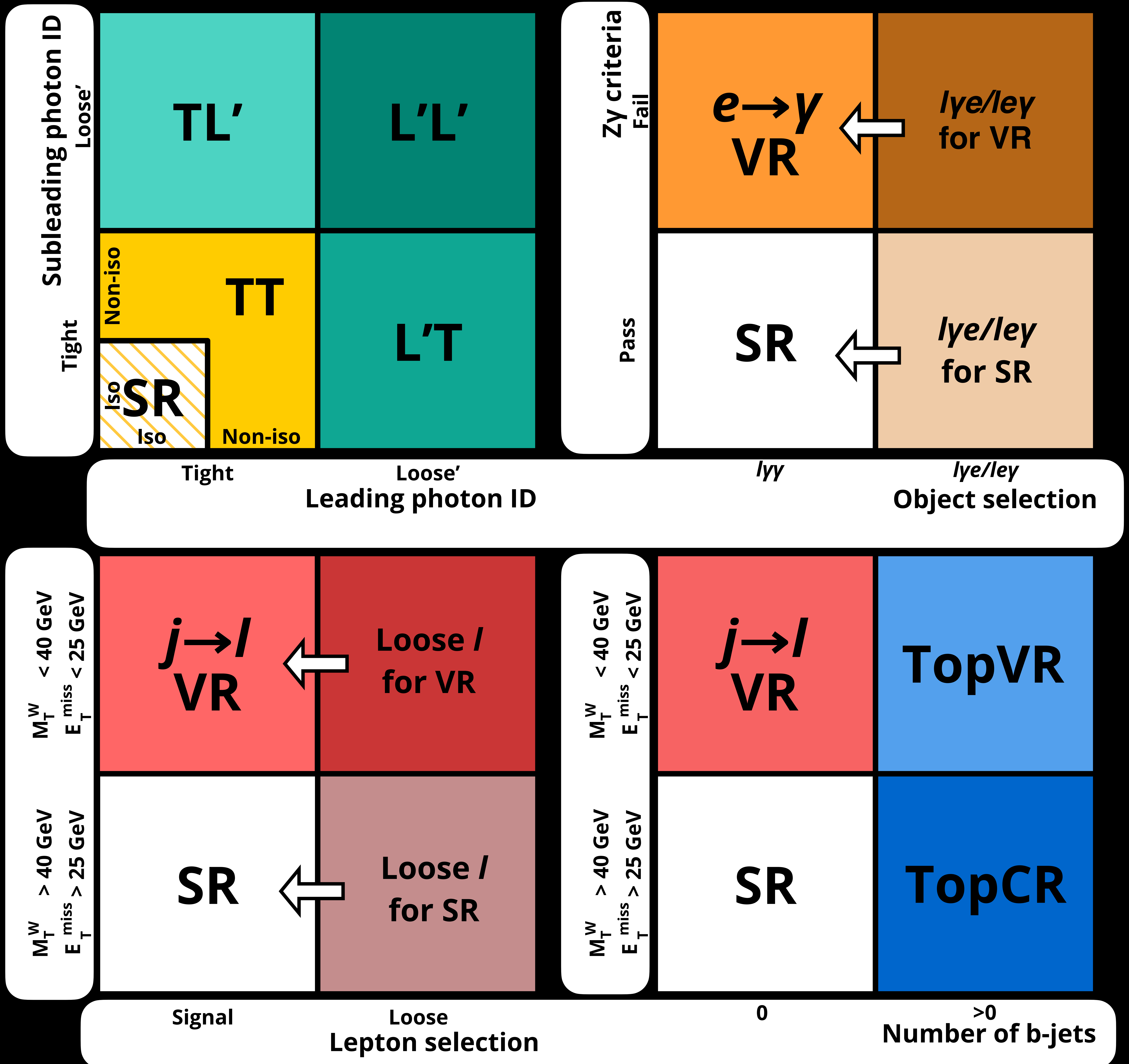

Measuring the W polarization in WZ processes

- $\frac{1}{\sigma}\frac{d\sigma}{d\cos\theta_{W^\pm}} = \frac{3}{8}\left[(1 \mp \cos(\theta_{W^\pm}))^2 f_L^W + (1 \pm \cos(\theta_{W^\pm}))^2 f_R^W + 2\sin^2(\theta_{W^\pm}) f_0^W\right]$ and
  $\frac{d\sigma}{\sigma d\cos\theta_Z} = \frac{3}{8}\left[(1+\cos^2(\theta_Z) - 2c\cos(\theta_Z))f_L^Z + (1+\cos^2(\theta_Z) + 2c\cos(\theta_Z))f_R^Z + 2\sin^2(\theta_Z) f_0^Z\right]$
- Single boson spin density matrix derived from joint spin density matrix
  - Individual helicity fractions: f_0 (longitudinal), f_L and f_R (left and right handed transverse helicity states)

- θ^W: angular distance between the momenta of the W boson and the charged lepton from its primary decay

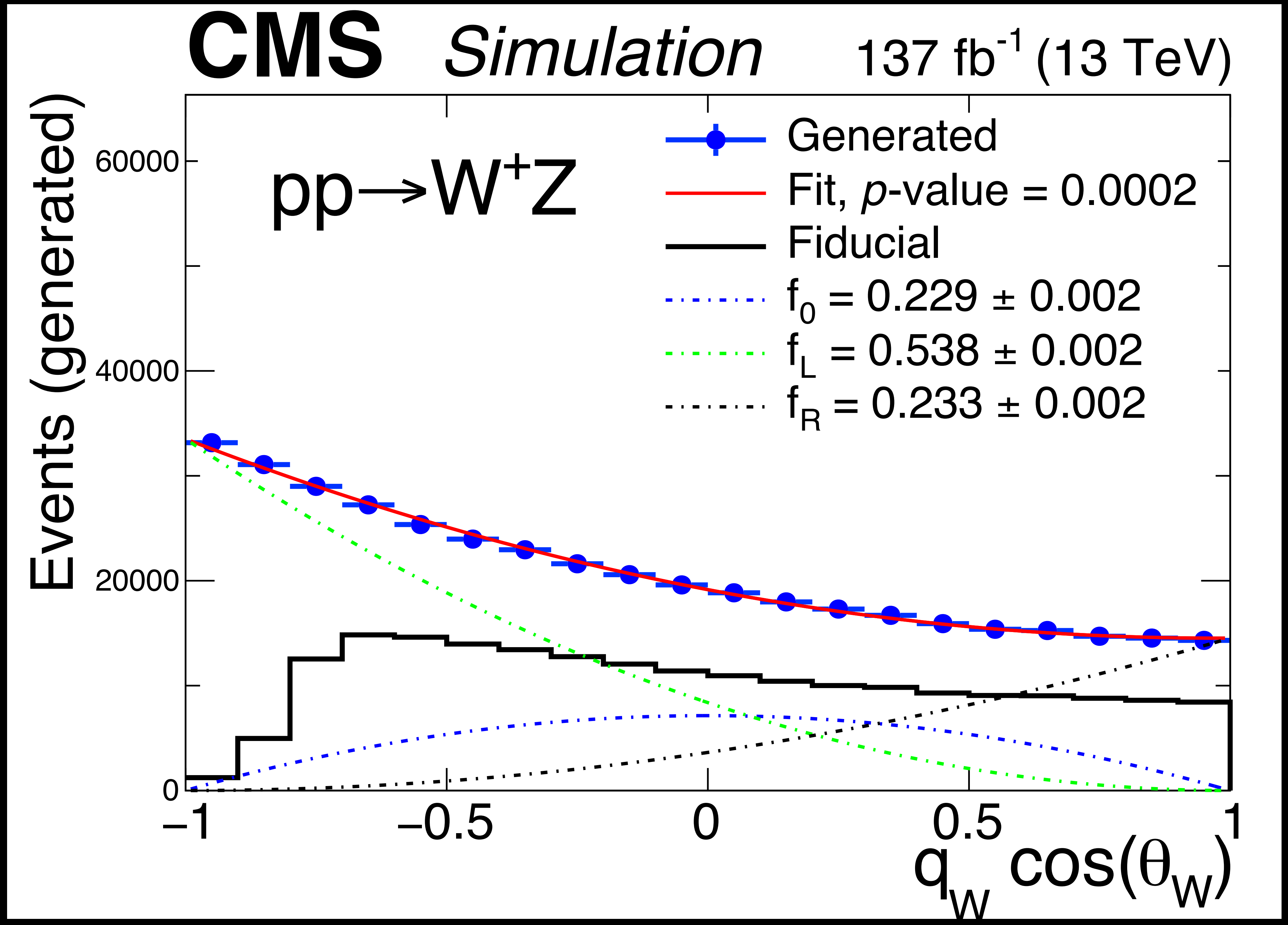

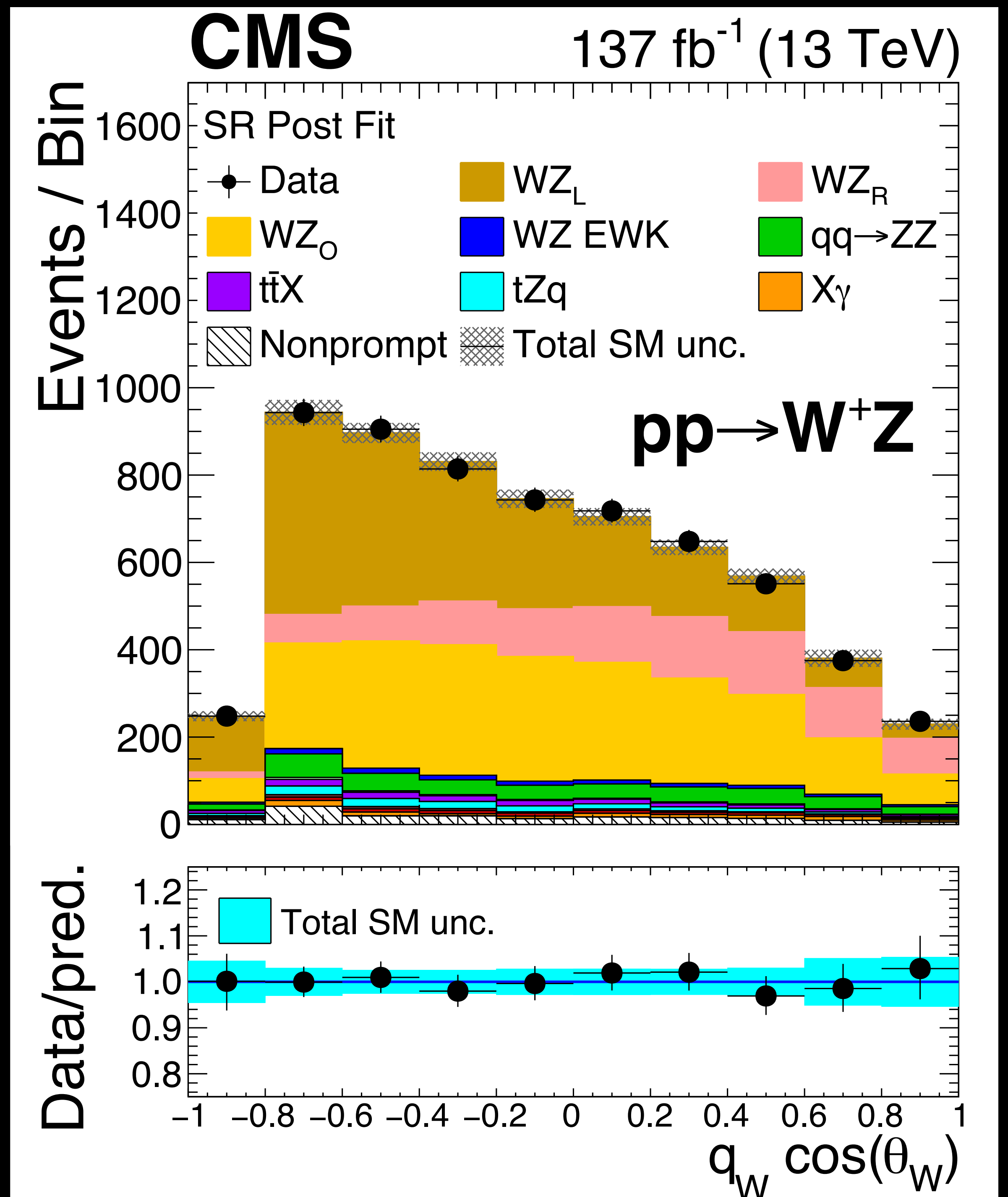

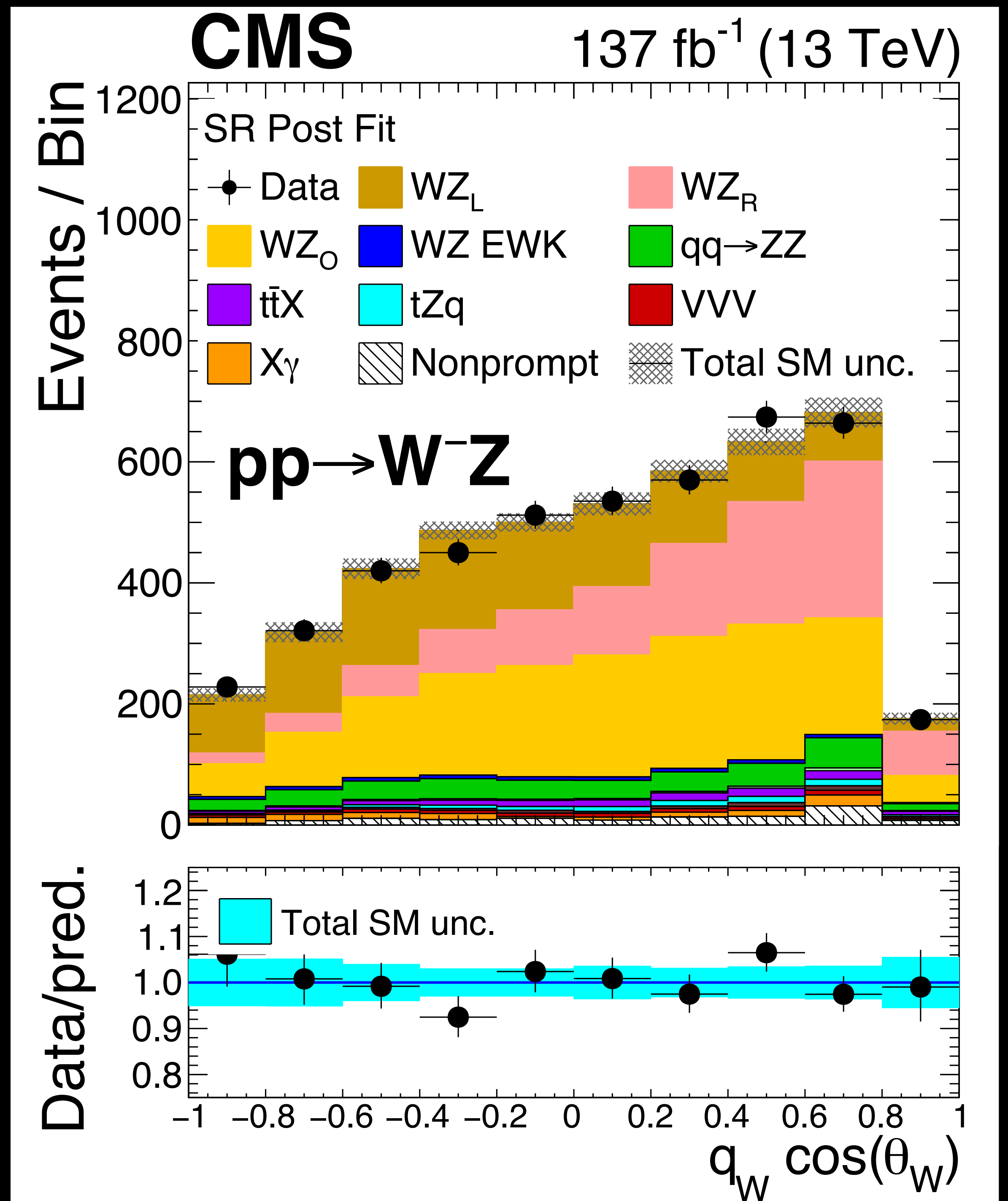

Content of the talk

- ATLAS
  - Diboson polarization fractions and Radiation Amplitude Zero effect in WZ production
    - https://atlas.web.cern.ch/Atlas/GROUPS/PHYSICS/PAPERS/STDM-2020-01/
  - Measurement of ZZ production cross-sections in the four-lepton final state
    - https://atlas.web.cern.ch/Atlas/GROUPS/PHYSICS/PAPERS/STDM-2022-17/
  - Evidence of pair-production of longitudinally polarised vector bosons and study of CP properties in $ZZ \to 4l$ events
    - https://atlas.web.cern.ch/Atlas/GROUPS/PHYSICS/PAPERS/STDM-2021-05/
  - Observation of gauge boson joint-polarisation states in WZ production
    - https://atlas.web.cern.ch/Atlas/GROUPS/PHYSICS/PAPERS/STDM-2022-01/
- CMS
  - Measurement of the $pp \to WZ$ inclusive and differential cross sections, polarization angles and search for anomalous gauge couplings at $\sqrt{s} = 13$ TeV
    - https://cms-results.web.cern.ch/cms-results/public-results/publications/SMP-20-014/index.html
  - Measurements of production cross sections of polarized same-sign W boson pairs in association with two jets in proton-proton collisions at $\sqrt{s} = 13$ TeV
    - https://cms-results.web.cern.ch/cms-results/public-results/preliminary-results/SMP-20-006/index.html
  - Measurement of the τ lepton polarization in Z boson decays
    - https://cms-results.web.cern.ch/cms-results/public-results/publications/SMP-18-010/index.html

https://arxiv.org/pdf/2308.03041

The pileup background consists of events in which one or both photons do not originate from the primary vertex, mainly due to a limited photon pointing resolution. The fraction of photons originating from a pileup vertex is calculated in a subset of SR data where at least one photon is converted. Since the fraction of photons that convert is independent of their production vertex, the relative fractions of signal and pileup photons in the converted sample is representative of the fractional number of signal and pileup photons in the full SR. Converted photons that are required to have at least one ID track with silicon hits [49] and a conversion radius, defined as the radial distance of the conversion vertex, of less than 400 mm are used for this estimate because the presence of an ID track allows for the calculation of a longitudinal impact parameter. The difference between the longitudinal impact parameters of the converted photon and the primary vertex, Δz, is Gaussian-distributed and expected to be close to zero for photons from the hard scatter, while pileup photons are expected to have a much broader distribution [55]. The $|\Delta z| > 55$ mm tails of the distribution are used to estimate the fraction of pileup photons in the SR. The statistical uncertainty on the pileup background is 56%, due to the limited number of events in the estimation region.

https://arxiv.org/pdf/2310.04350

For the polarisation measurements, dedicated systematic uncertainties are considered in the modelling of the polarisation templates, including theoretical uncertainties from higher-order corrections, PDFs and α_S described above, and the uncertainties associated with the reweighting methods as described in Section 6.1. For both the $q\bar{q} \to ZZ$ and $gg \to ZZ$ polarisation templates, the theoretical uncertainties from QCD scales are taken from the MoCaNLO calculations by varying the QCD scales as described above, while for the template of the interference term, which is reweighted from the inclusive Sherpa $q\bar{q} \to ZZ$ samples, these theoretical uncertainties are estimated from the Sherpa sample. The parton showering and hadronisation uncertainty is estimated for the signal by comparing the nominal Pythia 8 parton showering with the alternative Herwig 7 [95, 96] algorithm. Uncertainties from the NLO EW corrections are estimated by taking the difference between the additive and the multiplicative prescription in MoCaNLO [66]. For the 1D reweighting method in Section 6.1, the uncertainty is estimated by comparing the reweighted templates using the nominal observable and an alternative observable: the rapidity difference of the two Z bosons. For the additional 2D reweighting, the residual difference between the sum of the four templates and the inclusive prediction from the Sherpa sample is taken as an uncertainty.